



The  
University  
Of  
Sheffield.

**Department of Chemistry**  
**University of Sheffield**

---

*Chemical Probes to Investigate the Antibiotic  
Behaviour at the Molecular Level*

By  
Shuwen Ma

A thesis submitted in partial fulfilment of the requirements for the degree of  
Doctor of Philosophy

Supervisor: Prof. Simon Jones

## Abstract

This project aimed to design and synthesise a number of fluorescent chemical probes to develop a greater understanding the behaviour of antibiotic resistance, providing essential information that will be critical in the future research to prepare new antibacterial agents. In particular, the antibiotic interaction and function with peptidoglycan at the molecular level was called for special concern.

The work described in the thesis was mainly focused on the preparation of the fluorescent probes of thiazolidinone and quinazolinone and the synthesis of cyclic phosphonates which were supposed to show antibiotic activity. The small molecular transglycosylase inhibitor thiazolidinone showed good inhibitory effect against *S. aureus* with MIC of 16  $\mu\text{g}/\text{mL}$ . The MIC of PBP inhibitor quinazolinone is 2  $\mu\text{g}/\text{mL}$  against *S. aureus*. A series of chemical probes based on thiazolidinone and quinazolinone were successfully synthesised. However, the bioactivities of the prepared thiazolidinone and quinazolinone probes against *S. aureus* were limited and not qualified for labelling study, which required the development of new chemical probes. Cyclic phosphonates were supposed to inhibit nucleophilic serine and zinc-dependent  $\beta$ -lactamases as well as PBPs. Chemistry reactions were developed to prepare novel phosphonates, such as Kabachnik-Fields reaction, providing a great opportunity to discover new antibiotics.

## **Acknowledgements**

Firstly, I would like to show my appreciation towards Prof. Simon Jones and Prof. Simon Foster for giving me the opportunity to carry out my PhD and providing support and guidance throughout all elements of this project.

I am grateful to all members of the Jones and Foster groups, not only for scientific help but also for making the research life more enjoyable. Specifically thank Dr. Dan Cox and Dr. Victoria A Lund for their guidance in chemistry and biology respectively at the beginning of my PhD.

I am also greatly appreciative of the China Scholarship Council-Sheffield Joint Programme and the Great Britain-China Educational Trust for funding my study and life in Sheffield.

Lastly, but most importantly thank to my wonderful parents for their constant support and unconditional love.

## Abbreviations

The following abbreviations appear in this thesis:

~	Approximately
%	Percentage
Å	Angstrom(s)
AcOH	Acetic acid
ANR	Ames non-reverting
app	Apparent
aq.	Aqueous
ATCC	American Type Culture Collection
ATR	Attenuated total reflection
$\beta$	Beta
<i>B. anthracis</i>	<i>Bacillus anthracis</i>
Boc	<i>tert</i> -Butoxycarbonyl
Boc <sub>2</sub> O	Di- <i>tert</i> -butyl dicarbonate
BuOH	Butanol
°C	Degree Celsius
$\delta$	Chemical shift in parts per million
CDCl <sub>3</sub>	Deuterated chloroform
CH <sub>3</sub> C(OEt) <sub>3</sub>	Triethyl orthoformate
cm <sup>-1</sup>	Wavenumber(s)
COL	Colindale (The Central Public Health Laboratory)
Con.	Concentration
conc.	Concentrated
CuSO <sub>4</sub>	Copper(II) sulfate
D-Ala	D-Alanine
D-Ala-D-Ala	D-Alanyl-D-alanine
DCC	<i>N,N'</i> -Dicyclohexylcarbodiimide
DCM	Dichloromethane
D-Glu	D-Glutamic acid
DMAP	4-Dimethylaminopyridine
DMAPP	Dimethylallyl diphosphate

DMF	Dimethylformamide
DMP	Dess–Martin periodinane
DMSO	Dimethyl sulfoxide
DNA	Deoxyribonucleic acid
Dr.	Doctor
<i>E. coli</i>	<i>Escherichia coli</i>
<i>E. faecalis</i>	<i>Enterococcus faecalis</i>
<i>E. faecium</i>	<i>Enterococcus faecium</i>
Enz	Enzyme
ES <sup>+</sup>	Positive charge electrospray mass spectrometry
ES <sup>-</sup>	Negative charge electrospray mass spectrometry
ESKAPE	<i>Enterococcus faecium</i> , <i>Staphylococcus aureus</i> , <i>Klebsiella pneumoniae</i> , <i>Acinetobacter baumannii</i> , <i>Pseudomonas aeruginosa</i> and <i>Enterobacter species</i>
Et <sub>3</sub> N	Triethylamine
EtOAc	Ethyl acetate
EtOH	Ethanol
FeCl <sub>3</sub>	Iron(III) chloride
FPP	Isoprenoid farnesyl diphosphate
FPPS	Farnesyl diphosphate synthase
g	Gas
g	Gram(s)
GlcNAc	<i>N</i> -Acetylglucosamine
Gly	Glycine
h	Hour(s)
HBr	Hydrobromic acid
HCl	Hydrogen chloride
H <sub>2</sub> O	Water
HPLC	High performance liquid chromatography
H <sub>2</sub> SO <sub>4</sub>	Sulphuric acid
Hz	Hertz
hVISA	Hetero-resistant vancomycin-intermediate <i>Staphylococcus aureus</i>

IC <sub>50</sub>	Half-maximal inhibitory concentration
ICCB	Institute of Chemistry and Cell Biology
IPP	Isopentenyl diphosphate
<i>J</i>	Coupling constant (in NMR spectroscopy)
KCl	Potassium chloride
K <sub>2</sub> CO <sub>3</sub>	Potassium carbonate
KH <sub>2</sub> PO <sub>4</sub>	Potassium dihydrogen phosphate
KI	Potassium iodide
KOH	Potassium hydroxide
L-Ala	L-Alanine
LiAlH <sub>4</sub>	Lithium aluminium hydride
lit.	Literature
L-Lys	L-Lysine
μg	Microgram(s)
μM	Micromolar
μL	Microlitre(s)
M	Molar
MeCN	Acetonitrile
MeI	Iodomethane
MeOD	Deuterated methanol
MeOH	Methanol
Me <sub>2</sub> S	Dimethyl sulfide
MgSO <sub>4</sub>	Magnesium sulphate
MIC	Minimum inhibitory concentration
min	Minute(s)
mL	Millilitre(s)
mm	Millimetre(s)
mmol	Millimole
mol%	Mole percent
m.p.	Melting point
MraY	Phospho-MurNAc-pentapeptide translocase
MRSA	Methicillin-resistant <i>Staphylococcus aureus</i>
MSSA	Methicillin-sensitive <i>Staphylococcus aureus</i>

MurA	UDP- <i>N</i> -acetylglucosamine enolpyruvyl transferase
MurB	UDP- <i>N</i> -acetylenolpyruvylglucosamine reductase
MurC	UDP- <i>N</i> -acetylmuramoyl-L-alanine synthetase
MurD	UDP- <i>N</i> -acetylmuramoyl-L-alanine: D-glutamate ligase
MurE	UDP- <i>N</i> -acetylmuramoyl-L-alanyl-D-glutamate: meso-2,6-diaminopimelate ligase
MurF	UDP- <i>N</i> -acetylmuramoyl-tripeptide-D-alanyl-D-alanine ligase
MurG	UDP- <i>N</i> -acetylglucosamine- <i>N</i> -acetylmuramoyl-(pentapeptide) pyrophosphoryl undecaprenol <i>N</i> -acetylglucosamine transferase
MurNAc	<i>N</i> -Acetylmuramic acid
m/z	Mass to charge ratio
NaCl	Sodium chloride
NaH	Sodium hydride
NaHCO <sub>3</sub>	Sodium bicarbonate
Na <sub>2</sub> HPO <sub>4</sub>	Sodium Phosphate
NaI	Sodium iodide
NaN <sub>3</sub>	Sodium azide
NaOAc	Sodium acetate
NaOH	Sodium hydroxide
ng	Nanogram(s)
NH <sub>3</sub>	Ammonia
NHS	<i>N</i> -Hydroxysuccinimide
NH <sub>4</sub> SCN	Ammonium thiocyanate
nm	Nanometre(s)
nM	Nanomolar
NMR	Nuclear magnetic resonance
NOE	Nuclear Overhauser effect
O <sub>3</sub>	Ozone
OD <sub>600</sub>	Optical density (of a sample measured at a wavelength of 600 nanometres)
<i>p</i>	Para

PBP	Penicillin-binding protein
PBS	Phosphate buffered saline
PDB	Protein Data Bank
PEG	Polyethylene glycol
PET	Positron emission tomography
PhD	Doctor of Philosophy
PPh <sub>3</sub>	Triphenylphosphine
ppm	Parts per million
PPTS	Pyridinium <i>p</i> -toluenesulfonate
Prof.	Professor
quan.	Quantitative
RNA	Ribonucleic acid
rpm	Revolutions per minute
RT	Room temperature
<i>S. aureus</i>	<i>Staphylococcus aureus</i>
Ser	Serine
<i>S. pneumoniae</i>	<i>Streptococcus pneumoniae</i>
TBAI	Tetra-n-butylammonium iodide
<i>tert</i>	Tertiary
TBAF	Tetra-n-butylammonium fluoride
TBDMSCl	<i>tert</i> -Butyldimethylsilyl chloride
TFA	Trifluoroacetic acid
THF	Tetrahydrofuran
TLC	Thin layer chromatography
tRNA	Transfer ribonucleic acid
TSA	Tryptic soy agar
TSB	Tryptic soy broth
TsCl	4-Toluenesulfonyl chloride
UDP	Undecaprenyl phosphate
UP	Undecaprenyl monophosphate
UPP	Isoprenoid undecaprenyl diphosphate
UPPP	Undecaprenyl diphosphate phosphatase
UPPS	Undecaprenyl diphosphate synthase

USA	United States of America
VISA	Vancomycin-intermediate <i>Staphylococcus aureus</i>
VRSA	Vancomycin-resistant <i>Staphylococcus aureus</i>
W	Watt
wt%	Mass fraction
ZINC	ZINC is not commercial

- i. Abstract
- ii. Acknowledges
- iii. Abbreviations
- ix. Contents

## Contents

Chapter 1 Introduction .....	1
1.1 Mode of Action of Antibiotics.....	2
1.2 Bacterial Cell Wall .....	4
1.3 Biosynthesis of Peptidoglycan .....	6
1.4 Penicillin-Binding Proteins .....	11
1.4.1 Function .....	11
1.4.2 Classification .....	12
1.5 Staphylococcus aureus .....	13
1.6 Molecular Imaging Probes .....	15
1.6.1 Fluorescent Derivative of Moenomycin A .....	16
1.6.2 Fluorescent Beta-lactone Probes.....	18
1.7 Project Aims.....	21
Chapter 2 Thiazolidinone Synthesis and Analysis.....	22
2.1 Moenomycins and Thiazolidinone in the Literature.....	22
2.1.1 Moenomycins .....	22
2.1.2 Thiazolidinone.....	24
2.2 Synthesis and MIC Testing of Thiazolidinone .....	25
2.3 Synthesis and MIC Testing of Thiazolidinone Probe I.....	28
2.4 Structure-Activity Relationship of Thiazolidinones .....	31
2.5 Synthesis and MIC Testing of Thiazolidinone Probe II.....	37
Chapter 3 Quinazolinone Synthesis and Analysis.....	43
3.1 Quinazolinones in the Literature .....	43
3.2 Synthesis and MIC Testing of Small Molecule Quinazolinones .....	45
3.3 Design of Quinazolinone Probes.....	51
3.4 Synthesis and MIC Testing of Quinazolinone Probe I .....	52
3.4.1 Attempted Synthesis of Quinazolinone Probe I with an Alkyne-PEG Linker .....	52

3.4.2 Synthesis of Quinazolinone Probe I with an Azide-PEG Linker.....	55
3.4.3 MIC Testing of Quinazolinone Probe I.....	57
3.5 Synthesis and MIC Testing of Quinazolinone Probe II.....	59
3.5.1 Synthesis of Small Molecule Quinazolinone.....	59
3.5.2 Attempted Synthesis of Quinazolinone Probe II with an Alkyne-PEG Linker.....	60
3.5.3 Synthesis of Quinazolinone Probe II with an Azide-PEG Linker.....	61
3.5.4 MIC Testing of Quinazolinone Probe II.....	62
3.6 Labelling of Quinazolinone Probe II.....	63
3.6.1 Post-click labelling.....	64
3.6.2 Pre-click labelling.....	65
6.7 Synergism of Quinazolinones with Beta-lactam Antibiotic.....	69
3.7.1 MIC Testing of Ampicillin.....	69
3.7.2 Synergism of Quinazolinones with Ampicillin.....	70
Chapter 4 Cyclic Phosphonate Synthesis and Analysis.....	76
4.1 Cyclic Phosph(on)ates and Cyclic Boronates in the literature.....	76
4.1.1 Cyclic Phosph(on)ates.....	76
4.1.2 Cyclic Boronates.....	77
4.2 Retrosynthetic Analysis.....	80
4.3 Synthesis of <i>tert</i> -Butyl Protected Benzoates.....	80
4.4 Synthesis of Methyl Protected Benzoates.....	82
4.5 Simplified Target and Retrosynthetic Analysis.....	83
4.6 Two Synthetic Routes towards Benzeneacetaldehyde.....	84
4.7 Kabachnik-Fields Reaction.....	87
Chapter 5 Conclusion and Future Work.....	89
5.1 Thiazolidinones.....	89
5.2 Quinazolinones.....	91
5.3 Cyclic phosphonates.....	93
Chapter 6 Experimental Procedures.....	95
6.1 Biological Experimental.....	95
6.1.1 Growth Media.....	95
6.1.2 <i>Staphylococcus Aureus</i> Strains.....	95
6.1.3 Measurement by Optical Density.....	95

6.1.4 Determination of MIC by Microdilution method.....	96
6.1.5 Labelling Peptidoglycan Synthesis.....	96
6.1.5.1 16% (w/v) Paraformaldehyde.....	97
6.1.5.2 Phosphate Buffered Saline (PBS).....	98
6.1.5.3 Click-iT® Reaction Buffer Mix.....	98
6.1.6 Fluorescence Microscopy .....	98
6.2 Chemical Experimental .....	99
6.2.1 Solvents and Reagents.....	99
6.2.2 Chromatography.....	99
6.2.3 Melting point .....	99
6.2.4 IR spectroscopy.....	100
6.2.5 NMR spectroscopy.....	100
6.2.6 Mass spectroscopy.....	100
6.2.7 Chemical Synthesis .....	101
References .....	166

## **Chapter 1 Introduction**

Antibiotics were introduced into the area of medicine and enjoyed a high reputation in the 1940s. Especially, A. Fleming's discovery, penicillin, was purified and first clinically used by H. Florey and E. Chain to treat bacterial infections. It was later praised as the miracle drug.<sup>1</sup> During the Second World War, the large-scale generation of penicillin by a British-American collaboration treated most battlefield infections and saved millions of lives. With penicillin, the mortality of pneumonia in the American army decreased to less than 1% in World War II, much lower than the approximate 18% in World War I.<sup>2</sup>

However, the remarkable capacity of bacteria to regenerate in approximate 30 minutes makes it possible for them to mutate and adapt to new hosts and environments.<sup>3</sup> Since ancient times, naturally occurring antibiotics spawned the resistance genes by placing a selective pressure on bacteria and favouring the fittest and more adapted strains. The use, overuse and misuse of modern prescription antibiotics has driven further the evolution of antibiotic resistance.<sup>4,5</sup> The golden era of antibiotic discovery ended in the 1960s and the rapid emergence of resistant bacteria occurs globally. The antibiotic resistance crisis and the lack of new antibacterial development make bacterial infections become a serious health threat again.<sup>6,7</sup>

Therefore, it is urgent to investigate the behaviour of antimicrobial resistance and conduct further studies to prepare new antibacterial agents. The development of chemical tools enables imaging, manipulating and tracking the biological processes of the living

world. Chemical probes not only provide the valuable insight into the complex biological systems, but also inspire new ideas and methods leading to new scientific discoveries on human health and medicine. <sup>8</sup>

### 1.1 Mode of Action of Antibiotics

Antibiotics are medicines to target bacterial infections, either destroying (bactericidal) or slowing down (bacteriostatic) the growth of bacteria.<sup>9</sup> The mechanism of antibiotic action can mainly be divided into four categories on the basis of their intracellular targets: cell wall synthesis inhibition, cell membrane disruption, protein synthesis inhibition and nucleic acid synthesis inhibition (Figure 1).<sup>10, 11</sup>

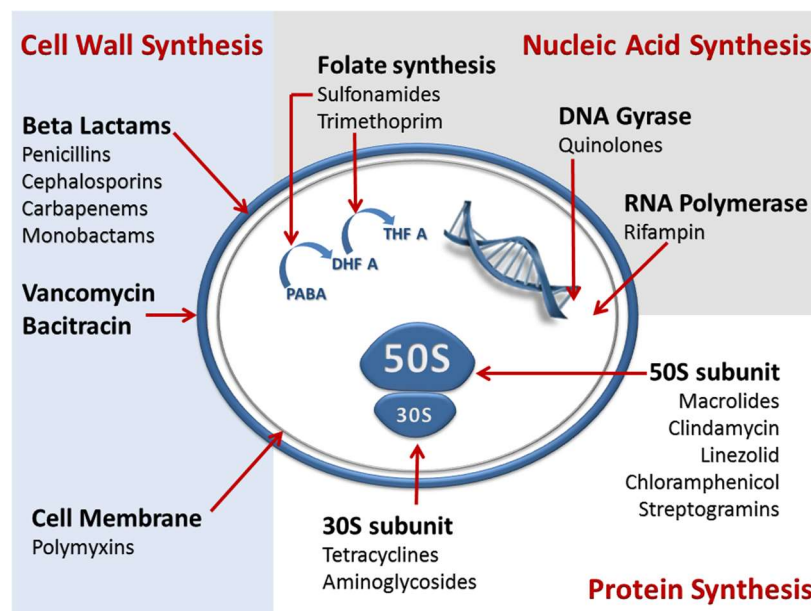


Figure 1. Mechanism of action of antibiotics. Adapted with permission from Royal Society of Chemistry.<sup>10</sup>

Inhibition of cell wall synthesis is the most common mechanism, e.g. penicillin, cephalosporins, carbapenems and vancomycin.  $\beta$ -Lactam antibiotics, such as penicillin, containing a core structure of a  $\beta$ -lactam ring, inhibit the transpeptidase (also known as penicillin-binding protein) during the cell wall synthesis.<sup>12</sup> The structure of penicillin is similar to D-Ala-D-Ala, which the transpeptidase normally binds to (Figure 2). As a mimic of D-Ala-D-Ala, penicillin binds to transpeptidase and occupies the active site, inhibiting the formation of the peptidoglycan cross-links. Therefore, the cell wall is weakened the osmotic damage leads to bursting or lysing the cells.<sup>12, 13</sup>



Figure 2. Structural comparison of penicillin (left) and D-Ala-D-Ala (right).

Another target of antibiotics is the outer membrane of gram-negative bacteria, such as polymyxins.<sup>10</sup> Polycationic peptide antibiotics (e.g. polymyxin B and polymyxin E) can destabilise the lipopolysaccharide of the outer membrane. The permeability of the bacterial membrane is then increased and the cytoplasmic content leaks, finally resulting in the death of cells.<sup>14</sup>

Nucleic acid synthesis can be interfered by antibiotics from different levels, such as Inhibition of nucleotide synthesis or interconversion. In addition, the template function of DNA can be impaired, and the replication and transcription of DNA can be prevented by interfering with the polymerases involved in the process.<sup>15</sup> For example, rifamycins

inhibit DNA-directed RNA polymerase by binding strongly to its  $\beta$  subunit. The conformation of the RNA polymerase is thereby distorted, and it cannot initiate RNA synthesis.<sup>16</sup>

Inhibition of protein synthesis is the second largest class of mechanism. The bacterial protein synthesis is mainly blocked by antibiotics at the 30S subunit or 50S subunit of the 70S bacterial ribosome.<sup>17, 18</sup> Take tetracyclines as an example, they are bacteriostatic agents and bind reversibly to the acceptor site of the 30S ribosomal subunit. While the aminoacyl tRNA attempts to bind to the acceptor site of the ribosome, it is blocked by tetracyclines.<sup>19</sup> Therefore, the binding of the aminoacyl tRNA is prevented and the protein biosynthesis is ultimately terminated.

## **1.2 Bacterial Cell Wall**

Bacteria are classified as prokaryotes that do not have membrane-bound structures and the most noteworthy is the lack of well-defined nucleus. They come in a variety of shapes, from spheres, rods, spirals to branched filaments, and other more complicated forms.<sup>20</sup> They differ from cells of higher organisms, as bacteria are usually in the face of dilute, inhospitable and unpredictable environments.<sup>21</sup> The osmotic pressure within the cell is much higher than the outside environment because of the high concentration of dissolved solute inside the cell cytoplasm. In order to survive and grow, the bacterial cell wall has evolved as a rigid, porous, protective layer enclosing the bacterium to maintain the cell

shape and osmotic stability.<sup>22, 23</sup>

The cell wall composition varies between bacterial species but mainly consists of peptidoglycan, also called murein. Peptidoglycan is a unique and essential polymer of long, linear glycan strands cross-linked by short peptides.<sup>22, 24</sup> Its thickness and mesh-like structure make it possible to divide bacteria into two large groups (gram-positive and gram-negative) by a staining and washing technique developed by Hans Christian Gram in 1884 and this eponymous stain is still widely used nowadays.<sup>21</sup> Gram-positive bacteria are able to remain dark blue or violet after Gram staining because their thick cell wall (20-80 nm) traps the dye. In contrast, the cell wall of gram-negative bacteria is relatively thin (7-8 nm) and releases the dye readily when washed with an alcohol or acetone solution. After washing, a counter stain (commonly safranin or fuchsine) will be added and gram-negative bacteria will be stained pink. Gram-positive bacteria also pick up the counter stain but it is indiscernible because the primary crystal violet stain is much darker.<sup>25</sup>

The cell wall of gram-negative bacteria only consists of a single layer of peptidoglycan in the periplasmic space between the inner and outer lipid membranes. The outer membrane invariably contains lipopolysaccharides on its outer leaflet which are toxic and classified as an endotoxin that elicits a strong immune response when infecting animals. It is relatively permeable and assists non-vesicle-mediated transport through channels such as porins or specialized transporters (Figure 3a). Though gram-positive bacteria lack the outer membrane, there are several layers of peptidoglycan framing the

cell wall. A group of teichoic acids are perpendicular to the peptidoglycan sheets which is unique to the gram-positive cell wall. They are essential to viability and the teichoic acid polymers anchored to the lipid membrane are referred to as lipoteichoic acids, activating the immune system of infected hosts and promoting inflammation. (Figure 3b).<sup>26</sup>

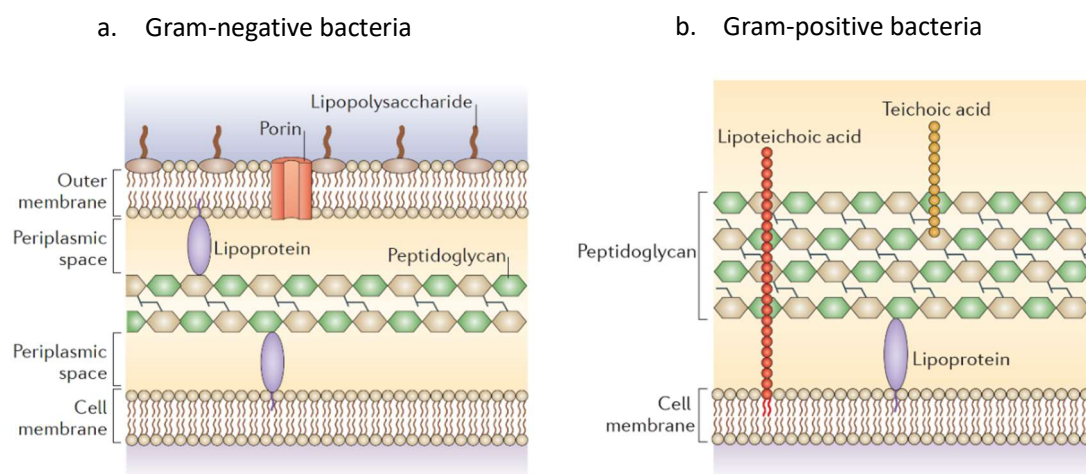


Figure 3. The cell wall structures of gram-negative bacteria (a) and gram-positive bacteria (b). Adapted with permission from Springer nature.<sup>26</sup>

### 1.3 Biosynthesis of Peptidoglycan

The biosynthesis of peptidoglycan can be divided into three overall stages. The first stage occurs in the cytoplasm. UDP-*N*-acetylmuramyl pentapeptide (UDP-MurNAc pentapeptide) is synthesised through a series of reactions starting from UDP-*N*-acetylglucosamine (UDP-GlcNAc), catalysed by UDP-*N*-acetylglucosamine enolpyruvyl transferase (MurA), UDP-*N*-acetylenolpyruvylglucosamine reductase (MurB), UDP-*N*-

acetylmuramoyl-L-alanine synthetase (MurC), UDP-*N*-acetylmuramoyl-L-alanine: D-glutamate ligase (MurD), UDP-*N*-acetylmuramoyl-L-alanyl-D-glutamate: meso-2,6-diaminopimelate ligase (MurE) and UDP-*N*-acetylmuramoyl-tripeptide-D-alanyl-D-alanine ligase (MurF).<sup>27, 28</sup> On the other hand, the combination of two molecules of (C<sub>5</sub>) isopentenyl diphosphate (IPP) and dimethylallyl diphosphate (DMAPP) leads to (C<sub>15</sub>) isoprenoid farnesyl diphosphate (FPP), which is catalysed by farnesyl diphosphate synthase (FPPS).<sup>29</sup> The synthesised FPP combines with another eight IPPs to form (C<sub>55</sub>) isoprenoid undecaprenyl diphosphate (UPP) in presence of undecaprenyl diphosphate synthase (UPPS).<sup>30</sup> After that, the cleavage of a phosphate group from UPP leads to undecaprenyl monophosphate (UP), assisted by undecaprenyl diphosphate phosphatase (UPPP) (Figure 4).<sup>31-33</sup>

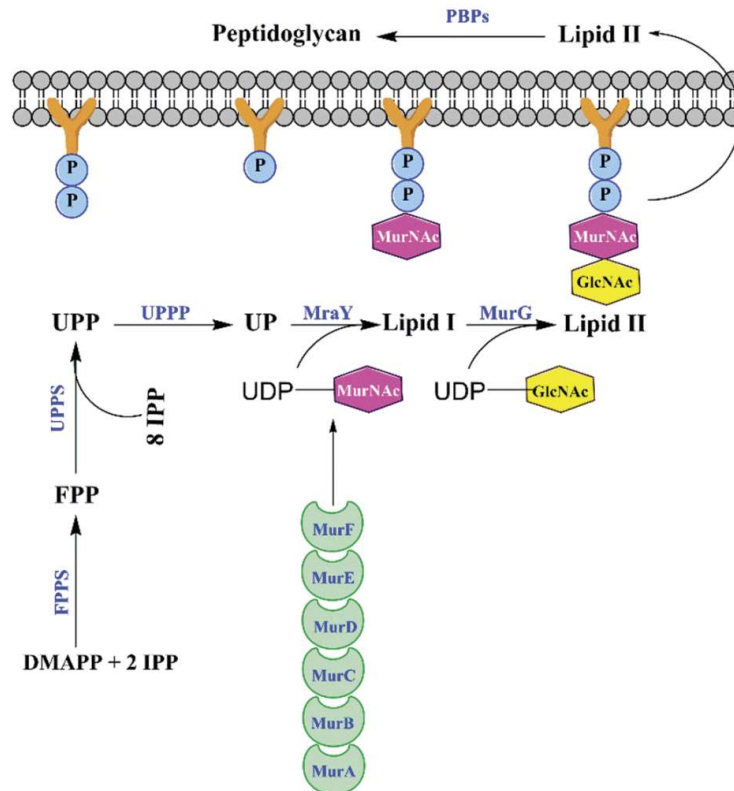


Figure 4. The simplified pathway for biosynthesis of peptidoglycan. Adapted with permission from Public Library of Science.<sup>32</sup>

In the second stage, phospho-MurNAc-pentapeptide translocase (MraY) catalyses the reaction of UP and UDP-*N*-acetylmuramyl pentapeptide at the inner leaflet of the inner membrane to form MurNAc-(pentapeptide)-pyrophosphoryl-undecaprenol (lipid I).<sup>34</sup> The addition of GlcNAc from UDP-GlcNAc to lipid I, catalysed by UDP-*N*-acetylglucosamine-*N*-acetylmuramoyl-(pentapeptide) pyrophosphoryl undecaprenol *N*-acetylglucosamine transferase (MurG), yields GlcNAc- $\beta$ -(1,4)-MurNAc-(pentapeptide)-pyrophosphoryl-undecaprenol (lipid II), the substrate of polymerisation in the final step (Figure 5).<sup>22</sup>

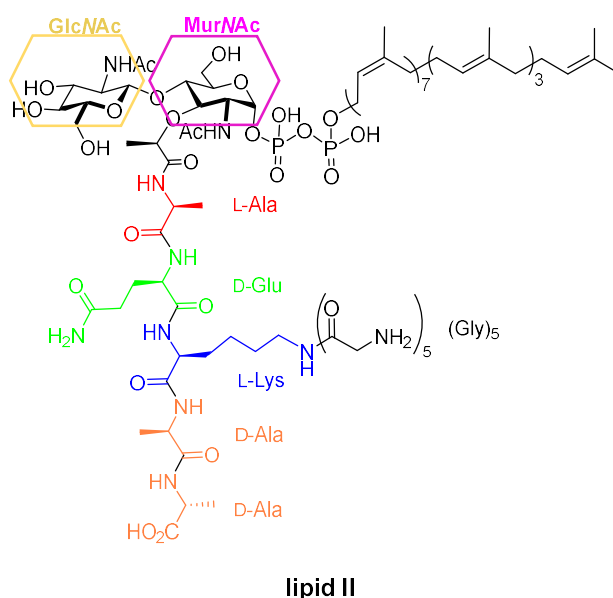


Figure 5. The chemical structure of lipid II (*Staphylococcus aureus*).

The final stage of the biosynthesis of peptidoglycan proceeds in two steps: the polymerization of the disaccharide phospholipid lipid II to form the glycan chains of alternating *N*-acetylglucosamine (GlcNAc) and *N*-acetylmuramic acid (MurNAc) (transglycosylation) and the cross-linking between glycan chains (transpeptidation),

which take place at the outer side of the cytoplasmic membrane.<sup>35</sup>

During transglycosylation, the pyrophosphate bond between the undecaprenyl group and MurNAc is split by a transglycosylase and the reducing end of MurNAc is likely to transfer to the hydroxyl group at C-4 carbon of GlcNAc to form a glycosidic bond (Figure 6).<sup>36</sup> The released undecaprenyl pyrophosphate is dephosphorylated and ready to join in a new round of synthesis.<sup>22</sup> The exact mechanism of transglycosylation process is still not known.

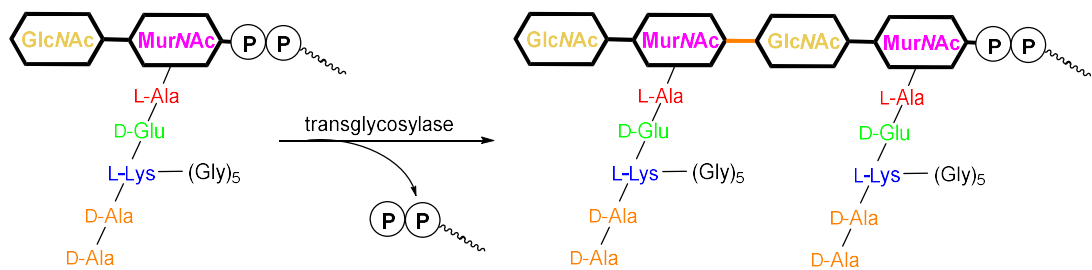


Figure 6. Transglycosylation involved in the biosynthesis of bacterial peptidoglycan (*Staphylococcus aureus*).

In the transpeptidation step, the transpeptidase/PBP binds to the donor peptide strand and allows the serine attack and the cleavage of D-Ala-D-Ala bond of peptide stem, releasing the terminal D-Ala.<sup>37</sup> The resulting enzyme-substrate intermediate is then transferred to an accepter peptide, which varies between different bacteria, and releases the PBP enzyme.<sup>38</sup> In the case of *Staphylococcus aureus*, D-Ala of the donor peptide is transferred to the last amino acid of the pentaglycine cross bridge of the accepter to form a new peptide bond (Figure 7).<sup>22</sup> Many antibiotics kill bacteria by

inhibiting transpeptidation such as  $\beta$ -lactams.

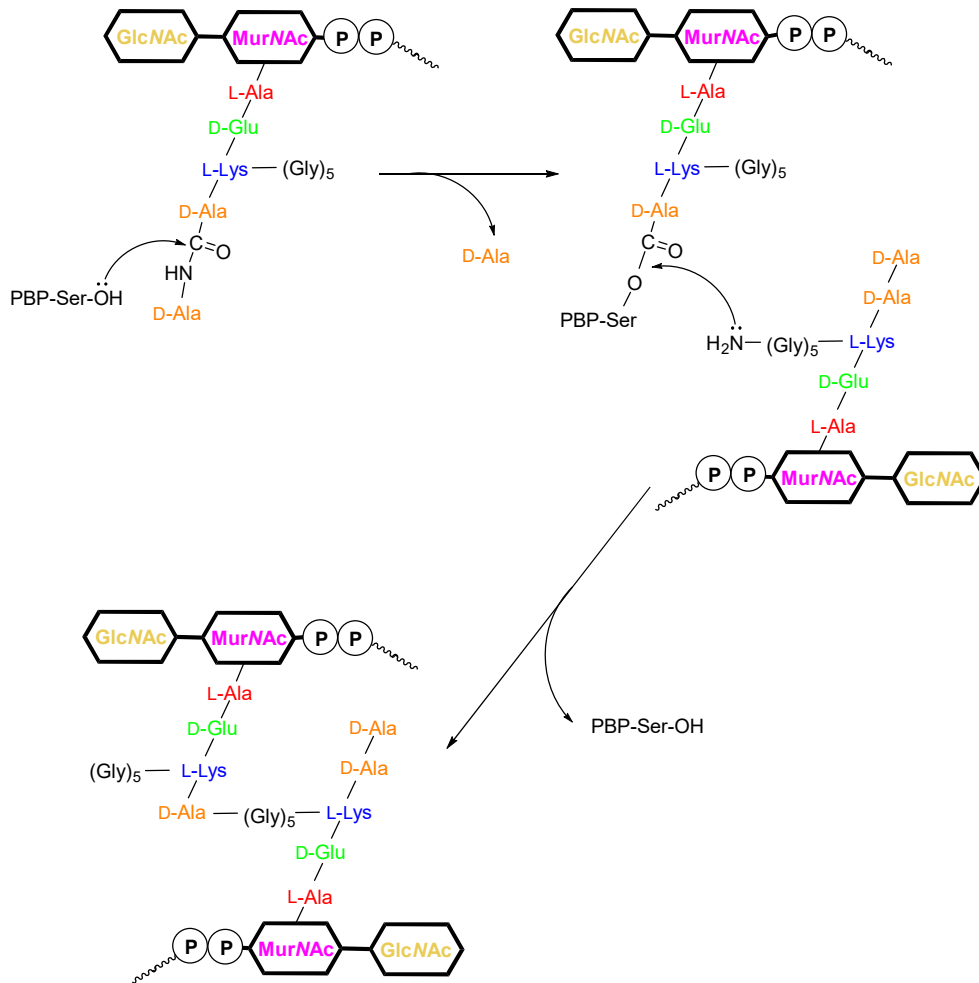


Figure 7. Details of transpeptidation involved in the biosynthesis of bacterial peptidoglycan (*Staphylococcus aureus*).

## 1.4 Penicillin-Binding Proteins

### 1.4.1 Function

Penicillin-binding proteins (PBPs) are membrane-associated macromolecules and play key roles in the cell wall synthesis process. In the final stage of the extracellular biosynthesis of peptidoglycan, PBPs catalyze the polymerization of the glycan strand of the disaccharide phospholipid lipid II (transglycosylation) and the cross-linking between glycan chains (transpeptidation).<sup>39, 40</sup>

In addition, some PBPs take part in DD-carboxypeptidation, hydrolysing the last D-alanine (D-Ala) of stem pentapeptides. Some PBPs take part in endopeptidation to hydrolyse the peptide bond connecting two glycan strands, the reverse activity of transpeptidation.<sup>41, 42</sup> For instance, PBP5 is a DD-carboxypeptidase that removes the terminal D-Ala from pentapeptide side chains; PBP4 and PBP7 are endopeptidases that cleave cross-linked side chains of tetrapeptide subunits (Figure 8).<sup>42, 43</sup>

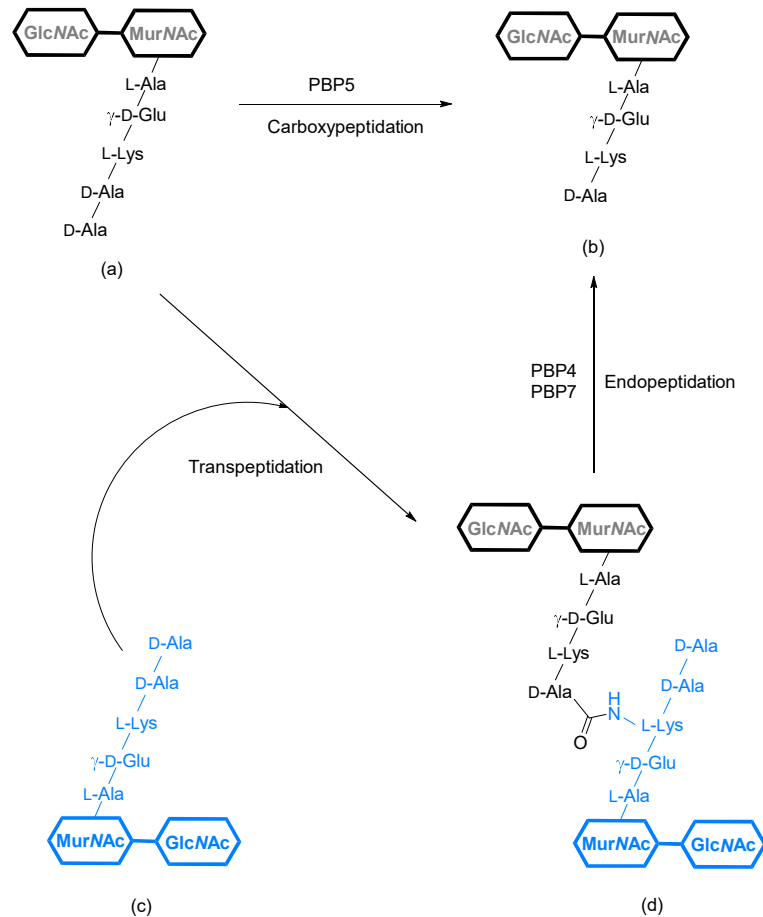


Figure 8. Activities of different PBPs on peptidoglycan subunits. The acyl-enzyme (a) has two possible routes: carboxypeptidation, releasing the shortened peptidoglycan strand (b), or cross-link formation with an acceptor strand from a neighboring peptidoglycan polymer (c) which provides the amino group for transpeptidation. Endopeptidases cleave cross-linked side chains (d) during peptidoglycan synthesis.

### 1.4.2 Classification

The PBP family is divided in three classes A, B and C (Table 1). Class A and B are high-molecular mass PBPs which are multimodular PBPs responsible for peptidoglycan polymerization and insertion into pre-existing cell wall.<sup>44</sup> Class A PBPs are bifunctional enzymes with transglycosylase and transpeptidase activities such as PBP1a and PBP1b from *Streptococcus pneumoniae*.<sup>45</sup> The N-terminal domains of class B PBPs act only as transpeptidases such as PBP2a from *Staphylococcus aureus*.<sup>46</sup> Class C PBPs are low-

molecular mass PBPs and generally act as DD-carboxypeptidases and endopeptidases, such as PBP4, PBP5 from *Escherichia coli* and PBP7 from *Mycobacterium tuberculosis* mentioned above.<sup>13, 44, 47</sup>

Table 1. Classification of PBPs

Classification	Characteristics	Examples
<b>Class A</b>	high-molecular mass bifunctional enzymes: transglycosylases and transpeptidases	PBP1a and PBP1b ( <i>Streptococcus pneumoniae</i> )
<b>Class B</b>	high-molecular mass transpeptidases	PBP2a ( <i>Staphylococcus aureus</i> )
<b>Class C</b>	low-molecular mass DD-carboxypeptidases and endopeptidases	PBP4 and PBP5 ( <i>Escherichia coli</i> ) PBP7 ( <i>Mycobacterium tuberculosis</i> )

## 1.5 *Staphylococcus aureus*

*Staphylococcus aureus* (*S. aureus*) is a gram-positive bacterium, which can cause many diseases, ranging from the most common skin infections to life-threatening systemic and chronic infections, such as septicemia, endocarditis, pneumonia and osteomyelitis.<sup>48, 49</sup> Of greater concern is methicillin-resistant *S. aureus* (MRSA) which was first reported in a British hospital but rapidly spread all over the world.<sup>50</sup> Further, because of the resistance to multiple antibiotics, there are limiting treatment options for MRSA.<sup>51</sup>

Typical first-line treatment of severe MRSA infection includes vancomycin or linezolid (Figure 9).<sup>52</sup> However, these antibiotics have limitations. Reduced susceptibility or microbial resistance to vancomycin has emerged in some common pathogenic organisms, such as vancomycin-intermediate *S. aureus* (VISA), hetero-resistant vancomycin-intermediate *S. aureus* (hVISA) and vancomycin-resistant *S. aureus* (VRSA).<sup>53</sup> These resistant strains are associated with increased morbidity and mortality, even higher than that caused by methicillin-sensitive *Staphylococcus aureus* (MSSA).<sup>54</sup> Despite linezolid being effective against MRSA, it is bacteriostatic and its long-term use potentially leads to the development of peripheral neuropathy, thrombocytopenia and myelosuppression.<sup>55</sup>

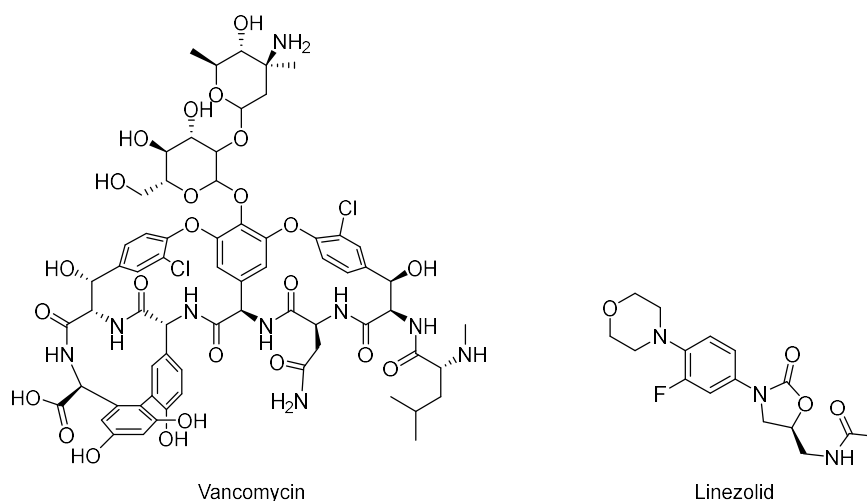


Figure 9. The structure of vancomycin (left) and linezolid (right).

Four PBPs are located in *S. aureus*: PBP1, PBP2, PBP3 and PBP4. Only PBP2 is Class A bifunctional enzyme with both transglycosylase and transpeptidase activities, which is located at the septum.<sup>56</sup> PBP1 and PBP3 are Class B monofunctional enzymes with high-molecular weight, that take part in transpeptidation. PBP4 is only low-molecular mass

PBP (Class C).<sup>57</sup> Both PBP1 and PBP2 are essential for *S. aureus* growth which means PBP3 and PBP4 are non-essential. Receiving the most attention, PBP2a is specific for MRSA, which confers resistance to  $\beta$ -lactam antibiotics by allosteric gating of its active site.<sup>58</sup>

## 1.6 Molecular Imaging Probes

In spite of remarkable advances in chemistry and biology, small molecule drug discovery remains a slow, costly and low-yielding activity, and productivity has fallen in recent years.<sup>59</sup> Molecular imaging, defined as the *in vivo* visualization, characterization and measurement of biological processes at the cellular and molecular level, takes advantage of traditional diagnostic imaging techniques, so that can reduce the workload and enhance the efficiency of the drug development.<sup>60, 61</sup> As a key component of molecular imaging, the molecular imaging probe is expected to proceed clinical translation, which must be able to specifically reach the target of interest *in vivo* and remain long enough to be detected.<sup>62</sup>

A molecular imaging probe typically consist of a targeting moiety, a signal agent and a linker to connect them (Figure 10). The targeting moiety is broadly considered as any target ligand including small molecules, proteins and nanoparticles, which can interact with the specific targets or biomarkers during the biological process. The signal agents

usually produce the signals for imaging purpose, such as the positron-emitting radionuclides (e.g.  $^{18}\text{F}$ ,  $^{131}\text{I}$  and  $^{90}\text{Y}$ ) in the positron emission tomography (PET) imaging probe and the fluorescent molecules (e.g. fluorescein and BODIPY) in the optical imaging.<sup>63-66</sup> The middle linker effectively minimize the interaction between the targeting moiety and the signal agent. It possesses a more significant function to modify the pharmacokinetics of the imaging probe mainly by altering the length, flexibility, hydrophilicity or charges.<sup>62, 67</sup>



Figure 10. The model of the molecular imaging probe.

### 1.6.1 Fluorescent Derivative of Moenomycin A

New antibiotics, such as  $\beta$ -lactam antibiotics and vancomycin, have been developed which are focused on targets involved in the cell wall synthesis and remodelling.<sup>13, 68</sup> However, most of these antibiotics work as inhibitors of peptidoglycan transpeptidation, and the direct inhibition of transglycosylation activity has so far not been exploited.<sup>69</sup> Moenomycin A is known to bind to the active site of bacterial peptidoglycan glycosyltransferases and inhibits cell wall biosynthesis.<sup>70</sup> It is potentially useful to study the mechanism of the transglycosylation reaction and discover other structural classes of molecules that target the same active site.



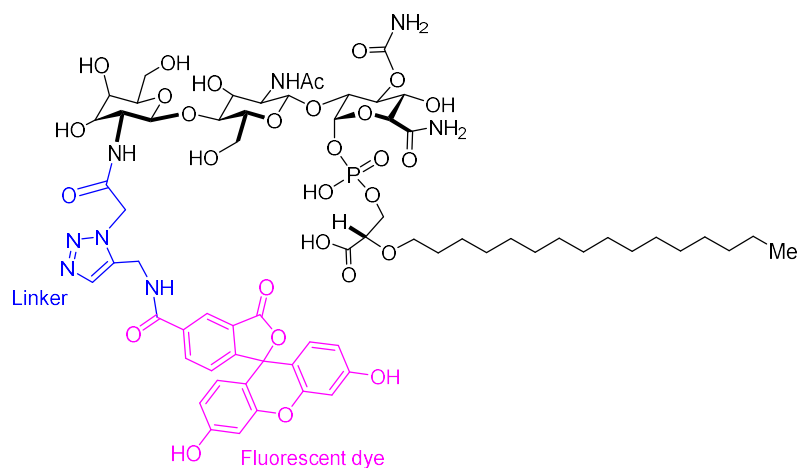


Figure 12. The structure of the truncated fluorescent analogue of moenomycin.

### 1.6.2 Fluorescent Beta-lactone Probes

$\beta$ -Lactam antibiotics are commonly regarded as a class of the most clinically effective antibiotics to inhibit PBP transpeptidation which leads to cell lysis and treatment of bacterial infections.<sup>73</sup> The fluorophore-labelled penicillin (Figure 13) has been used in a standard strategy to study the catalytic activity of the PBPs. However, penicillin-based compounds label all PBPs, so the discrete characterization of individual PBP homologues is still difficult to achieve.<sup>74, 75</sup>

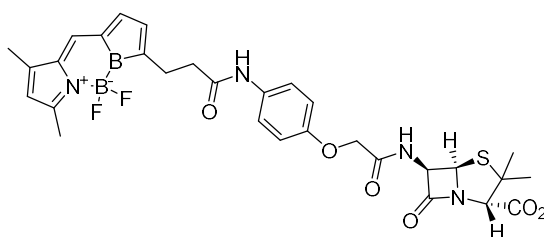


Figure 13. The structure of fluorophore-labelled penicillin.

To overcome this difficulty, S. Sharifzadeh *et al.* identified a comparatively simple  $\beta$ -lactone scaffold that can be applied to develop PBP-selective imaging reagents.<sup>76</sup> These new lactone probes were examined for the bioactivity of inhibiting the functions of PBPs in *S. pneumoniae*, an ovoid-shaped gram-positive bacteria that causes serious diseases such as pneumonia, bacteremia and meningitis.<sup>75</sup>

Among these identified  $\beta$ -lactone antibiotics, the fluorescein-functionalised probe **1** labelled PBP1b and PBP2x in *S. pneumoniae*. Remarkably, the probe **2** only labelled PBP2x in *S. pneumoniae* and the derivative **3** could label PBP1b, PBP2x, and PBP2b. With the linker and dye, the MICs of probes **2** and **3** were tested to be 80  $\mu\text{g}/\text{mL}$  against *S. pneumoniae*, much lower than the MIC of the parent natural  $\beta$ -lactone antibiotic SQ 26,517, which is 500  $\mu\text{g}/\text{mL}$  (Figure 14).<sup>74, 76</sup>

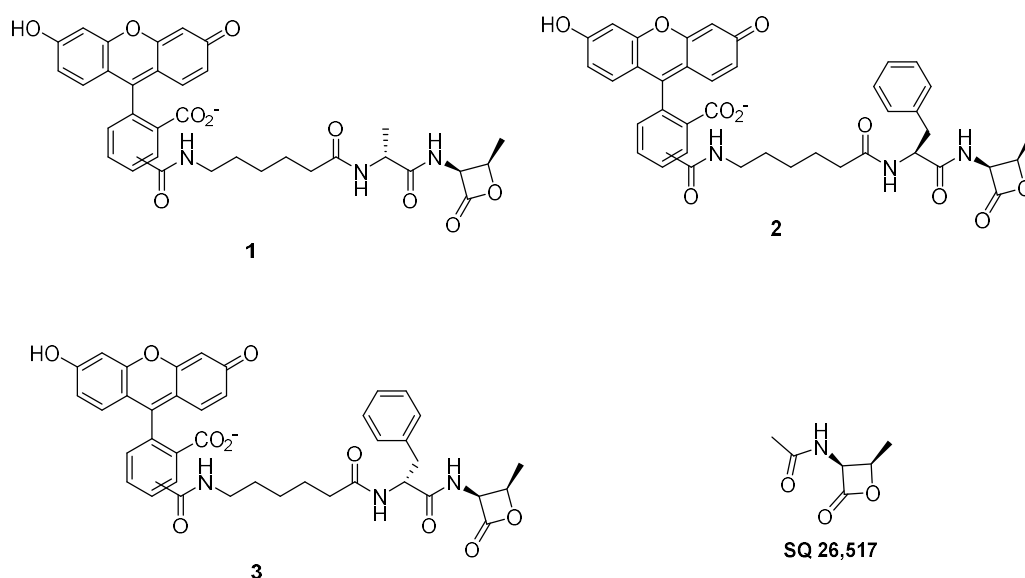


Figure 14. The structures of fluorescent  $\beta$ -lactone probes and SQ 26,517

These fluorescent  $\beta$ -lactone probes provided an effective way to monitor PBP2x and PBP2b activity in live *S. pneumoniae*. Using these probes, it was found that PBP2b and PBP2x colocalize as a single ring in early division. During the middle to late division, PBP2x stay at the central septal site while PBP2b remains at the outer division ring.<sup>74</sup> The research finding highlights the importance of the developing PBP-selective probes.

## 1.7 Project Aims

The rapid emergence and worldwide spread of infections caused by antibiotic resistant bacteria represents a serious health threat. The identification and development of new and efficient antibiotic classes is scarce. New chemical tools for imaging and tracking biological systems is critical to our future understanding of the bacteria world, which affect medicine and human health.

The purpose of this project is to develop fluorescent chemical probes which are used to study the behaviour of antibiotic resistance. Specifically, this work studies the antibiotic interaction and function with peptidoglycan at the molecular level. This is achieved by preparing novel antibiotics and fluorescent chemical probes, and investigating the activity with superbug methicillin-resistant staphylococcus aureus. The chemical probes will be designed based on transglycosylase inhibitor thiazolidinone **4** and PBP inhibitor quinazolinone **5**, and MICs will be tested to confirm their antibiotic activity. In addition, this project will also try to design and synthesise new cyclic phosphonates **6** which are supposed to inhibit nucleophilic serine and zinc-dependent  $\beta$ -lactamases as well as PBPs (Figure 15).

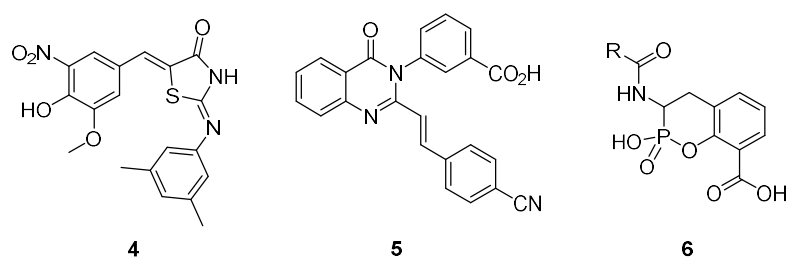


Figure 15. The structures of thiazolidinone **4**, quinazolinone **5** and cyclic phosphonates **6**.

## Chapter 2 Thiazolidinone Synthesis and Analysis

### 2.1 Moenomycins and Thiazolidinone in the Literature

#### 2.1.1 Moenomycins

Although the mechanism of the transpeptidation reaction is reasonably well understood, the active site of the transglycosylase is still unknown, and the mechanism of the transglycosylation step is largely unexplored.<sup>77</sup> Moenomycins are the only known group of antibiotics that directly inhibit bacterial peptidoglycan glycosyltransferases. They are classified as phosphoglycolipid natural products based on the chemical structure, containing 3-phosphoglyceric acid, a unique structural element among bacterial secondary metabolites.<sup>78</sup> The majority of known moenomycin-type natural products were discovered by the end of the 1970s but exact structures have been determined only for some members of the family.<sup>72</sup> Moenomycin A, the founding member of the moenomycin family, was first described in 1965. Its structure has been determined, consisting of a highly functionalized pentasaccharide attached via a unique phosphoglycerate linkage to an isoprenoid chain (Figure 16).<sup>72, 78</sup>

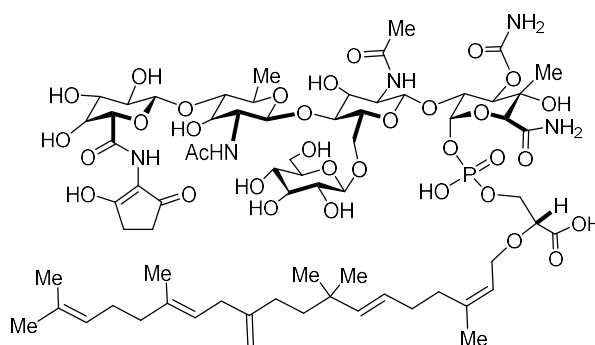


Figure 16. Structure of moenomycin A

The moenomycins are potent antibiotics. For instance, the minimal inhibitory concentration (MIC) of moenomycin A against various gram-positive bacteria ranges from 1 ng/mL to 100 ng/mL, which is over 10-1000 times more effective than vancomycin.<sup>71</sup> Despite impressive antibiotic activity, their clinical use in humans is prevented because of suboptimal pharmacology.<sup>79</sup> The 25-carbon lipid tail is suggested to make moenomycins very stable detergent-like molecules that tend to aggregate in aqueous solutions and partition into membranes. The amphiphilic nature results in moenomycins having a long half-life in the bloodstream, and ultimate hemolytic activity and poor oral bioavailability.<sup>72</sup>

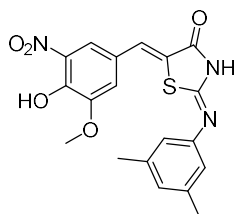
Nevertheless, moenomycins were successfully commercialized as animal growth promoters, under the trade names Flavomycin and Flavophospholipol.<sup>80</sup> Concerns have been raised of the wide use of antibiotics in animal nutrition might put these compounds into natural habitats where antibiotic resistance was primarily evolved, and eventually narrow down the options for treating human diseases.<sup>81</sup> As a result, in 1985, all animal feed antibiotic additives were banned in Sweden and in 2006, this ban came into effect in the entire territory of the European Union.<sup>82</sup> However, during the long-term use, there was no report of animal microflora that showed significant resistance to moenomycins. Flavomycin is still approved as an animal growth promoter in the USA and many other countries for cattle, swine and poultry.<sup>83</sup>

### 2.1.2 Thiazolidinone

With the truncated moenomycin derivative probe (described in section 1.6.1), Gampe group was able to identify low-micromolar inhibitors of peptidoglycan transglycosylase enzymes. Compared with moenomycin A, the affinity of the simplified probe to transglycosylases was attenuated, but the binding was tight enough to discover transglycosylase inhibitors in the displacement assay.<sup>84</sup>

110,000 Compounds of the ICCB library collection at Harvard Medical School were screened to test the binding affinity to *S. aureus* SgtB. Thiazolidinone **4** was discovered to bind to the active sites of transglycosylases, not only *S. aureus* SgtB, but also other transglycosylases used in the study including *S. aureus* PBP2, *E. faecalis* PBP2a and *E. coli* PBP1b. The antibiotic activity of thiazolidinone **4** was confirmed by MIC tests. It inhibits both MSSA and MRSA at the concentration of 16  $\mu\text{g/mL}$  and the MIC against *B. anthracis* is 4  $\mu\text{g/mL}$  (Table 2).<sup>84</sup>

Table 2. Structure and MIC Results of Thiazolidinone **4**



**4**

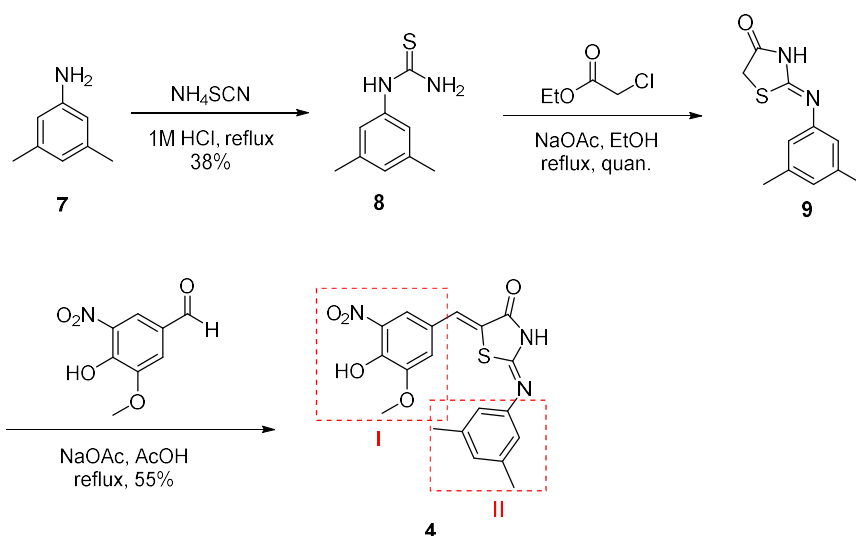
Entry	MIC ( $\mu\text{g/mL}$ )
<i>S. aureus</i> ATCC 29213 (MSSA)	16
<i>S. aureus</i> USA 300 (MRSA)	16
<i>B. anthracis</i> ANR-1	4

The discovery of transglycosylase inhibitor, thiazolidinone **4**, provides the idea to develop fluorescent chemical probes based on this small molecule, investigating the mechanism of peptidoglycan transglycosylation.

## 2.2 Synthesis and MIC Testing of Thiazolidinone

The project to prepare thiazolidinone probes started with the synthesis of 2-[(3,5-dimethylphenyl)amino]-5-[(4-hydroxy-3-methoxy-5-nitrophenyl)methylene]-4(5*H*)-thiazolone **4**. When thiazolidinone **4** was made successfully and tested to confirm the bioactivity, the appropriate linker and fluorescent agent could be added subsequently to develop new chemical probes.

The first step in the synthesis of thiazolidinone **4** was to couple 3,5-dimethylaniline **7** with ammonium thiocyanate in 1M HCl (Scheme 1). A precipitate of thiourea **8** was obtained in 38% yield. This was then reacted with ethyl chloroacetate giving rise to thiazolone **9**, followed by the condensation with 5-nitrovanillin to give the target compound **4** in 55% yield.



Scheme 1. Synthetic route to 2-[(3,5-dimethylphenyl)amino]-5-[(4-hydroxy-3-methoxy-5-nitrophenyl)methylene]-4(5*H*)-thiazolone **4**.

From Tan and Thenmozhiyal's studies about phenylmethylenethiohydantoin, the  $^1\text{H}$  NMR chemical shift of the olefinic proton of *Z* isomer (6.40 – 7.40 ppm) is higher than that of *E* isomer (5.80 – 6.30 ppm).<sup>85, 86</sup> The experimental data from the  $^1\text{H}$  NMR spectra of thiazolidinone **4** showed the diagnostic olefinic proton was at 7.20 ppm which was in the range of the *Z* form. Therefore, the geometrical isomerism of thiazolidinone **4** was more likely to be *Z* form, which was confirmed by X-ray crystallography (Figure 17).

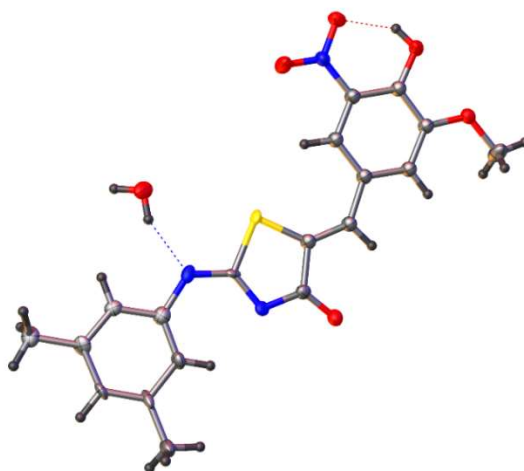


Figure 17. Crystal structure of thiazolidinone **4** along with a water molecule.

The antibiotic activities of thiazolone **9** and thiazolidinone **4** were tested by determining the MIC of each. If the intermediate thiazolone **9** had shown significant antibiotic activity, this relatively simple molecule would have been chosen to develop thiazolone probes. However, it did not inhibit the growth of MSSA (methicillin-sensitive *Staphylococcus aureus*) SH1000 at the concentration up to 120 µg/mL, and the OD<sub>600</sub> values were over 2.5 at the concentration equal or lesser than 120 µg/mL. The activity of thiazolidinone **4** was observed to be 8 µg/mL against *Bacillus subtilis* (Table 3, Figure 18). The new chemical probes in the project were prepared in small scales, therefore their antimicrobial susceptibility was tested by broth microdilution in 96-well microplates instead of 5 mL tubes. For consistency, the activity of thiazolidinone **4** against *Staphylococcus aureus* SH1000 was tested in 96-well microplates and the MIC was established to be 16 µg/mL (Table 4).

Table 3. OD<sub>600</sub> Results of Thiazolidinone **4** against *Bacillus subtilis*

Con. Entry	0*	0.5 µg/mL	1 µg/mL	2 µg/mL	4 µg/mL	8 µg/mL	16 µg/mL	32 µg/mL	32 µg/mL (no bacteria)	Nutrient Broth**
<b>4</b>	2.160	2.253	2.277	2.307	2.287	0.346	0.074	0.160	0.121	0.000

\*There were bacteria and nutrient broth in the tube. No thiazolidinone **4** was added. \*\* There was only nutrient broth in the tube. No bacteria and thiazolidinone **4** were added.

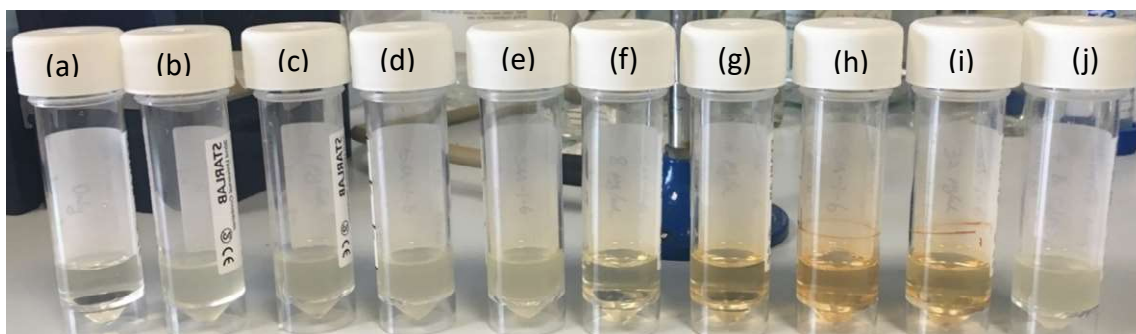


Figure 18. MIC result of thiazolidinone **4** against *Bacillus subtilis*. (a) There was only nutrient broth in the tube. (b) The concentration of thiazolidinone **4** was 0.5  $\mu\text{g/mL}$ . (c) The concentration of thiazolidinone **4** was 1  $\mu\text{g/mL}$ . (d) The concentration of thiazolidinone **4** was 2  $\mu\text{g/mL}$ . (e) The concentration of thiazolidinone **4** was 4  $\mu\text{g/mL}$ . (f) The concentration of thiazolidinone **4** was 8  $\mu\text{g/mL}$ . (g) The concentration of thiazolidinone **4** was 16  $\mu\text{g/mL}$ . (h) The concentration of thiazolidinone **4** was 32  $\mu\text{g/mL}$ . (i) There were thiazolidinone **4** and nutrient broth in the tube. No bacteria were added. (j) There were bacteria and nutrient broth in the tube. No thiazolidinone **4** was added.

Table 4. OD<sub>600</sub> Results of Thiazolidinone **4** against *Staphylococcus aureus* SH1000

Con. Entry	0*	0.25 $\mu\text{g/mL}$	0.5 $\mu\text{g/mL}$	1 $\mu\text{g/mL}$	2 $\mu\text{g/mL}$	4 $\mu\text{g/mL}$	8 $\mu\text{g/mL}$	16 $\mu\text{g/mL}$	32 $\mu\text{g/mL}$	64 $\mu\text{g/mL}$	128 $\mu\text{g/mL}$	TSB**
<b>4</b>	0.943	0.928	0.918	0.923	0.892	0.642	0.260	0.083	0.092	0.128	0.100	0.000

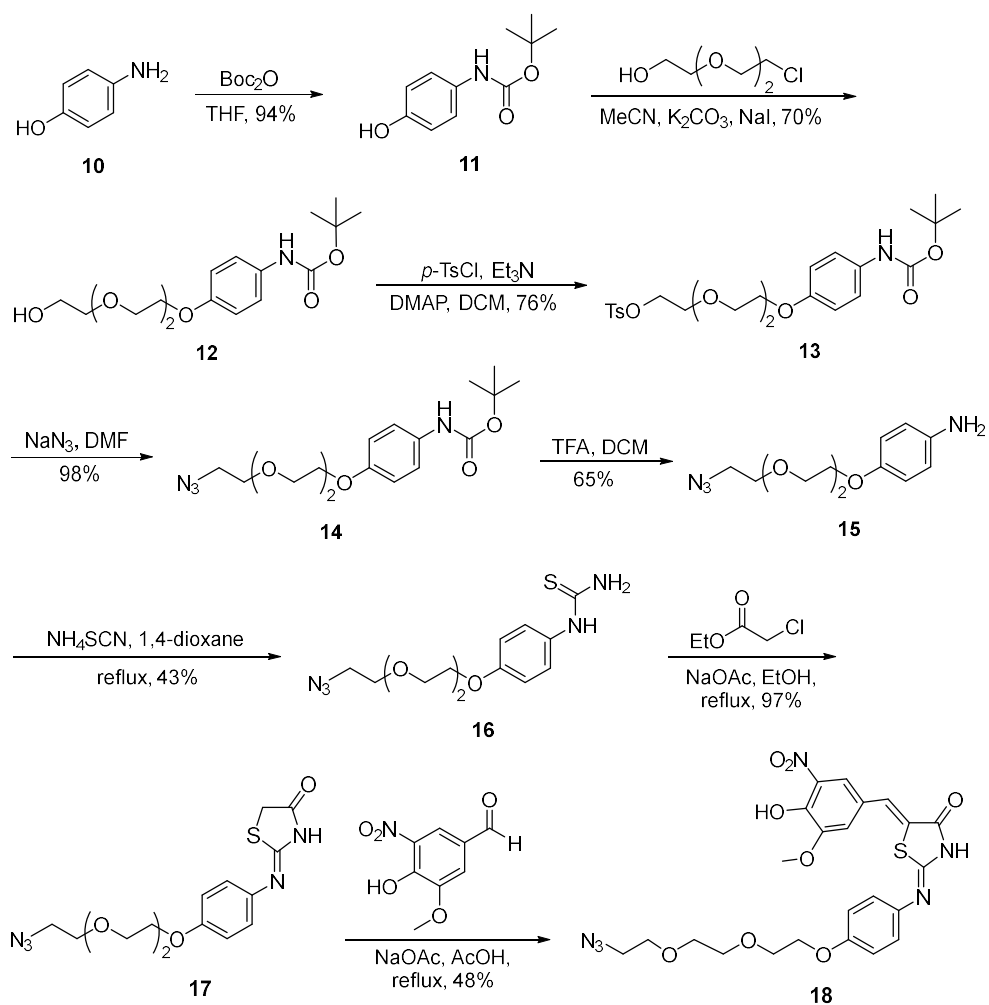
\*There were bacteria and TSB in the microplates. No thiazolidinone **4** was added. \*\* There was only TSB in the microplates. No bacteria and thiazolidinone **4** were added.

### 2.3 Synthesis and MIC Testing of Thiazolidinone Probe I

Since the small molecule thiazolidinone **4** showed good antibiotic activity, the next step was to design and synthesise corresponding thiazolidinone probes by addition of an azido polyethylene glycol (PEG) linker, where the fluorescent dye could be attached later by click chemistry. The synthesis of thiazolidinone probe I started from commercial 4-aminophenol **10**. A regioselective protection was conducted in a solution of THF by slow addition of the readily available di-*tert*-butyl dicarbonate. Thin layer chromatography

(TLC) indicated consumption of the starting material and a single product **11** was obtained in 94% yield (Scheme 2). The Boc protected aminophenol **11** was reacted with 2-[2-(2-chloroethoxy)ethoxy]ethanol to give polyether **12** followed by reaction with *p*-toluenesulfonyl chloride catalysed by 4-dimethylaminopyridine leading to tosylate **13** in good yield (76%). This tosylate **13** was converted into an azide **14** by nucleophilic substitution reaction with sodium azide (98% yield). Finally the Boc group was removed with trifluoroacetic acid to give amine **15** in 60% yield.

With the aniline **15** bearing the azido PEG linker in place, a similar strategy as described in section 2.2 was used for the synthesis of the thiazolidinone probe I **18** (Scheme 2). Ammonium thiocyanate was reacted with the aniline **15** to give the thiourea **16** (43% yield) in 1,4-dioxane instead of 1M HCl. In the presence of aq. HCl, no product was obtained which is possibly due to the poor water solubility of the materials. The thiourea **16** was cyclised with ethyl chloroacetate to form the cyclised product **17** in high yield (96%), that was converted to the target thiazolidinone **18** by Knoevenagel condensation with 5-nitrovanillin. The isolation of the thiazolidinone probe I **18** was completed by HPLC separation to give pure probe **18** in 48% yield. The <sup>1</sup>H NMR value of olefinic proton of thiazolidinone **18** was in the range of 7.15 - 7.26 ppm, located in the range of *Z* form (6.40 – 7.40 ppm),<sup>85, 86</sup> so the configuration was speculated to be *Z* isomer.



Scheme 2. Synthetic route to 2-[[4-[2-(2-azidoethoxy)ethoxy]phenyl]imino]-5-(4-hydroxy-3-methoxy-5-nitrobenzylidene)thiazolidin-4-one **18**.

The thiazolidinone probe **I 18** was tested for antibiotic activity but did not display antibacterial activity at concentrations up to 128  $\mu\text{g/mL}$  for *S. aureus* SH1000 (Table 5). Compared with the results in Table 4, although the small molecule thiazolidinone **4** showed good antibiotic activity to inhibit the growth of *S. aureus* at 16  $\mu\text{g/mL}$ , without two methyl groups and with the PEG linker at the aromatic ring II, the bioactivity of the thiazolidinone probe **I 18** decreased dramatically.

Table 5. OD<sub>600</sub> Results of Thiazolidinone Probe I **18** against *Staphylococcus aureus* SH1000

Con. Entry	0*	0.25 μg/mL	0.5 μg/mL	1 μg/mL	2 μg/mL	4 μg/mL	8 μg/mL	16 μg/mL	32 μg/mL	64 μg/mL	128 μg/mL	TSB**
<b>18</b>	0.935	0.909	0.896	0.878	0.906	0.821	0.802	0.834	0.469	0.438	0.157	0.000

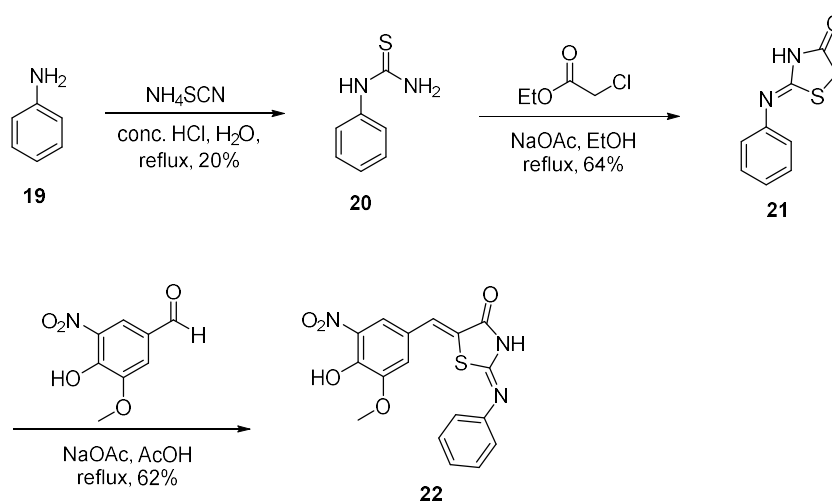
\*There were bacteria and TSB in the microplates. No thiazolidinone **18** was added. \*\* There was only TSB in the microplates. No bacteria and thiazolidinone **18** were added.

## 2.4 Structure-Activity Relationship of Thiazolidinones

The antibacterial activity result of the thiazolidinone probe I **18** indicated that the addition of the PEG linker at the aromatic ring II without the two methyl groups was not very successful. There is no report published about the relationship between the structure of the thiazolidinone and activity to help design active probes. Therefore, this was first studied before the design of new thiazolidinone probes.

A series of small molecule thiazolidinone derivatives were prepared for the study. 5-(4-Hydroxy-3-methoxy-5-nitrobenzylidene)-2-(phenylimino)thiazolidin-4-one **22** was first chosen since it lacked the two methyl groups on the aromatic ring II compared with the original thiazolidinone **4**, starting from aniline **19** (Scheme 3). Concentrated HCl was added to aniline **19** followed by ammonium thiocyanate in water, leading to thiourea **20** in 20% yield. The next step was the cyclisation of thiourea **20** and ethyl chloroacetate leading to thiazolone **21** in 64% yield. Finally, the condensation of thiazolone **21** with 5-

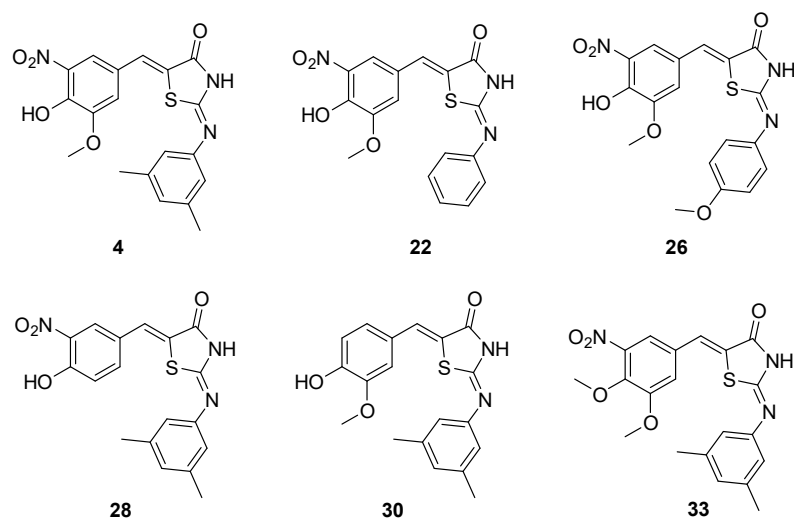
nitrovanillin gave thiazolidinone **22** in 62% yield. The  $^1\text{H}$  NMR spectra of thiazolidinone **22** showed olefinic proton was in the range of 7.48 – 7.86 ppm, which indicated that the configuration was more likely to be *Z* isomer (6.40 – 7.40 ppm) than *E* isomer (5.80 – 6.30 ppm).<sup>85, 86</sup>



Scheme 3. Synthetic route to 5-(4-hydroxy-3-methoxy-5-nitrobenzylidene)-2-(phenylimino)thiazolidin-4-one **22**.

Compared with thiazolidinone **4**, thiazolidinone **22** displayed a limited inhibitory effect against *S. aureus* SH1000 at the concentration of 64  $\mu\text{g/mL}$ , which reduced the  $\text{OD}_{600}$  from 0.808 to 0.283 but could not inhibit the growth of all bacteria (Table 6). The MIC could not be tested at a higher concentration because of the low solubility in the liquid broth required for bacterial growth, and therefore the compound may have more potent activity but this could not be confirmed.

Table 6. The OD<sub>600</sub> results of thiazolidinones against *S. aureus* SH1000

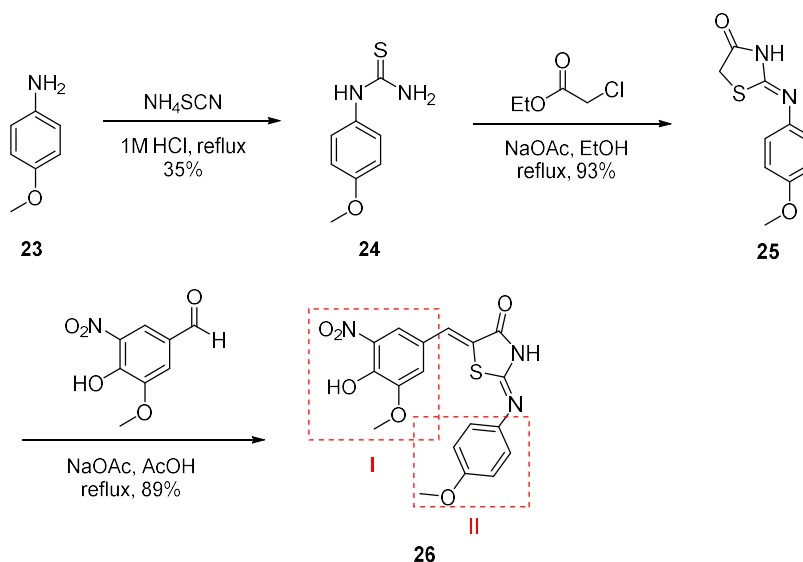


Con. Entry	0*	0.5 μg/mL	1 μg/mL	2 μg/mL	4 μg/mL	8 μg/mL	16 μg/mL	32 μg/mL	64 μg/mL	TSB**
4	0.808	0.897	0.820	0.858	0.790	0.418	0.060	0.043	0.055	0.000
22	0.808	0.866	0.782	0.819	0.763	0.777	0.428	0.359	0.286	0.000
26	0.783	0.915	0.769	0.835	0.813	0.754	0.640	0.666	0.589	0.000
28	0.790	0.973	0.876	0.902	1.011	0.982	0.956	0.952	0.920	0.000
30	0.837	0.884	0.814	0.826	0.668	0.664	0.605	0.409	0.271	0.000
33	0.779	0.850	0.724	0.774	0.719	0.700	0.677	0.861	0.663	0.000

\*No thiazolidinone compounds were added. \*\*No bacteria and thiazolidinone compounds were added.

Another thiazolidinone derivate, 5-(4-hydroxy-3-methoxy-5-nitrobenzylidene)-2-((4-methoxyphenyl)imino)thiazolidin-4-one **26**, was prepared, which replaced the two methyl groups with a single *para*-methoxy group. The synthetic route started from the reaction of *p*-anisidine **23** with ammonium thiocyanate in 1M HCl resulting in thiourea **24** in 35% yield (Scheme 4). Secondly, the cyclisation of thiourea **24** and ethyl chloroacetate gave rise to thiazolone **25** in 93% yield, followed by Knoevenagel condensation with 5-nitrovanillin to give the target compound **26** in 89% yield. Similar to thiazolidinones **4** and **22**, the <sup>1</sup>H NMR value of olefinic proton of thiazolidinone **26**

was at a high chemical shift (7.32 – 7.80 ppm), so the configuration was speculated to be *Z* isomer (6.40 – 7.40 ppm), rather than *E* isomer (5.80 – 6.30 ppm).<sup>85, 86</sup>

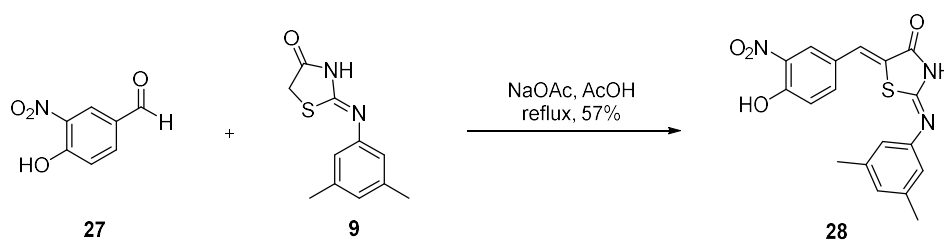


Scheme 4. Synthetic route to 5-(4-(4-hydroxy-3-methoxy-5-nitrobenzylidene)-2-(4-methoxyphenyl)imino]thiazolidin-4-one **26**.

The antibacterial activity of thiazolidinone **26** against *S. aureus* SH1000 was also tested (Table 6). Unfortunately, it was not as effective as thiazolidinone **4** and **22** in the inhibition of the growth of *S. aureus* SH1000. The electronegative oxygen attached to the aromatic ring II might reduce the inhibitory effect of compound **26**. These results demonstrated that without two methyl groups on the aromatic ring, the thiazolidinone probe I **18** was less active than thiazolidinone **4** and the addition of the PEG linker resulted in inactivity.

The substitutions on the aromatic ring I were also investigated. Thiazolidinone **29** lacks the methoxy group compared with thiazolidinone **4**. The synthesis built upon the pre-

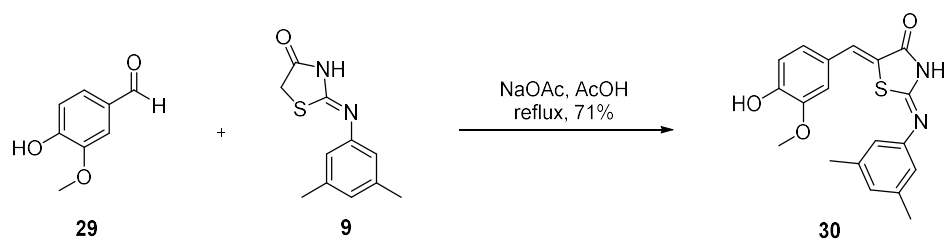
prepared thiazolone **9**. Condensation of 4-hydroxy-3-nitrobenzaldehyde **27** with thiazolone **9** led to thiazolidinone **28** in 57% yield (Scheme 5). The  $^1\text{H}$  NMR value of olefinic proton of thiazolidinone **28** was 7.34 ppm, located in the range of *Z* form (6.40 – 7.40 ppm),<sup>85, 86</sup> so the configuration was speculated to be *Z* isomer.



Scheme 5. Synthetic route to 2-((3,5-dimethylphenyl)imino)-5-(4-hydroxy-3-nitrobenzylidene)thiazolidin-4-one **28**.

However, without the methoxy group on the aromatic ring I, thiazolidinone **28** did not show any antibacterial activity against *S. aureus* SH1000 (Table 6). When 64  $\mu\text{g}/\text{mL}$  thiazolidinone **28** was added, the density of the bacteria did not decrease ( $\text{OD}_{600}$  was 0.920), compared with the culture without thiazolidinone **28** ( $\text{OD}_{600}$  was 0.790). The result indicated the importance of methoxy group for an inhibitory effect.

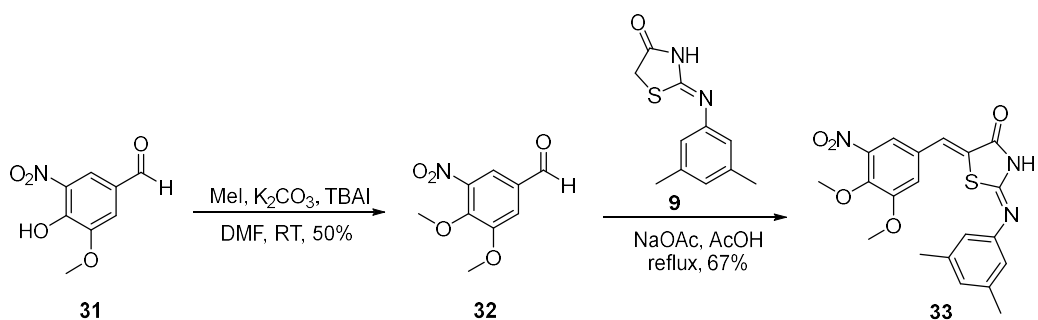
The impact of the nitro group was also investigated afterwards. 2-[(3,5-Dimethylphenyl)imino]-5-(4-hydroxy-3-methoxybenzylidene)thiazolidin-4-one **30** was prepared by condensation of vanillin **29** and thiazolone **9**, achieved in 71% yield (Scheme 6). The  $^1\text{H}$  NMR chemical shift of the olefinic proton of thiazolidinone **30** was in the range of 6.95 - 7.10 ppm, so thiazolidinone **30** was supposed to be *Z* isomer (6.40 - 7.40 ppm), rather than *E* isomer (5.80 - 6.30 ppm).<sup>85, 86</sup>



Scheme 6. Synthetic route to 2-[(3,5-dimethylphenyl)imino]-5-(4-hydroxy-3-methoxybenzylidene)thiazolidin-4-one **32**.

Thiazolidinone **30** without the nitro group is more soluble in tryptic soy broth (TSB) than other thiazolidinones. Lack of nitro group did not affect the antibacterial activity as much as lack of the methoxy group. Thiazolidinone **30** showed an inhibitory effect against *S. aureus* SH1000 but the MIC was higher than 64  $\mu\text{g/mL}$  (Table 6). When 64  $\mu\text{g/mL}$  thiazolidinone **30** was added, the  $\text{OD}_{600}$  value was 0.270, higher than 0.100, indicating that some bacteria still grew.

Since methoxy and nitro groups were necessary for antibacterial activity, the linker for the chemical probe was proposed to be added to the hydroxy group of thiazolidinone **4**. 5-(3,4-Dimethoxy-5-nitrobenzylidene)-2-((3,5-dimethylphenyl)imino)thiazolidin-4-one **33** was prepared for testing the effect on antibacterial activity through methylation of the hydroxy group. The synthesis started from methylation of 5-nitrovanillin **31** in presence of iodomethane (50% yield). Methylated 3,4-dimethoxy-5-nitrobenzaldehyde **32** was reacted with thiazolone **9** to form thiazolidinone **33** in 67% yield (Scheme 7). The  $^1\text{H}$  NMR value of olefinic proton of thiazolidinone **33** was 7.34 ppm, located in the range of *Z* form (6.40 - 7.40 ppm),<sup>85, 86</sup> so the configuration was speculated to be *Z* isomer.



Scheme 7. Synthetic route to 5-(3,4-dimethoxy-5-nitrobenzylidene)-2-[(3,5-dimethylphenyl)imino]thiazolidin-4-one **33**.

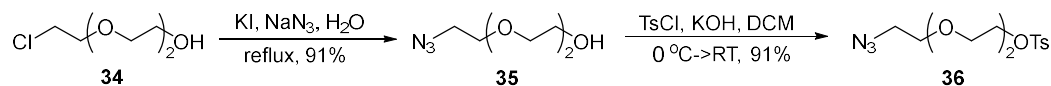
Thiazolidinone **33** did not display great antibacterial activity against *S. aureus* SH1000 (Table 6). Thus, it was not a good idea to use the hydroxy group for installation of the linker for the chemical probe.

## 2.5 Synthesis and MIC Testing of Thiazolidinone Probe II

Based on the study of relationship between structure and activity, it is difficult to improve the antibacterial activity by changing the structure of thiazolidine **4**. Therefore, the linker was proposed to be added to the methoxy group to minimize the change of structure.

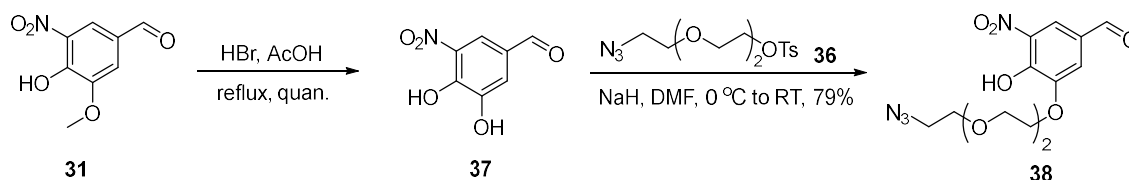
The linker for the second thiazolidinone probe was prepared from commercial 2-[2-(2-chloroethoxy)ethoxy]ethanol **34**. The first step of synthesis was azidation of alcohol **34** by sodium azide, catalysed by potassium iodide. The product 2-[2-(2-azidoethoxy)ethoxy]ethanol **35** was obtained in a high yield (91%). Subsequently, a tosyl group was introduced by reacting azidated alcohol **35** with 4-toluenesulfonyl chloride

under alkaline conditions, leading to 2-[2-(2-azidoethoxy)ethoxy]ethyl-4-methylbenzenesulfonate **36** in 91% yield (Scheme 8).



Scheme 8. Synthetic route to 2-[2-(2-Azidoethoxy)ethoxy]ethyl-4-methylbenzenesulfonate **36**.

Before adding the tosylate **36** to the aldehyde, the 5-nitrovanillin **31** was demethylated in presence of hydrobromic acid and acetic acid to form 3,4-dihydroxy-5-nitrobenzaldehyde **37** in quantitative yield. Coupling of the demethylated aldehyde **37** with the tosylate **36**, facilitated by sodium hydride, gave rise to the product **38** in 79% yield (Scheme 9).

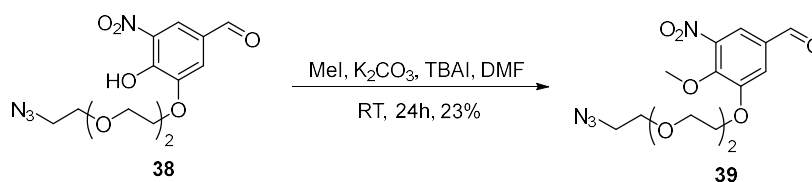


Scheme 9. Synthetic route to 3-[2-[2-(2-azidoethoxy)ethoxy]ethoxy]-4-hydroxy-5-nitrobenzaldehyde **38**.

The proton of *meta*-hydroxy group of the demethylated aldehyde **37** is more acidic than the proton of *para*-hydroxy group, so the linker **36** is more likely to be added to the *meta*-hydroxy group to form the desired product **38**. Experimental 1D  $^1\text{H}$  and  $^{13}\text{C}$  NMR spectra of the product could only confirm that the linker **36** was coupled with one of the hydroxy groups but the position on the aromatic ring I could not be determined. In addition, the

broadness of one of the aromatic proton signals really made it difficult to characterise and no useful correlations were found from 2D  $^1\text{H}$  and  $^{13}\text{C}$  NMR spectra.

The product **38** was further functionalised to identify the structure. It was methylated in presence of iodomethane, potassium carbonate and tetrabutylammonium iodide. The starting material **38** was not totally consumed, and the methylated product **39** was isolated in 23% yield, which was enough for characterisation (Scheme 10).



Scheme 10. Methylation of 3-[2-[2-(2-azidoethoxy)ethoxy]ethoxy]-4-hydroxy-5-nitrobenzaldehyde **38**.

NOE spectra of the methylated product **39** showed that one of the aromatic CH groups not only gave a NOE correlation to the aldehyde proton (9.91 ppm) but also gave a through-space NOE correlation to the first CH<sub>2</sub> group (4.31 ppm) on the linker (Figure 19). In other words, the linker was *meta* to the aldehyde group, rather than *para*, which confirmed the isolation of the desired product.

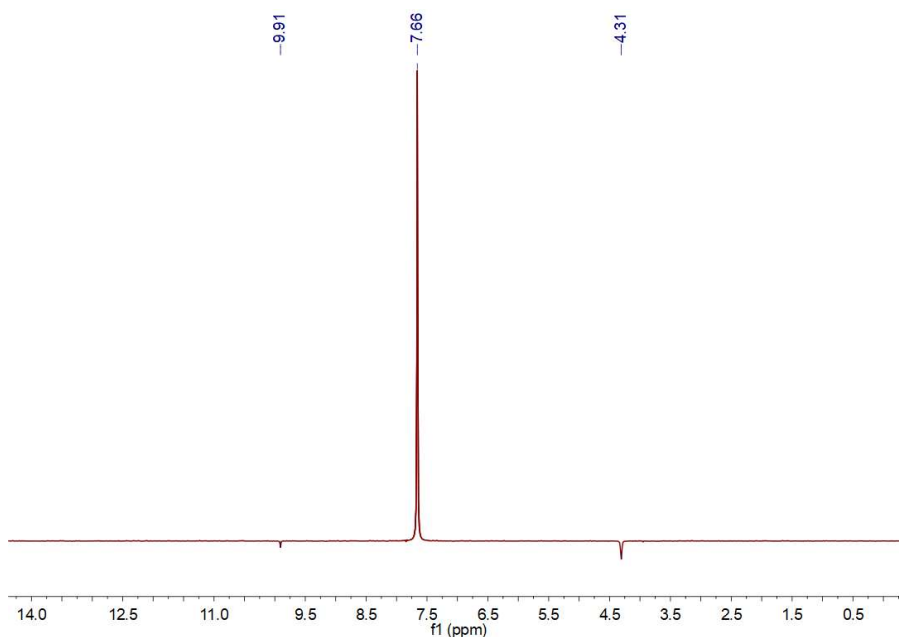
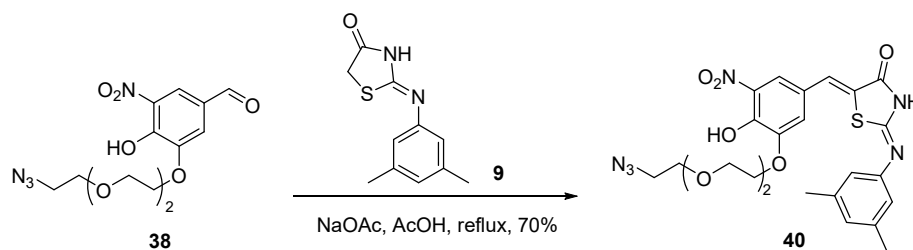


Figure 19. NOE correlations of the aromatic CH group of **39** to the aldehyde proton and the first CH<sub>2</sub> group on the linker.

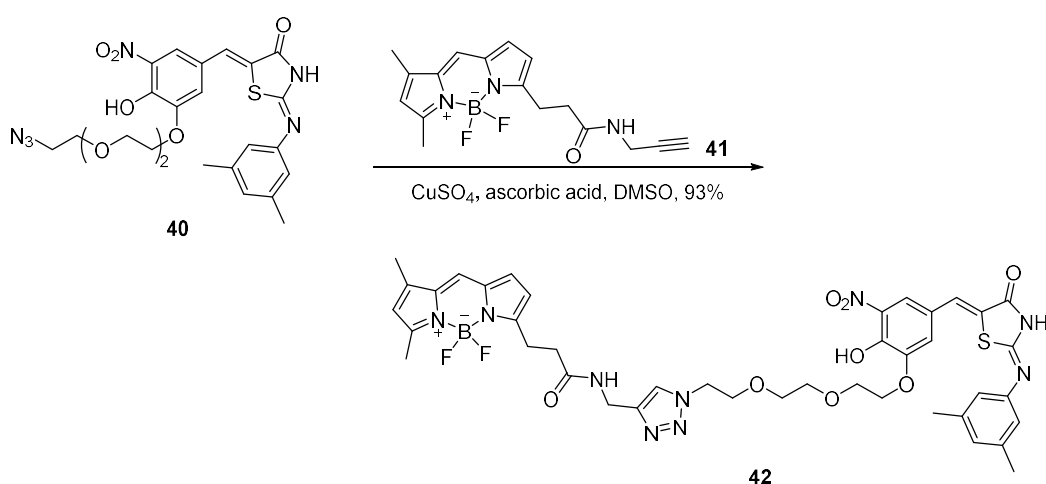
With the linker installed in aldehyde **38**, thiazolidinone **40** was synthesised by Knoevenagel condensation of aldehyde **38** with thiazolone **9** in 70% yield (Scheme 11). Similar to the thiazolidinones without the linker, the <sup>1</sup>H NMR value of the olefinic proton of thiazolidinones **40** was 7.29 ppm, so the configuration was speculated to be *Z* isomer (6.40 - 7.40 ppm), rather than *E* isomer (5.80 - 6.30 ppm).<sup>85, 86</sup>



Scheme 11. Synthetic route to 5-[3-[2-[2-(2-azidoethoxy)ethoxy]ethoxy]-4-hydroxy-5-nitrobenzylidene]-2-[(3,5-dimethylphenyl)imino]thiazolidin-4-one **40**.

When testing the antibacterial activity of thiazolidinone **40**, it was first dissolved in DMSO at the concentration of 1 mg/mL. Then the organic solution was diluted in the aqueous TSB. Again, thiazolidinone **40** encountered the solubility problem in the aqueous TSB and precipitated at a concentration of 8  $\mu\text{g/mL}$ . Thiazolidinone **40** was unable to inhibit the growth of *S. aureus* SH1000 at the concentration lower than 8  $\mu\text{g/mL}$ , and more concentrated solutions could not be tested because of the low solubility.

A charged and water soluble BODIPY dye **41** was considered to be installed on the thiazolidinone **40** to improve the solubility in TSB. Thiazolidinone probe II **42** was prepared by click reaction of thiazolidinone **40** and BODIPY dye **41**, catalysed by copper sulphate and ascorbic acid. Purification through HPLC separation gave the final product **42** in 93% yield (Scheme 12). Owing to the small amount of sample prepared, thiazolidinone probe II **42** was characterised by mass spectrometry and HPLC.



Scheme 12. Synthetic route to thiazolidinone probe II **42**.

With the charged BODIPY dye, thiazolidinone probe II **42** dissolved well in TSB. However, it did not display an inhibitory effect against *S. aureus* SH1000 at concentrations of up to 128  $\mu\text{g/mL}$  (Table 7). Addition of the linker and the dye largely reduced the affinity of thiazolidinone to the transglycosylases of *S. aureus* SH1000.

Table 7. OD<sub>600</sub> Results of Thiazolidinone Probe II **42** against *Staphylococcus aureus* SH1000

Con. Entry	0*	0.25 $\mu\text{g/mL}$	0.5 $\mu\text{g/mL}$	1 $\mu\text{g/mL}$	2 $\mu\text{g/mL}$	4 $\mu\text{g/mL}$	8 $\mu\text{g/mL}$	16 $\mu\text{g/mL}$	32 $\mu\text{g/mL}$	64 $\mu\text{g/mL}$	128 $\mu\text{g/mL}$	TSB**
<b>42</b>	0.835	0.694	0.700	0.688	0.712	0.721	0.672	0.724	0.643	0.680	0.503	0.000

\*There were bacteria and TSB in the microplates. No thiazolidinone **42** was added. \*\* There was only TSB in the microplates. No bacteria and thiazolidinone **42** were added.

Neither thiazolidinone probe I **18** or probe II **42** were active for further imaging study, but they provided the base for investigating the activity of thiazolidinones. The thiazolidinone project ended here because it was too difficult to design an effective probe based on a thiazolidinone framework. Any changes of the substitutions on the aromatic ring I of thiazolidinone **4** resulted decreasing the antibacterial activity. The electronegative oxygen on the PEG linker attached to the bottom aromatic ring also reduced the inhibitory effect of thiazolidinone. Although replacing the PEG linker with electron-donating carbon linker on the aromatic ring II might be helpful to increase the activity, the solubility in aqueous broth would become even lower, which was also unacceptable for bioactivity testing.

## Chapter 3 Quinazolinone Synthesis and Analysis

### 3.1 Quinazolinones in the Literature

Quinazolinones are non- $\beta$ -lactam antibacterials that target inhibiting PBPs, so they can circumvent the known mechanisms of resistance to  $\beta$ -lactam antibiotics and hold great promise in recourse against MRSA infections.<sup>87</sup> Recently, some 4-quinazolinone derivatives have been identified by R. Bouley *et al.* from *in silico* screening of the PBP2a active site utilizing the ZINC database containing 1.2 million drug-like compounds.<sup>87, 88</sup> High-ranking compounds were screened for antibacterial activity against the ESKAPE (*Enterococcus faecium*, *Staphylococcus aureus*, *Klebsiella pneumoniae*, *Acinetobacter baumannii*, *Pseudomonas aeruginosa* and *Enterobacter species*) panel, which led to the discovery of compound **43** (Figure 20).<sup>89, 90</sup> This compound displayed good activity against *S. aureus* ATCC 29213 with a MIC of 2  $\mu$ g/mL and modest activity against *E. faecium* (MIC of 16  $\mu$ g/mL), but did not have activity against gram-negative bacteria of the panel.<sup>87</sup>

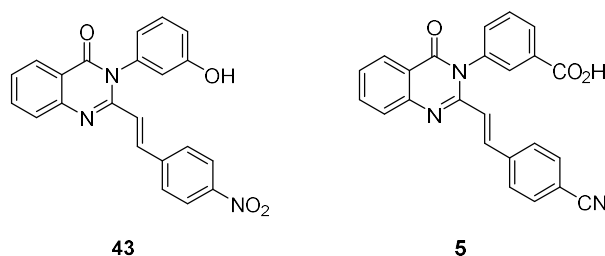


Figure 20. The structures of quinazolinone derivatives **43** and **5**.

Quinazolinone **5** was subsequently identified as a lead compound when synthesising a focused library of analogues. It displayed potent activity against *S. aureus*, including MRSA, and showed good oral bioavailability.<sup>87, 88</sup> This compound inhibits the biosynthesis of the cell wall in *S. aureus* by binding to DD-transpeptidases involved in cross-linking of peptidoglycan. This mechanism is consistent with the action of  $\beta$ -lactams which often inhibit more than one PBP.<sup>44</sup> For example, quinazolinone **5** works by inhibiting PBP1 and PBP2a in MRSA. This compound also binds to the allosteric site of PBP2a.<sup>91</sup>

To study the structure-activity relationship, more than 70 4(3*H*)-quinazolinones were synthesised by Bouley group, with potent activity against MRSA strains. For example, quinazolinones **44** and **45** exhibit excellent antibacterial activity against *S. aureus* ATCC 29213 with MICs of 0.003  $\mu\text{g}/\text{mL}$  and 0.004  $\mu\text{g}/\text{mL}$ , respectively (Figure 21).<sup>88</sup>

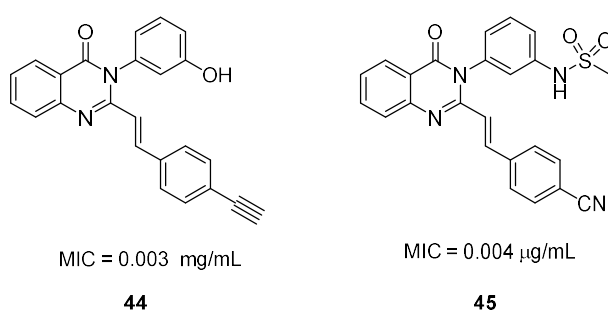
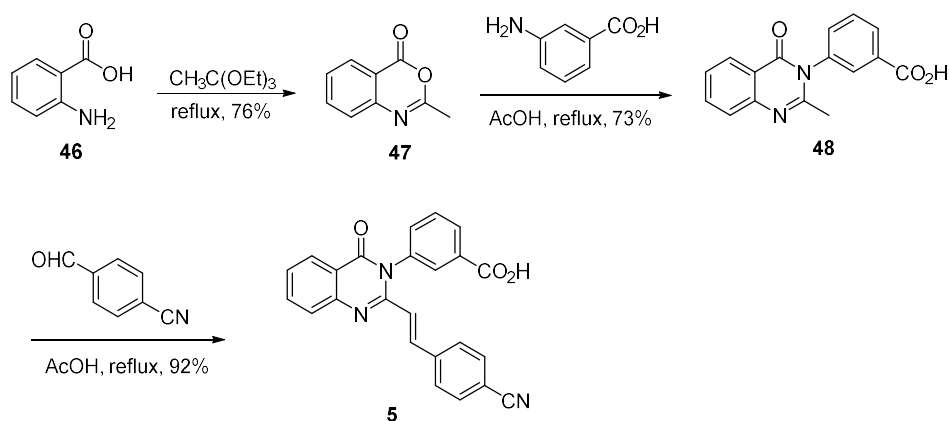


Figure 21. The structures of quinazolinones **44**, **45** and MICs against *S. aureus* ATCC 29213.

### 3.2 Synthesis and MIC Testing of Small Molecule Quinazolinones

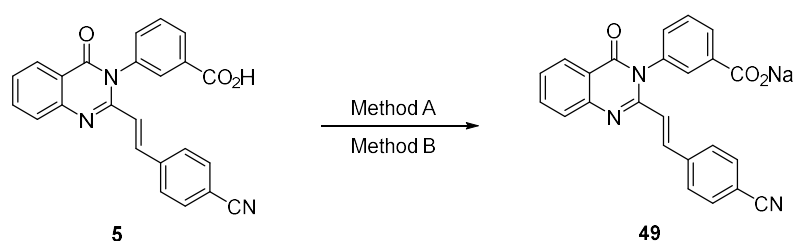
Since the antibiotic activity of quinazolinone **5** inhibited PBP1 and PBP2a in MRSA, a labelled version of this was selected as potential tool to probe cell wall biology. The small molecule quinazolinone **5** was prepared first and the antibiotic activity was confirmed by MIC testing. Secondly, the PEG linker ending with an alkyne or azide group was added followed by the click reaction with dye ATTO 488 or BODIPY.

Quinazolinone **5** was synthesised following a reported three-step synthetic route,<sup>87</sup> by cyclisation of anthranilic acid **46** and triethyl orthoacetate at 160 °C giving rise to 2-methylbenzoxazinone **47** in 76% yield. 3-Aminobenzoic acid was added to 2-methylbenzoxazinone **47** in acetic acid leading to ring-opening and ring-closing amination affording 2-methylquinazolinone **48** with a yield of 73%. In order to obtain the target quinazolinone **5**, an aldol-type condensation of the intermediate quinazolinone **48** and 4-formylbenzotrile was carried out at 130 °C to give the *E*-product **5** in 92% yield (Scheme 13). The coupling constant of the alkene protons **5** in the <sup>1</sup>H NMR spectrum is 15.5 Hz which is indicative of an *E* alkene.



Scheme 13. Synthetic route to (*E*)-3-(3-carboxyphenyl)-2-(4-cyanostyryl)quinazolin-4(3*H*)-one **5**.

The sodium salt of quinazolinone **49** was prepared afterwards in two different ways. Method A followed the reported synthetic route<sup>1</sup> to react quinazolinone **5** and sodium 2-ethylhexanoate in ethanol. The product **49** was achieved as a precipitate in 96% yield. Method B was to add NaOH to a quinazolinone **5** solution in THF which produced the sodium salt **49** in quantitative yield (Scheme 14). The second approach resulted in a slightly higher yield and was easier to conduct.



Scheme 14. Two synthetic routes to sodium (*E*)-3-(3-carboxyphenyl)-2-(4-cyanostyryl)quinazolin-4(3*H*)-one **49**. Conditions: method A: sodium 2-ethylhexanoate, EtOH, 0 °C, 96%; method B: NaOH, THF, RT, quantitative.

Both quinazolinone **5** and the sodium salt **49** showed an antibacterial effect against *S. aureus* SH1000 tested by an agar disk-diffusion method (Figure 22). This method

provides qualitative results and is commonly used for antimicrobial susceptibility testing. However, it is not appropriate for quantitatively determining MICs. Therefore, the MICs were tested afterwards by a broth dilution method, with the results indicating that the compounds were unable to inhibit the growth of *S. aureus* SH1000 in the TSB at a concentration up to 128  $\mu\text{g/mL}$  (Table 8). Based on the agar disk diffusion testing, quinazolinone **5** and the sodium salt **49** showed bioactivity, however they were not very effective and could not kill *S. aureus* SH1000 in the broth at a concentration of 128  $\mu\text{g/mL}$ .



Figure 22. Ampicillin was used as a positive control to inhibit the growth of *S. aureus* SH1000 on TSA (tryptic soy agar). Water and DMSO were used as negative controls which were unable to inhibit the growth of *S. aureus* SH1000. Both quinazolinone **5** and the sodium salt **49** displayed antibacterial effect against *S. aureus* SH1000 on TSA disks.

Table 8. OD<sub>600</sub> Results of Quinazolinones **5** and **49** against *S. aureus* SH1000<sup>a</sup>

Con. / Entry	0*	0.5 $\mu\text{g/mL}$	1 $\mu\text{g/mL}$	2 $\mu\text{g/mL}$	4 $\mu\text{g/mL}$	8 $\mu\text{g/mL}$	16 $\mu\text{g/mL}$	32 $\mu\text{g/mL}$	64 $\mu\text{g/mL}$	128 $\mu\text{g/mL}$	TSB**
<b>5</b>	0.707	0.556	0.559	0.558	0.422	0.353	0.219	0.187	0.121	0.258	0.000
<b>49</b>	0.672	0.497	0.437	0.358	0.384	0.299	0.277	0.231	0.256	0.270	0.000

\*NO quinazolinone compounds were added. \*\*No bacteria and quinazolinone compounds were added.

<sup>a</sup>Alternative wild-type MSSA with 11bp *rsbU*+ deletion replaced to restore a functional sigB.

Compared with the MIC testing method used by Bouley *et al.* for quinazolinones,<sup>87</sup> the broth and *S. aureus* strains are different from what were used in these experiments. Bouley *et al.* used Mueller-Hinton II broth to grow bacteria, so TSB was replaced by Mueller-Hinton II to grow *S. aureus*. Another common intermediate, nutrient broth, was also tried to check the influence of different broths. However, no change was observed. Bouley *et al.* tried nine different *S. aureus* strains to test antibiotic activities of quinazolinone **5** (Table 9).<sup>87</sup> However, these strains were unavailable, and so other different MSSA (Newman, NewHG) and MRSA (COL, JE2) strains were used. This time, quinazolinone **5** and sodium salt **49** displayed inhibitory effect against all selected MSSA (Newman, NewHG) and MRSA (COL, JE2) strains with the same MIC of 2 µg/mL (Table 10). They also showed a significant antibacterial effect against *S. aureus* Newman, NewHG, COL and JE2 strains on agar disks (Figure 23). The resulting bioactivities are different between SH1000 and other selected *S. aureus* strains (Newman, NewHG, COL and JE2) may because of the different genome sequences.<sup>92-94</sup> However, the precise mechanism of quinazolinone **5** inhibiting different *S. aureus* strains remains to be discovered.

Table 9. MIC Results of Quinazolinone **5** against a Panel of Staphylococcal Strains

Strains		MIC ( $\mu\text{g/mL}$ )
MSSA	<i>S. aureus</i> ATCC 29213 <sup>a</sup>	2
	<i>S. aureus</i> NRS128 <sup>b</sup>	4
MRSA	<i>S. aureus</i> NRS70 <sup>c</sup>	2
	<i>S. aureus</i> NRS123 <sup>d</sup>	2
	<i>S. aureus</i> NRS100 <sup>e</sup>	16
	<i>S. aureus</i> NRS119 <sup>f</sup>	8
	<i>S. aureus</i> NRS120 <sup>f</sup>	8
	<i>S. aureus</i> VRS1 <sup>g</sup>	16
	<i>S. aureus</i> VRS2 <sup>h</sup>	2

<sup>a</sup>Quality control methicillin-sensitive *S. aureus* (MSSA) strain.

<sup>b</sup>MSSA strain, *mecA* negative, resistant to erythromycin, clindamycin and penicillin.

<sup>c</sup>Clinical MRSA strain isolated in Japan, *mecA* positive, resistant to erythromycin, clindamycin, oxacillin and penicillin.

<sup>d</sup>Community-acquired MRSA strain, *mecA* positive, resistant to methicillin, oxacillin, penicillin and tetracycline.

<sup>e</sup>MRSA strain, *mecA* positive, resistant to oxacillin, penicillin and tetracycline.

<sup>f</sup>Clinical MRSA strain, *mecA* positive, resistant to linezolid, ciprofloxacin, gentamicin, oxacillin, penicillin and trimethoprim/sulfamethoxazole.

<sup>g</sup>Clinical MRSA isolate from Michigan, *mecA* positive, *vanA* positive, resistant to vancomycin, ciprofloxacin, clindamycin, erythromycin, gentamicin, oxacillin and penicillin.

<sup>h</sup>Clinical MRSA isolate from Pennsylvania, *mecA* positive, *vanA* positive, resistant to vancomycin, ciprofloxacin, clindamycin, erythromycin, gentamicin, oxacillin and penicillin.

Table 10. OD<sub>600</sub> Results of Quinazolinones **5** and **49** against Staphylococcal Strains

Con. Entry	0*	0.5 μg/mL	1 μg/mL	2 μg/mL	4 μg/mL	8 μg/mL	16 μg/mL	32 μg/mL	64 μg/mL	128 μg/mL	TSB**
<i>S. aureus</i> Newman <sup>a</sup>											
<b>5</b>	0.596	0.233	0.113	0.023	0.012	0.009	0.011	0.011	0.014	0.019	0.000
<b>49</b>	0.673	0.402	0.192	0.023	0.007	0.014	0.008	0.008	0.010	0.013	0.000
<i>S. aureus</i> NewHG <sup>b</sup>											
<b>5</b>	0.609	0.278	0.208	0.042	0.014	0.013	0.017	0.017	0.015	0.023	0.000
<b>49</b>	0.673	0.402	0.192	0.023	0.007	0.014	0.008	0.008	0.010	0.013	0.000
<i>S. aureus</i> COL <sup>c</sup>											
<b>5</b>	0.559	0.426	0.349	0.100	0.074	0.061	0.056	0.085	0.033	0.041	0.000
<b>49</b>	0.667	0.377	0.187	0.084	0.061	0.055	0.027	0.03	0.033	0.036	0.000
<i>S. aureus</i> JE2 <sup>d</sup>											
<b>5</b>	0.633	0.246	0.174	0.080	0.021	0.011	0.009	0.012	0.013	0.018	0.000
<b>49</b>	0.515	0.338	0.214	0.025	0.014	0.015	0.013	0.016	0.014	0.013	0.000

\*NO quinazolinone compounds were added. \*\*No bacteria and quinazolinone compounds were added.

<sup>a</sup>Wild-type MSSA strain isolated from a human infection in 1952.

<sup>b</sup>MSSA strain, Newman derivative in which the gene encoding regulator SaeS has been repaired.

<sup>c</sup>Wild-type MRSA strain isolated from a human infection in the early 1960s.

<sup>d</sup>MRSA, parental strain of Nebraska Mutant Library, also known as USA300 strain.

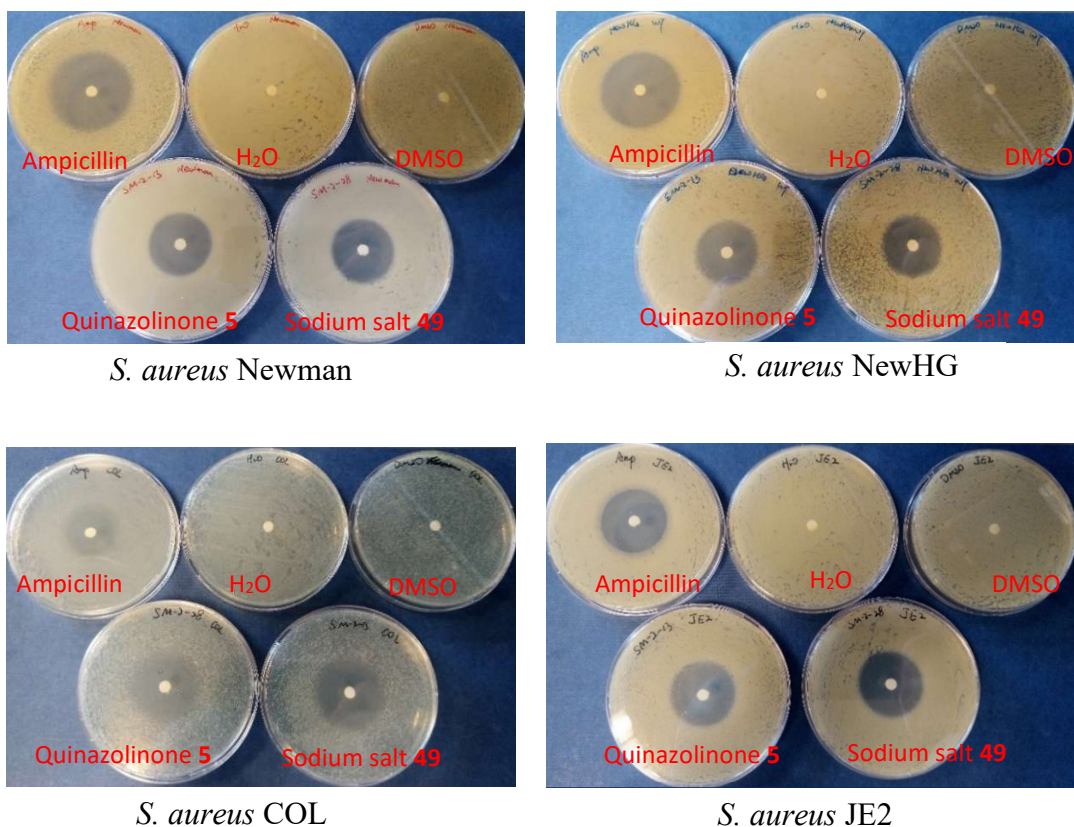


Figure 23. Agar disk-diffusion testing of quinazolinone **5** and the sodium salt **49** against MSSA (Newman, NewHG) and MRSA (COL, JE2) strains. Ampicillin was used as a positive control to inhibit the growth of Staphylococcal Strains on TSA. Water and DMSO were used as negative controls.

### 3.3 Design of Quinazolinone Probes

The crystal structure for the complex of quinazolinone **5** and *S. aureus* PBP2a reveals that quinazolinone **5** binds to the allosteric site of *S. aureus* PBP2a by salt-bridge interactions of the carboxylic acid group on the aromatic rings I (Figure 24).<sup>1</sup> Additionally, the aromatic rings II and III are unblocked by *S. aureus* PBP2a which provides space to add the linker and dye on the ring II or III for quinazolinone probes meanwhile avoid affecting the interactions with *S. aureus* PBP2a.

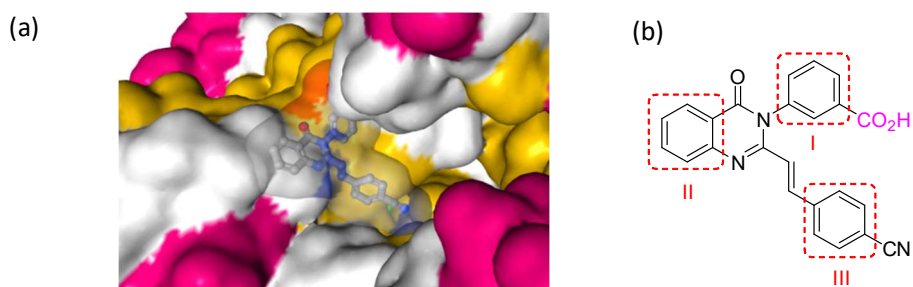


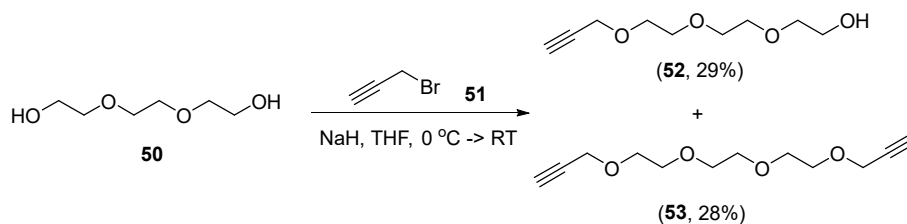
Figure 24. (a) Crystal structure of PBP2a from MRSA in complex with quinazolinone **5** (PDB code 4CJN). (b) Structures of quinazolinone **5**. Aromatic rings I, II, and III are highlighted by red boxes.

In consideration of the following click reaction to connect the linker and dye, a linker ending with an alkyne or azide group was needed to be added to the on the aromatic ring II or III of quinazolinone **5**, so that a dye with an azide or alkyne group can couple with the linker by azide-alkyne cycloaddition.

### 3.4 Synthesis and MIC Testing of Quinazolinone Probe I

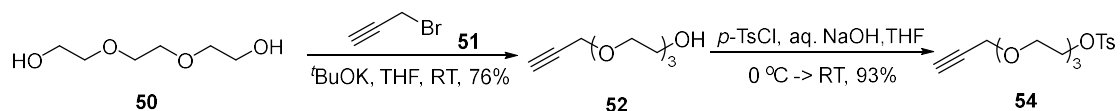
#### 3.4.1 Attempted Synthesis of Quinazolinone Probe I with an Alkyne-PEG Linker

According to the crystal structure, quinazolinone probe I was designed by coupling PEG linker to the aromatic rings II of quinazolinone **5**. A linker ending with an alkyne group was attempted firstly to add to ring II, prepared from triethylene glycol **50**. By reacting with 1 equivalent propargyl bromide **51** in the presence of 1 equivalent sodium hydride, 2 equivalent triethylene glycol **50** was converted to mono-alkyne-PEG **52** (29%) and bis-alkyne by-product **53** (28%) (Scheme 15).



Scheme 15. Synthesis of 2-[2-[2-(2-propyn-1-yloxy)ethoxy]ethoxy]ethanol **52** and triethylene glycol dipropargyl ether **53**.

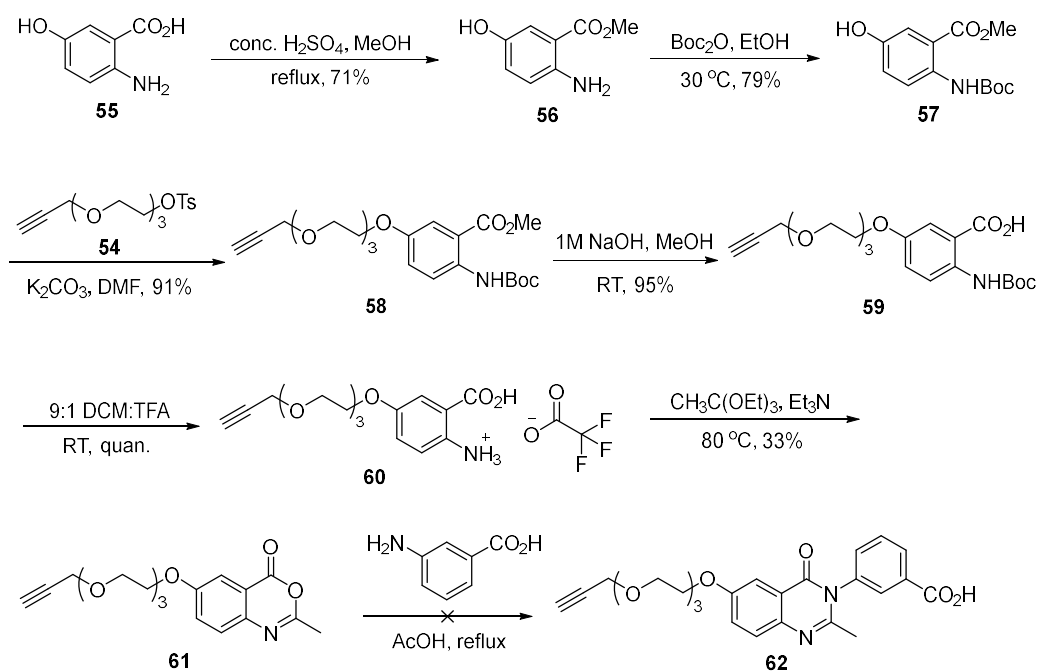
To improve the yield of mono-alkyne-PEG **52**, the reaction condition was optimised. Sodium hydride was replaced by the relatively weaker base potassium *tert*-butoxide, resulting in mono-alkyne-PEG **52** in a higher yield (76%). After that, *p*-toluenesulphonyl chloride and sodium hydroxide solution were used to introduce a tosyl group to mono-alkyne-PEG **52**, leading to tosylate **54** in good yield (93%), using sodium hydroxide solution (Scheme 16).



Scheme 16. Synthesis of 2-[2-[2-(prop-2-yn-1-yloxy)ethoxy]ethoxy]ethyl 4-methylbenzenesulfonate **54**.

Before adding the PEG linker **54**, the carboxyl group of 5-hydroxyanthranilic acid **55** was protected by methylation catalysed by concentrated sulfuric acid to give methyl 2-amino-5-hydroxybenzoate **56** in 71% yield. The amino group was protected subsequently by di-*tert*-butyl dicarbonate in ethanol to afford *tert*-butyl carbamate **57** in 79% yield. Next, the prepared PEG linker **54** was installed on the carbamate **57** in DMF, facilitated by potassium carbonate, giving rise to polyether **58** in 91% yield. Hydrolysis of the ester

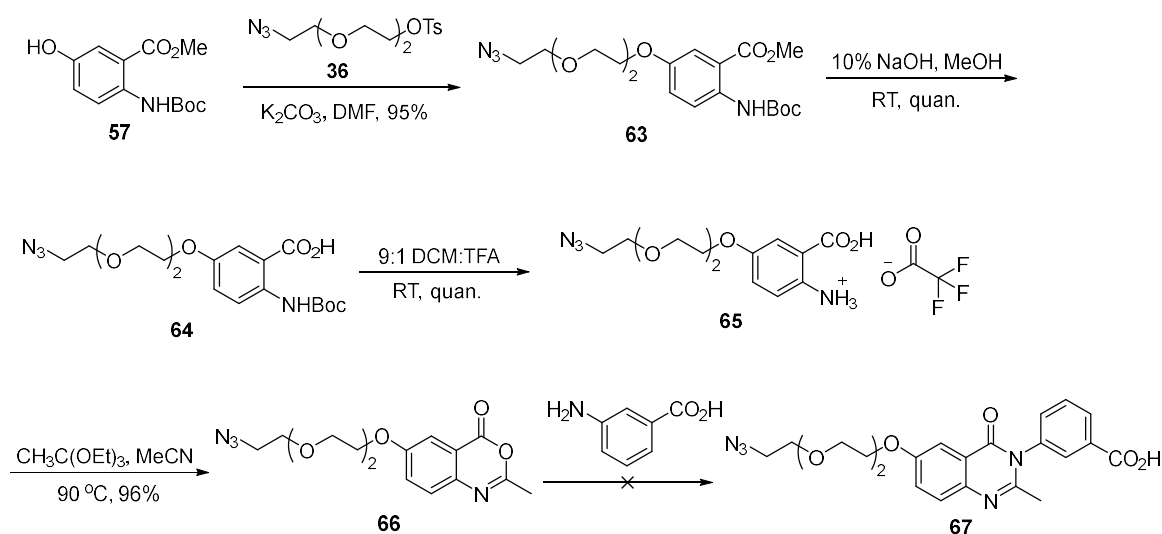
**58** was followed by dissolving in 1M NaOH and methanol. The pH of the aqueous phase was adjusted to 4 with 1M HCl to prepare carboxylic acid **59** in 95% yield. After that, TFA was used for Boc-deprotection of *tert*-butyl carbamate **59** to form TFA salt **60** in quantitative yield. The TFA salt **60** was neutralised with triethylamine and cyclised with triethyl orthoacetate at 80 °C to afford benzoxainone **61** in 33% yield. However, attempted formation of 2-methylquinazolinone **62** by reacting benzoxainone **61** and 3-aminobenzoic acid in acetic acid at 130 °C failed, and returned starting materials. (Scheme 17).



Scheme 17. Attempted synthesis of quinazolinone **62** with an alkyne-PEG linker.

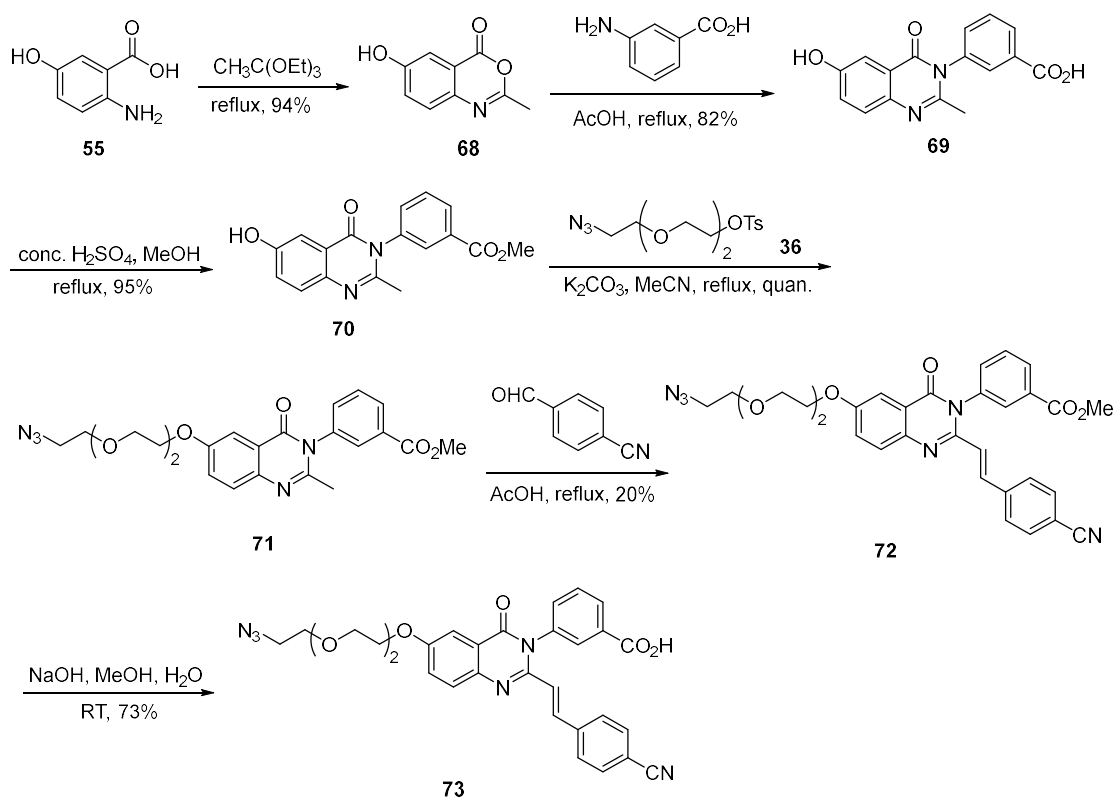
### 3.4.2 Synthesis of Quinazolinone Probe I with an Azide-PEG Linker

The azide-PEG linker **36** was also synthesised to prepare quinazolinone probes. With the azide-PEG linker **36** in hand (Scheme 8), it was installed to *tert*-butyl carbamate **57** in DMF, facilitated by potassium carbonate, giving rise to polyether **63** in 95% yield. Similar to preparation of quinazolinone with an alkyne-PEG linker, the deprotection of the carboxylic acid and amine groups were carried out sequentially. Hydrolysis of the ester **63** with 10% NaOH aqueous solution, and adjustment of the pH of the aqueous phase to 4 with 1M HCl, afforded carboxylic acid **64** in quantitative yield. TFA salt **65** was prepared in quantitative yield by Boc-deprotection of *tert*-butyl carbamate **64**. Cyclisation of TFA salt **65** and triethyl orthoacetate was carried out in acetonitrile at 90 °C to afford benzoxainone **66** in 96% yield. Formation of 2-methylquinazolinone **67** with an azide-PEG linker was attempted by amination of benzoxainone **66** with 3-aminobenzoic acid under different conditions, but unfortunately, the starting materials, benzoxainone **66** and 3-aminobenzoic acid, returned unchanged (Scheme 18).



Scheme 18. Attempted synthesis of quinazolinone **67** with an azide-PEG linker.

Given the problems with these approaches, a new synthetic route was designed to prepare 2-methylquinazolinone before installing the linker. Quinazolinone probe I **73** was prepared by reaction of triethyl orthoacetate with 5-hydroxyanthranilic acid **55** with no solvent leading to the cyclised product **68** in a high yield (94%). Ring-opening and ring-closing amination was followed by reacting oxazinone **73** with 3-aminobenzoic acid in acetic acid giving quinazolinone **69** in 82% yield. The carboxy group of quinazolinone **69** was protected by methylation in presence of concentrated sulfuric acid and methanol. Without the protection of the carboxy group, the linker **36** would have been added to both the hydroxy group and the carboxy group of quinazolinone **69** in the next step. After methylation, the prepared tosylate **36** was installed on the methylated quinazolinone **70** in acetonitrile, facilitated by potassium carbonate, giving rise to polyether **71** in quantitative yield. Subsequently, the condensation of polyether **71** and 4-formylbenzotrile in acetic acid led to quinazolinone **72** in 20% yield. Finally, the methylated quinazolinone **72** was deprotected with sodium hydroxide in water and methanol at room temperature, forming quinazolinone probe I **73** in 73% yield (Scheme 20). The coupling constant of the alkene protons of both **72** and **73** in the  $^1\text{H}$  NMR spectra is 15.5 Hz which indicates that they are *E* alkenes.



Scheme 19. Synthesis route to quinazolinone probe I **73**.

### 3.4.3 MIC Testing of Quinazolinone Probe I

Quinazolinone probe I **73** was tested for antibacterial effect, however, it only inhibited the growth of *S. aureus* COL at a concentration of 128  $\mu\text{g/mL}$ , and had no effect on other MSSA or MRSA strains (SH1000, Newman, NewHG and JE2) (Table 11).

Table 11. OD<sub>600</sub> Results of Quinazolinone Probe I **73** against Staphylococcal Strains

Con. Entry	0*	0.5 μg/mL	1 μg/mL	2 μg/mL	4 μg/mL	8 μg/mL	16 μg/mL	32 μg/mL	64 μg/mL	128 μg/mL	TSB**
<i>S. aureus</i> SH1000											
<b>73</b>	0.650	0.607	0.607	0.599	0.593	0.570	0.564	0.536	0.446	0.296	0.000
<i>S. aureus</i> Newman											
<b>73</b>	0.604	0.537	0.536	0.556	0.573	0.558	0.540	0.502	0.434	0.209	0.000
<i>S. aureus</i> NewHG											
<b>73</b>	0.588	0.682	0.682	0.673	0.716	0.670	0.649	0.630	0.510	0.214	0.000
<i>S. aureus</i> COL											
<b>73</b>	0.605	0.529	0.547	0.519	0.543	0.499	0.499	0.433	0.282	0.013	0.000
<i>S. aureus</i> JE2											
<b>73</b>	0.643	0.597	0.573	0.582	0.610	0.581	0.566	0.540	0.465	0.278	0.000

\*NO quinazolinone **73** was added. \*\*No bacteria and quinazolinone **73** were added.

This may be a result of the substitution on the aromatic ring II of quinazolinone. Previously reported compounds with different substitutions (-CO<sub>2</sub>H, -NO<sub>2</sub>, -NH<sub>2</sub>) on ring II, quinazolinones **74** (MIC = 64 μg/mL), **75** (MIC = 128 μg/mL) and **76** (MIC = 32 μg/mL) were less active than quinazolinone **5** (MIC = 2 μg/mL) without substitution on the ring II against *S. aureus* ATCC 29213 (Figure 25).<sup>88</sup> A similar trend was observed with substituted quinazolinone probe I **73**.

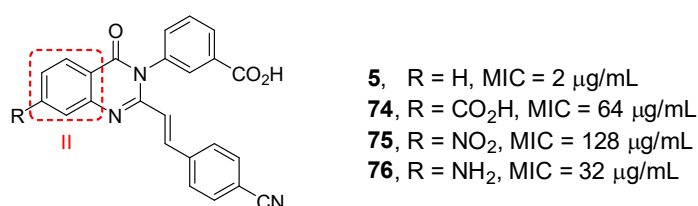


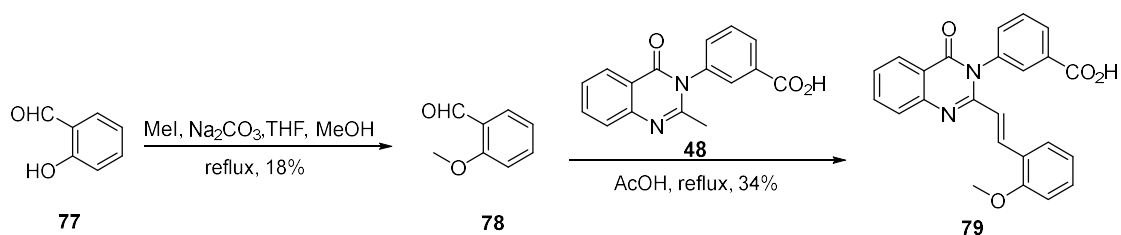
Figure 25. The MICs of quinazolinones **5**, **74**, **75** and **76**, determined for *S. aureus* ATCC 29213.

### 3.5 Synthesis and MIC Testing of Quinazolinone Probe II

#### 3.5.1 Synthesis of Small Molecule Quinazolinone

Installation of the linker on the aromatic ring II of quinazolinone had detrimental effect on antibacterial activity, therefore, the linker of quinazolinone probe II was designed on the aromatic ring III. Additionally, with a loss of nitrile group on ring III, the synthesis of quinazolinone probe II became easier.

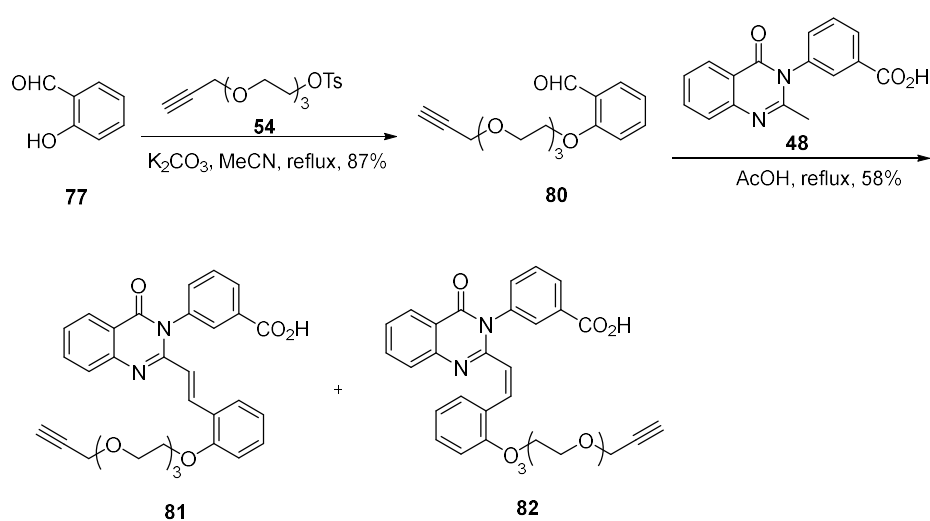
A simplified quinazolinone **79** was prepared first in order to test the feasibility of quinazolinone probe II. The first step was methylation of salicylaldehyde **77** in presence of iodomethane, sodium carbonate, methanol and THF, resulting in 2-methoxybenzaldehyde **78** in 18% yield. The condensation of aldehyde **78** and prepared quinazolinone **48** in acetic acid led to quinazolinone **79** in 34% yield (Scheme 20). The coupling constant of the alkene protons in the  $^1\text{H}$  NMR spectrum is 15.6 Hz which is indicative of an *E* alkene.



Scheme 20. Synthesis route to small molecule quinazolinone **79**.

### 3.5.2 Attempted Synthesis of Quinazolinone Probe II with an Alkyne-PEG Linker

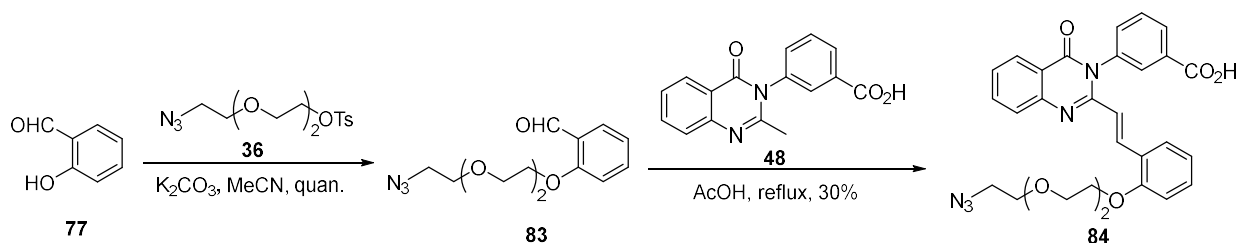
After the successful synthesis of quinazolinone **79**, the quinazolinone probe **81** with an alkyne-PEG linker on the aromatic ring III was attempted. The prepared alkyne-PEG linker **54** was added to the hydroxy group of 2-hydroxybenzaldehyde **77** in the presence of potassium carbonate and acetonitrile, resulting in the intermediate aldehyde **80** in 87% yield. Next, aldehyde **80** was attempted to react with 2-methylquinazolinone **48** to prepare quinazolinone probe **81** and a mixture of *E* (*J* 15.5 Hz) **81** and *Z* (*J* 12.4 Hz) **82** isomers of the final product was recognised from <sup>1</sup>H NMR spectrum (Scheme 21). However, the isolation of the major isomer **81** (*E*) using column chromatography failed twice due to isomerisation from *E* to *Z*. The ratio of *E* isomer **81** to *Z* isomer **82** was around 2:1. Further purification did not carried out because of the successful preparation of the single isomer, quinazolinone probe II with an azide-PEG linker, which was relatively more stable (described in the following section 3.5.3).



Scheme 21. Attempted synthesis of quinazolinones **81**, **82** with an alkyne-PEG linker.

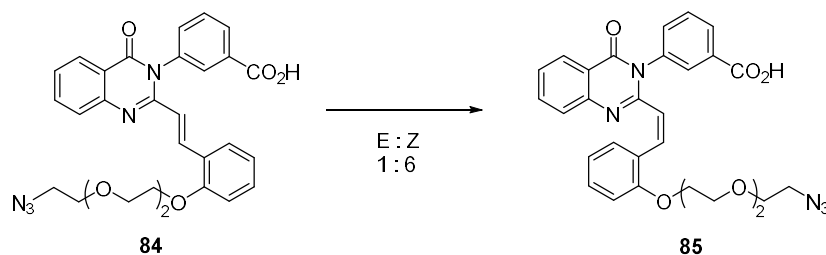
### 3.5.3 Synthesis of Quinazolinone Probe II **84** with an Azide-PEG Linker

The prepared azide-PEG linker **36** was used to prepare quinazolinone probe II **84**. First, coupling of salicylaldehyde **77** and azide-PEG linker **36** in acetonitrile, facilitated by potassium carbonate, gave rise to aldehyde **83** in quantitative yield. Secondly, condensation with aldehyde **83** and 2-methylquinazolinone **48** in acetic acid led to quinazolinone probe II **84** in 30% yield (Scheme 22).



Scheme 22. Synthesis route to quinazolinone probe II **84** with an azide-PEG linker.

Quinazolinone probe II **84** was isolated as an *E* isomer after the condensation reaction with a coupling constant of the alkene protons in the <sup>1</sup>H NMR spectrum shown as 15.6 Hz. However, it was not very stable when stored at ambient temperature. The *E* isomer **84** slowly transferred to the corresponding *Z* isomer **85** with a coupling constant of the alkene protons in the <sup>1</sup>H NMR spectrum shown as 12.4 Hz over a two month period with the final ratio of *E* isomer **84** (14%) to *Z* isomer **85** (86%) was around 1:6. In a study of influencing factors of transformation, the *E* isomer **84** solution in MeOD was heated at 40 °C, which did not speed up the transformation. However, when the *E* isomer **84** solution in MeOD was exposed to a lamp with a 23W power regular light source, it isomerised to *Z* isomer **85** quickly and the *E*:*Z* ratio turned 1:6 in just 3 hours (Scheme 23). Therefore, quinazolinone probe II **84** is sensitive to light not temperature.



Scheme 23. Transformation of quinazolinone probe II *E* isomer **84** to *Z* isomer **85**.

### 3.5.4 MIC Testing of Quinazolinone Probe II

The MIC of both *E* and *Z* isomers of quinazolinone probe **II** were tested. Quinazolinone (*E* isomer) **84** was unable to inhibit the growth of *S. aureus* SH1000 at a concentration up to 128  $\mu\text{g/mL}$ , but it showed inhibitory effect at the concentration of 32  $\mu\text{g/mL}$  against other MSSA (Newman, NewHG) and MRSA (COL, JE2) strains (Table 11). Unfortunately, quinazolinone (*Z* isomer) **85** was not as effective as quinazolinone (*E* isomer) **84**, and only had inhibitory effect on *S. aureus* COL at a concentration of 128  $\mu\text{g/mL}$ , but not on other *S. aureus* strains (SH1000, Newman, NewHG and JE2) (Table 12).

Table 12. OD<sub>600</sub> Results of Quinazolinone *E* isomer **84** and *Z* isomer **85** against *Staphylococcal* Strains

Con. Entry	0*	0.5 μg/mL	1 μg/mL	2 μg/mL	4 μg/mL	8 μg/mL	16 μg/mL	32 μg/mL	64 μg/mL	128 μg/mL	TSB**
<i>S. aureus</i> SH1000											
<b>84(E)</b>	0.701	0.620	0.611	0.585	0.552	0.487	0.407	0.387	0.384	0.380	0.000
<b>85(Z)</b>	0.663	0.627	0.600	0.611	0.604	0.583	0.525	0.436	0.340	0.194	0.000
<i>S. aureus</i> Newman											
<b>84(E)</b>	0.631	0.606	0.568	0.542	0.442	0.371	0.264	0.072	0.024	0.029	0.000
<b>85(Z)</b>	0.576	0.578	0.566	0.590	0.574	0.518	0.487	0.405	0.308	0.102	0.000
<i>S. aureus</i> NewHG											
<b>84(E)</b>	0.673	0.728	0.659	0.573	0.548	0.350	0.227	0.068	0.018	0.019	0.000
<b>85(Z)</b>	0.758	0.736	0.747	0.718	0.707	0.637	0.635	0.482	0.328	0.101	0.000
<i>S. aureus</i> COL											
<b>84(E)</b>	0.631	0.526	0.498	0.498	0.518	0.383	0.378	0.095	0.039	0.033	0.000
<b>85(Z)</b>	0.663	0.692	0.724	0.729	0.685	0.656	0.631	0.546	0.295	0.013	0.000
<i>S. aureus</i> JE2											
<b>84(E)</b>	0.650	0.615	0.616	0.525	0.317	0.240	0.129	0.073	0.012	0.020	0.000
<b>85(Z)</b>	0.601	0.657	0.698	0.725	0.740	0.641	0.494	0.441	0.223	0.107	0.000

\*NO quinazolinone compounds were added. \*\*No bacteria and quinazolinone compounds were added.

### 3.6 Labelling of Quinazolinone Probe II

Two different methods were used to label PBPs with quinazolinone probe II **84** and dye. During post-click labelling, fixed cells were prepared by treatment of bacteria with quinazolinone **84**. Then the appropriate dye was added and ligated by a click reaction to make them visible under the microscope. Conversely, for pre-click labelling, a click

reaction of fluorescent dye and quinazolinone antibiotic **84** was conducted and followed by purification, prior to treatment of bacteria.

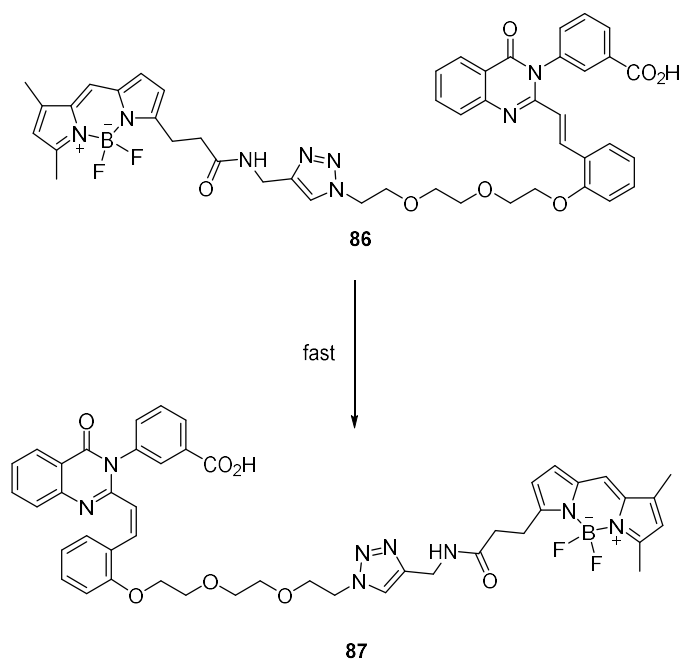
### 3.6.1 Post-click labelling

Quinazolinone (*E* isomer) **84** displayed great antibiotic activity and effectively inhibited the growth of *S. aureus* (Newman, NewHG, COL, JE2) at a concentration of 32 mg/mL, so it was used to label *S. aureus* cells. *S. aureus* SH1000 in TSB liquid media was incubated at 37 °C to reach an OD<sub>600</sub> of ~ 0.3. Quinazolinone (*E* isomer) **84** was added at a concentration of 80 mg/mL and the culture was continued to be incubated at 37 °C for 20 min. 1mL Sample was centrifugated and the resulting pellet was fixed with paraformaldehyde in PBS prior to click reaction.

The labelled sample by quinazolinone (*E* isomer) **84** was clicked with the dye ATTO 488 alkyne in presence of click buffer, additive and CuSO<sub>4</sub> solution, in order to visualise the PBP localisation. The resulting microscopy image showed that some cell walls were well labelled, such as the cells marked with the red frame in the Figure 26. However, some celled are unclearly labelled. The targeting PBPs are involved in the biosynthesis of peptidoglycan which is incorporated within the inner cell wall surface; therefore, the size of the dye and cell wall surface charges may make it difficult to permeate the cell wall and reach the target quinazolinone probes and PBPs.

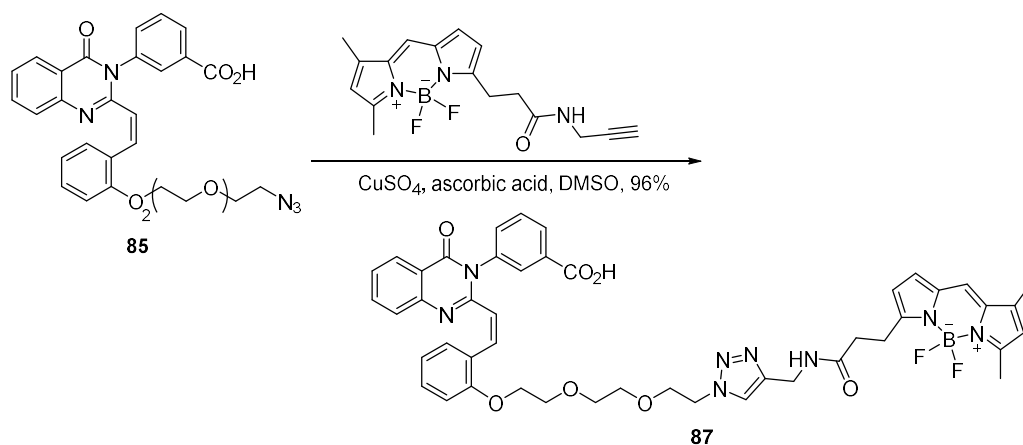


After the click chemistry, the fluorescent product (*E* isomer) **86** was more unstable than the starting material **84**, and quickly isomerised to the corresponding *Z* isomer **87** (Scheme 25). The isomerisation of the starting material, quinazolinone (*E* isomer) **84**, to the corresponding *Z* isomer **85** could be observed over a period of several days. However, the fluorescent product (*E* isomer) **86** started to isomerise to the corresponding *Z* isomer **87** in just few minutes. Therefore, the fluorescent *E* isomer **86** was isolated very carefully and protected from the light using aluminium foil.



Scheme 25. Transformation of fluorescent quinazolinone *E* isomer **86** to *Z* isomer **87**.

Fluorescent quinazolinone (*Z* isomer) **87** can also be prepared by click reaction of the relatively stable quinazolinone (*Z* isomer) **85** and dye BODIPY FL alkyne. The *Z* isomer product **87** was obtained in 96% yield after purification by HPLC (Scheme 26).



Scheme 26. Click chemistry to prepare fluorescent quinazolinone (*Z* isomer) **87**.

Both clicked products (*E* **86** and *Z* **87** isomers) were used to treat bacteria. However, they did not display much inhibition of the growth of *S. aureus*. The MIC of both against *S. aureus* COL is 128  $\mu\text{g}/\text{mL}$ , and were also unable to inhibit other *S. aureus* strains (SH1000, Newman, NewHG and JE2) at this concentration (Table 13). The fluorescent *E* isomer **86** might have similar biological activity as *Z* isomer **87**, or it might transfer quickly to *Z* isomer during the testing even though the samples were protected carefully from the light.

Table 13. OD<sub>600</sub> Results of Fluorescent Quinazolinone *E* isomer **86** and *Z* isomer **87** against Staphylococcal Strains

Con. Entry	0*	0.5 μg/mL	1 μg/mL	2 μg/mL	4 μg/mL	8 μg/mL	16 μg/mL	32 μg/mL	64 μg/mL	128 μg/mL	TSB**
<i>S. aureus</i> SH1000											
<b>86(E)</b>	0.604	0.572	0.605	0.567	0.606	0.584	0.543	0.555	0.448	0.255	0.000
<b>87(Z)</b>	0.627	0.651	0.633	0.643	0.623	0.572	0.546	0.479	0.399	0.175	0.000
<i>S. aureus</i> Newman											
<b>86(E)</b>	0.543	0.602	0.639	0.629	0.604	0.591	0.574	0.565	0.517	0.287	0.000
<b>87(Z)</b>	0.517	0.606	0.604	0.608	0.589	0.596	0.567	0.537	0.510	0.286	0.000
<i>S. aureus</i> NewHG											
<b>86(E)</b>	0.730	0.746	0.707	0.742	0.756	0.740	0.679	0.628	0.561	0.352	0.000
<b>87(Z)</b>	0.760	0.700	0.702	0.689	0.713	0.683	0.649	0.601	0.548	0.318	0.000
<i>S. aureus</i> COL											
<b>86(E)</b>	0.715	0.715	0.716	0.676	0.676	0.625	0.592	0.542	0.273	0.007	0.000
<b>87(Z)</b>	0.686	0.667	0.645	0.663	0.672	0.679	0.626	0.571	0.300	0.004	0.000
<i>S. aureus</i> JE2											
<b>86(E)</b>	0.623	0.638	0.604	0.609	0.606	0.586	0.557	0.523	0.447	0.325	0.000
<b>87(Z)</b>	0.639	0.620	0.616	0.653	0.638	0.647	0.584	0.533	0.443	0.314	0.000

\*NO quinazolinone compounds were added. \*\*No bacteria and quinazolinone compounds were added.

The MIC results of fluorescent quinazolinones (*E* and *Z* isomers) **86** and **87** displayed that they did not inhibit *S. aureus* strains (SH1000, Newman, NewHG and JE2). Although they show the inhibition of the growth of *S. aureus* COL at 128 μg/mL, the concentration is too high for PBP labelling. The further pre-click labelling will not be carried out until quinazolinone probes can be applied at a lower concentration, such as synergism with other antibiotics or preparing new more active quinazolinone probes.

## 6.7 Synergism of Quinazolinones with Beta-lactam Antibiotic

Recently, quinazolinone **5** was reported to show bactericidal synergy combined with commercial piperacillin-tazobactam against MSSA and MRSA strains.<sup>95</sup> Quinazolinone **5** inhibits the function of PBP1 and PBP2a, and PBP2a is unique to MRSA strains such as COL and JE2. Beta-lactam antibiotics kill *Staphylococcus aureus* bacteria by inhibiting the function of cell-wall PBP1 and PBP3 but they are ineffective against PBP2a.<sup>96</sup> Therefore, a synergism study of quinazolinones with the beta-lactam antibiotic, ampicillin, was performed. With ampicillin targeting PBP1, quinazolinones were supposed to inhibit the function of PBP2a and the growth of MRSA at a lower concentration.

### 3.7.1 MIC Testing of Ampicillin

Ampicillin was tested first against all Staphylococcal strains which were used for quinazolinones. As is well-known, ampicillin effectively kills MSSA bacteria and the MICs against SH1000, Newman and NewHG are lower than 0.5 µg/mL (Table 14). However, ampicillin cannot kill MRSA bacteria as effectively as MSSA. The MICs against COL and JE2 are 64 µg/mL and 32 µg/mL respectively.

Table 14. OD<sub>600</sub> Results of Ampicillin against Staphylococcal Strains

Con. Entry	0*	0.5 µg/mL	1 µg/mL	2 µg/mL	4 µg/mL	8 µg/mL	16 µg/mL	32 µg/mL	64 µg/mL	128 µg/mL	TSB**
<i>S. aureus</i> SH1000											
Ampicillin	0.630	0.035	0.004	0.002	0.006	0.007	0.023	0.006	0.003	0.004	0.000
<i>S. aureus</i> Newman											
Ampicillin	0.557	0.041	0.005	0.001	0.000	0.005	0.007	0.005	0.002	0.004	0.000
<i>S. aureus</i> NewHG											
Ampicillin	0.696	0.040	0.006	0.003	0.001	0.002	0.005	0.006	0.006	0.008	0.000
<i>S. aureus</i> COL											
Ampicillin	0.554	0.531	0.506	0.507	0.492	0.487	0.464	0.302	0.003	0.002	0.000
<i>S. aureus</i> JE2											
Ampicillin	0.614	0.370	0.330	0.279	0.254	0.189	0.139	-0.001	-0.002	-0.004	0.000

\*No ampicillin was added. \*\*No bacteria and ampicillin were added.

### 3.7.2 Synergism of Quinazolinones with Ampicillin

The prepared quinazolinones were used to treat MRSA combined with ampicillin at a fixed concentration (2 µg/mL). At 2 µg/mL, ampicillin is able to inhibit the function of PBP1 but unable to kill MRSA bacteria. With ampicillin addition, the MICs of quinazolinone **5** decrease from 2 µg/mL to 1 µg/mL against COL, from 2 µg/mL to 0.125 µg/mL against JE2 (Table 15).

Table 15. OD<sub>600</sub> Results of Quinazolinone **5** with 2 µg/mL Ampicillin against MRSA Strains

Con. Entry	0*	0.0625 µg/mL	0.125 µg/mL	0.25 µg/mL	0.5 µg/mL	1 µg/mL	2 µg/mL	4 µg/mL	8 µg/mL	16 µg/mL	32 µg/mL	TSB**
<i>S. aureus</i> COL												
<b>5</b>	0.631	0.550	0.512	0.438	0.264	0.061	0.057	0.019	0.012	0.008	0.008	0.000
<i>S. aureus</i> JE2												
<b>5</b>	0.635	0.152	0.068	0.023	0.015	0.003	0.004	0.007	0.004	0.002	0.002	0.000

\*No quinazolinone **5** was added. \*\*No bacteria and quinazolinone **5** were added.

When 2 µg/mL ampicillin added, quinazolinone **73** inhibits COL at the concentration of 128 µg/mL, but it is unable to inhibit the growth of the JE2 at this concentration, which is the same as without ampicillin (Table 16). The MIC of quinazolinone **84** (*E*) against COL is 32 µg/mL, either by itself or with 2 µg/mL ampicillin. But when 2 µg/mL ampicillin is added, its MIC decrease from 32 µg/mL to 4 µg/mL against JE2. With ampicillin addition, quinazolinone **85** (*Z*) is unable to inhibit COL bacteria at the concentration up to 128 µg/mL, but it inhibits JE2 bacteria at 32 µg/mL, lower than without 2 µg/mL ampicillin (Table 16).

The addition of 2 µg/mL ampicillin made no difference to fluorescent quinazolinones **86** (*E*) and **87** (*Z*). The MICs of these compounds against COL bacteria remain 128 µg/mL and they are unable to inhibit JE2 bacteria at this concentration even with 2 µg/mL ampicillin (Table 16).

Table 16. OD<sub>600</sub> Results of Quinazolinones with 2 µg/mL Ampicillin against MRSA Strains

Con. Entry	0*	0.25 µg/mL	0.5 µg/mL	1 µg/mL	2 µg/mL	4 µg/mL	8 µg/mL	16 µg/mL	32 µg/mL	64 µg/mL	128 µg/mL	TSB**
<i>S. aureus</i> COL												
<b>73</b>	0.673	0.570	0.560	0.546	0.572	0.552	0.556	0.513	0.499	0.355	0.002	0.000
<b>84(E)</b>	0.680	0.514	0.530	0.526	0.543	0.519	0.445	0.271	0.100	0.009 8	0.064	0.000
<b>85(Z)</b>	0.653	0.528	0.509	0.527	0.485	0.491	0.447	0.514	0.466	0.393	0.241	0.000
<b>86(E)</b>	0.606	0.529	0.573	0.594	0.587	0.547	0.525	0.557	0.492	0.333	0.026	0.000
<b>87(Z)</b>	0.642	0.538	0.525	0.534	0.549	0.565	0.495	0.529	0.469	0.356	0.005	0.000
<i>S. aureus</i> JE2												
<b>73</b>	0.645	0.261	0.261	0.264	0.259	0.269	0.265	0.262	0.263	0.275	0.170	0.000
<b>84(E)</b>	0.691	0.234	0.204	0.173	0.149	0.063	0.031	0.004	0.009	0.004	-0.001	0.000
<b>85(Z)</b>	0.691	0.243	0.242	0.236	0.226	0.197	0.175	0.142	0.068	0.013	0.000	0.000
<b>86(E)</b>	0.604	0.235	0.233	0.238	0.239	0.238	0.245	0.245	0.267	0.258	0.197	0.000
<b>87(Z)</b>	0.596	0.243	0.233	0.244	0.235	0.239	0.236	0.242	0.246	0.259	0.164	0.000

\*No quinazolinone compounds were added. \*\*No bacteria and quinazolinone compounds were added.

. OD<sub>600</sub> of 2 µg/mL ampicillin and COL bacteria in TSB is 0.586

. OD<sub>600</sub> of 2 µg/mL ampicillin and JE2 bacteria in TSB is 0.265

Making a comparison of the MIC results of quinazolinones used in the synergism study (Figure 27), quinazolinone **5** synergized with ampicillin against both MRSA strains COL and JE2 (Table 17). The combination of quinazolinone **84** or **85** with ampicillin showed bactericidal synergy against JE2, but not COL. Addition of ampicillin to quinazolinone **73**, **86** or **87** was not helpful to inhibit the growth of MRSA strains COL and JE2, which was unsuitable for labelling.

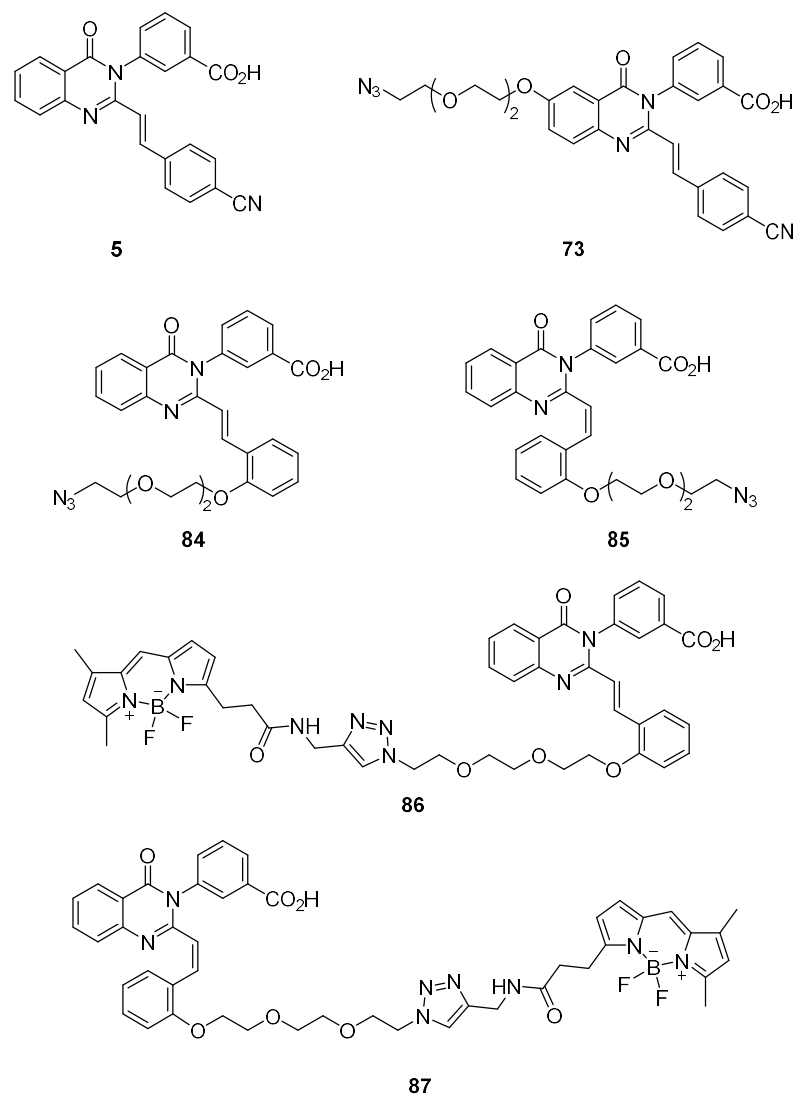


Figure 27. The structures of quinazolinones used in the synergism study with ampicillin.

Table 17. Comparison of MIC Results of Quinazolinones without/with 2 µg/mL Ampicillin against MRSA Strains

Entry	MIC (µg/mL) without Ampicillin	MIC (µg/mL) with Ampicillin
<i>S. aureus</i> COL		
<b>5</b>	2	1
<b>73</b>	128	128
<b>84(E)</b>	32	32
<b>85(Z)</b>	128	-
<b>86(E)</b>	128	128
<b>87(Z)</b>	128	128
<i>S. aureus</i> JE2		
<b>5</b>	2	0.125
<b>73</b>	-	-
<b>84(E)</b>	32	4
<b>85(Z)</b>	-	32
<b>86(E)</b>	-	-
<b>87(Z)</b>	-	-

- Unable to inhibit the growth of bacteria at the concentration up to 128 µg/mL

According to the experimental results achieved so far, although the antibiotic, quinazolinone **5**, displayed good antibiotic activity against *S. aureus*, the addition of the PEG linker and the fluorescent dye decreased bioactivity. For further labelling study, more active chemical probes are required. The substitutions on the aromatic ring II of quinazolinone are negative to the bioactivity against *S. aureus* (Section 3.4.3), so it is not ideal to adding the linker to the aromatic ring II. To simplify the chemical synthesis, the nitrile group was neglected when the PEG linker was added to the aromatic ring III of quinazolinone. However, the addition of the linker and the dye resulted in the isomerisation of quinazolinones and decreasing the antibiotic activity. When thinking of

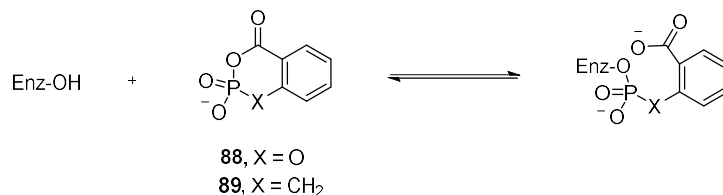
new probes with higher bioactivity, other more active quinazolinones, such as **44** and **45** (Section 3.1), can also be used to develop probes.

## Chapter 4 Cyclic Phosphonate Synthesis and Analysis

### 4.1 Cyclic Phosph(on)ates and Cyclic Boronates in the literature

#### 4.1.1 Cyclic Phosph(on)ates

Development of  $\beta$ -lactamase inhibitors is viable to prevent antibiotic resistance and save the effectiveness of  $\beta$ -lactam antibiotics in antimicrobial therapy.<sup>97, 98</sup> The mono- and bicyclic acyl phosph(on)ates studied by K. Kaur *et al.* have shown to inhibit class A and class C  $\beta$ -lactamases. Notably, the current  $\beta$ -lactamase inhibitors used in medicine shows high activity against class A enzymes, but they are not so effective against class C enzymes.<sup>99</sup> The cyclic phosph(on)ates **88** and **89** are reversible covalent inhibitors of *Enterobacter cloacae* P99  $\beta$ -lactamase (class C) (Scheme 27).<sup>97, 99</sup>



Scheme 27. The mode of action of cyclic phosph(on)ates **88** and **89**.

The cyclic phosphates **90** and **91** were prepared subsequently, where the substituents owned more degree of freedom for rotation (Figure 28). They were designed to be less likely to recyclise after the ring-opening reaction with the enzyme. Satisfyingly, both of them irreversibly inhibited *Enterobacter cloacae* P99  $\beta$ -lactamase (class C), and cyclic phosphate **90** irreversibly inhibited TEM-2  $\beta$ -lactamase (class A) as well.<sup>99</sup>

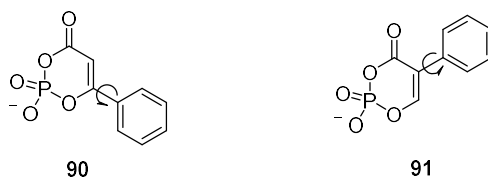


Figure 28. The structure of cyclic phosphates **90** and **91**.

#### 4.1.2 Cyclic Boronates

The interactions of boronic acid inhibitors with serine proteases have been reported a number of years ago, which provided the basis for the study of similar interactions with  $\beta$ -lactamases.<sup>100</sup> For example, cyclic boronic acid RPX7009 **92** can inhibit many class A, class C and some class D  $\beta$ -lactamases. The combination of RPX7009 **92** with carbapenem antibiotic biapenem **93** for phase 1 clinical trials is successful and the combination of RPX7009 **92** with carbapenem antibiotic meropenem **94** is in phase 3 clinical trials to evaluate the safety efficacy and tolerability (Figure 29).<sup>100, 101</sup>

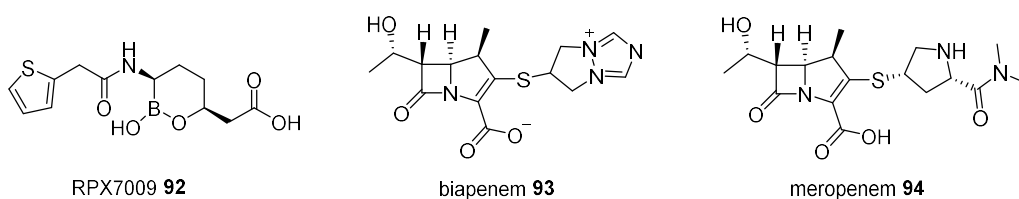


Figure 29. The structures of RPX7009 **92** and carbapenem antibiotics biapenem **93** and meropenem **94**.

However, the clinically useful inhibitors of class B zinc-dependent metallo- $\beta$ -lactamases had never been reported before Brem group's study in 2016. Many bacteria have acquired resistance to both serine- $\beta$ -lactamases (class A) and metallo- $\beta$ -lactamases (class B),

therefore, Brem *et al.* planned to identify dual action inhibitors against both serine- $\beta$ -lactamases and metallo- $\beta$ -lactamases.<sup>100</sup> Various boronic acids were screened and three cyclic boronates **95**, **96** and **97** were found from the patent literature. Using these cyclic boronates as models, two more cyclic boronates **98** and **99** were designed and synthesised by Brem group for bioactivity testing (Figure 30).<sup>102</sup>

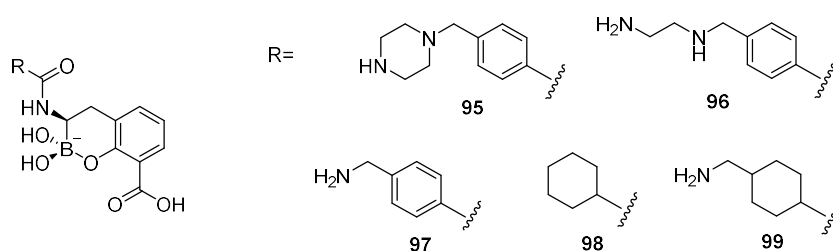


Figure 30. Structures of cyclic boronates **95**, **96**, **97**, **98** and **99**.

All these compounds **95**, **96**, **97**, **98** and **99** were tested to show potent inhibition against both serine- $\beta$ -lactamases and metallo- $\beta$ -lactamases by a mechanism involving mimicking of the tetrahedral intermediate of  $\beta$ -lactamase catalysis.<sup>102</sup> Since serine- $\beta$ -lactamases and PBPs targeting  $\beta$ -lactams are evolutionarily and mechanistically related, the serine- $\beta$ -lactamase inhibitor **97** was also tested for inhibition against PBPs.<sup>103</sup> Surprisingly, cyclic boronate **97** potently inhibited the non-essential PBP5 from *Escherichia coli* with  $IC_{50}$  value at 1.7 nM. Similar to the mechanism inhibiting  $\beta$ -lactamases, to inhibit PBP5, cyclic boronate **97** acts as a mimic of the tetrahedral intermediate 1 produced by nucleophilic attack during the PBP catalysis (Figure 31).<sup>102</sup>

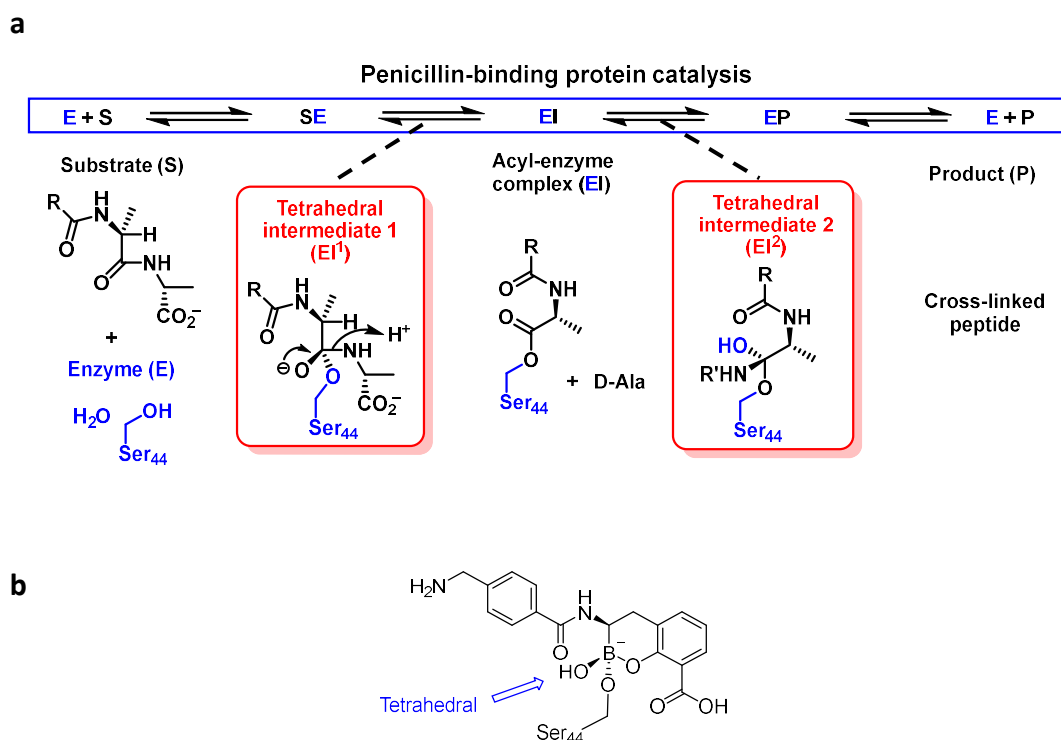


Figure 31. (a) Mode of action of PBP. (b) The binding mode of compound **97**.

Since cyclic boronates are able to effectively inhibit  $\beta$ -lactamases and PBP5, it is reasonable for us to attempt on phosphonates compounds which are particularly interested in and studied in Jones group. This project tried to design and synthesise some cyclic phosphonates which show the analogous transition state to cyclic boronates,  $\beta$ -lactamases and PBPs (Figure 32).

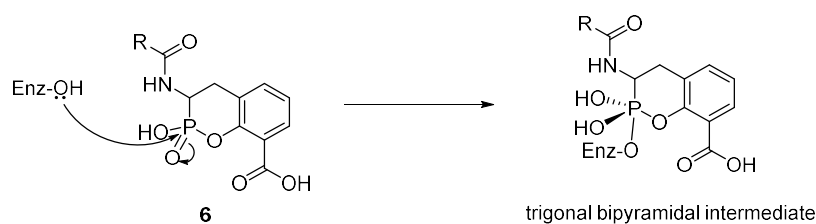
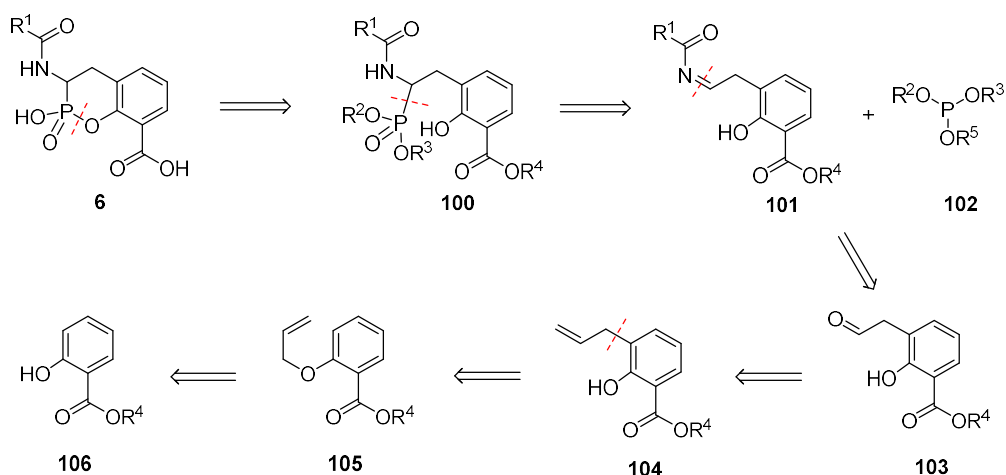


Figure 32. The speculative binding mode of cyclic phosphonate target **6**.

## 4.2 Retrosynthetic Analysis

Since there is no synthetic route reported to this class of cyclic phosphonate **6**, an independent synthesis is necessary. Consecutive disconnections of the six-membered heterocycle at the phosphorus-oxygen single bond and phosphorus-carbon single bond gives benzoate **101** and phosphite **102**. Benzoate **101** could be prepared from aldehyde **103**, itself prepared from alkene **104**, which in turn come from allyloxybenzoate **105** by Claisen rearrangement. Allyloxybenzoate **105** can be prepared from commercially available salicylic acid **106** (Scheme 28).

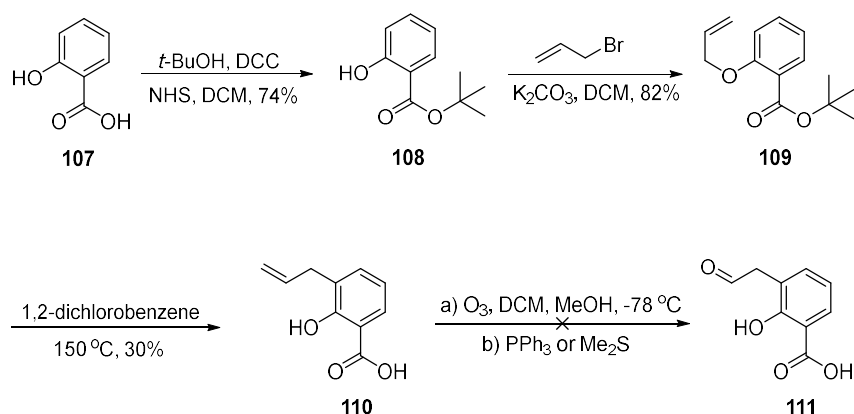


Scheme 28. Retrosynthetic analysis of cyclic phosphonate **6**

## 4.3 Synthesis of *tert*-Butyl Protected Benzoates

Based on the retrosynthetic analysis described in section 4.2, the carboxyl group of salicylic acid **107** needs to be protected before the consequent reactions. The large *tert*-

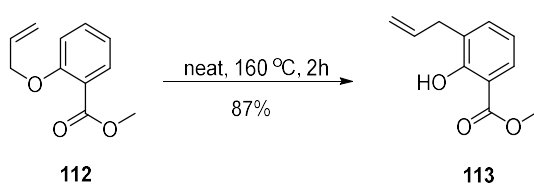
butyl group was a good choice because *tert*-butyl ester will not be hydrogenated or hydrolysed under alkaline conditions. First of all, *N,N'*-dicyclohexylcarbodiimide (DCC) and *N*-hydroxysuccinimide (NHS) were employed to promote the installation of the *tert*-butyl ester of salicylic acid **107** in DCM. The desired *tert*-butyl protected product **108** was achieved in 74% yield. This was followed by *O*-allylation, carried out using allyl bromide and potassium carbonate in DCM, to yield allyloxybenzoate **109** in 82%. After that, the 3,3-sigmatropic Claisen rearrangement was carried out by heating allyloxybenzoate **109** in 1,2-dichlorobenzene at 150 °C to yield *ortho*-rearranged product **110** in 30% yield (Scheme 29). However, the *tert*-butyl group had been cleaved from allyloxybenzoate **109** which was likely due to the high reaction temperature. Ozonolysis of the alkene **110** was followed to prepare aldehyde **111** by bubbling ozone in DCM and methanol at -78 °C and work-up with PPh<sub>3</sub> or Me<sub>2</sub>S. Unfortunately, the starting material **110** decomposed and the desired aldehyde **111** was not obtained.



Scheme 29. Synthetic route to 3-allyl-2-hydroxybenzoic acid **110**.

#### 4.4 Synthesis of Methyl Protected Benzoates

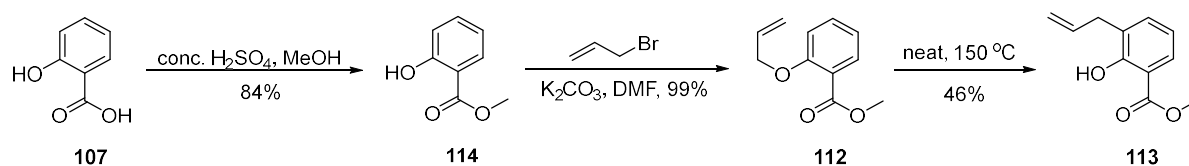
Owing to the failed synthesis of aldehyde **111**, a different protecting group was considered. The 3,3-sigmatropic Claisen rearrangement was successfully carried out by Patel *et al.* to prepare methyl benzoate **113** in a high yield (Scheme 30).<sup>104</sup> Therefore, methyl benzoate **113** was the next target for synthesis following Patel's method.



Scheme 30. Patel's method to prepare methyl benzoate **113**.

The starting material, salicylic acid **107**, was methylated by methanol under the acidic condition, affording the corresponding methyl ester **114** in 84% yield. Subsequently, *O*-allylation was carried out using allyl bromide and potassium carbonate in DMF and the resulting methyl 2-(allyloxy)benzoate **112** was obtained in 99% yield. Finally, Patel's method was followed to prepare the corresponding *ortho*-rearranged product **113**. When starting material **112** was used in a small scale (183 mg) at 150 °C, all materials evaporated probably as the boiling point of the reactant, methyl 2-(allyloxy)benzoate **112**, is 147-151 °C.<sup>105</sup> The heating temperature was decreased but the reaction did not occur. The reaction succeeded by increasing the amount of starting material **112** to 3 g. Most reactant still evaporated when heating at 150 °C, but some heated at reflux, resulting in the desired product **113** in 46% yield (Scheme 31). Although the *ortho*-rearranged

product **113** was obtained, the substantial waste of the starting material **112** was not ideal.



Scheme 31. Synthetic route to methyl protected benzoates.

#### 4.5 Simplified Target and Retrosynthetic Analysis

The large loss of starting material **112** during the Claisen rearrangement reaction led to the relatively low yield of the product **113**. Additionally, the next step, ozonolysis was also challenging. Therefore, a simplified target, cyclic phosphonate **122**, was taken into consideration for the reasons outlined below, which was easier for preparation (Figure 33).

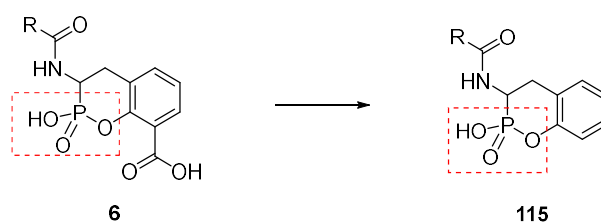
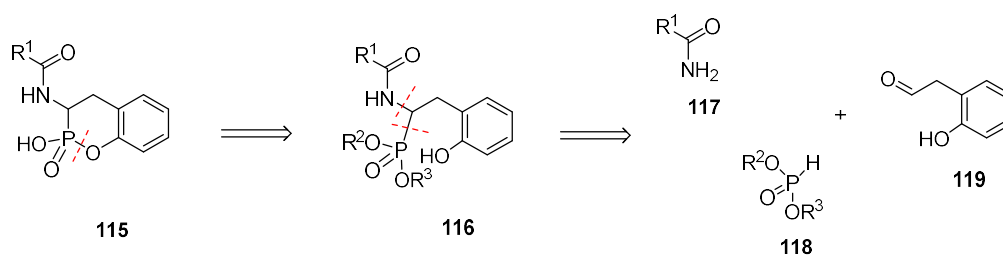


Figure 33. The simplification of target cyclic phosphonate.

The target cyclic phosphonate was supposed to inhibit  $\beta$ -lactamases and PBPs by mimicking the tetrahedral intermediate, it is important to keep the tetrahedral core (in red boxes in Figure 33). The carbonyl group might be ignored since it was not responsible

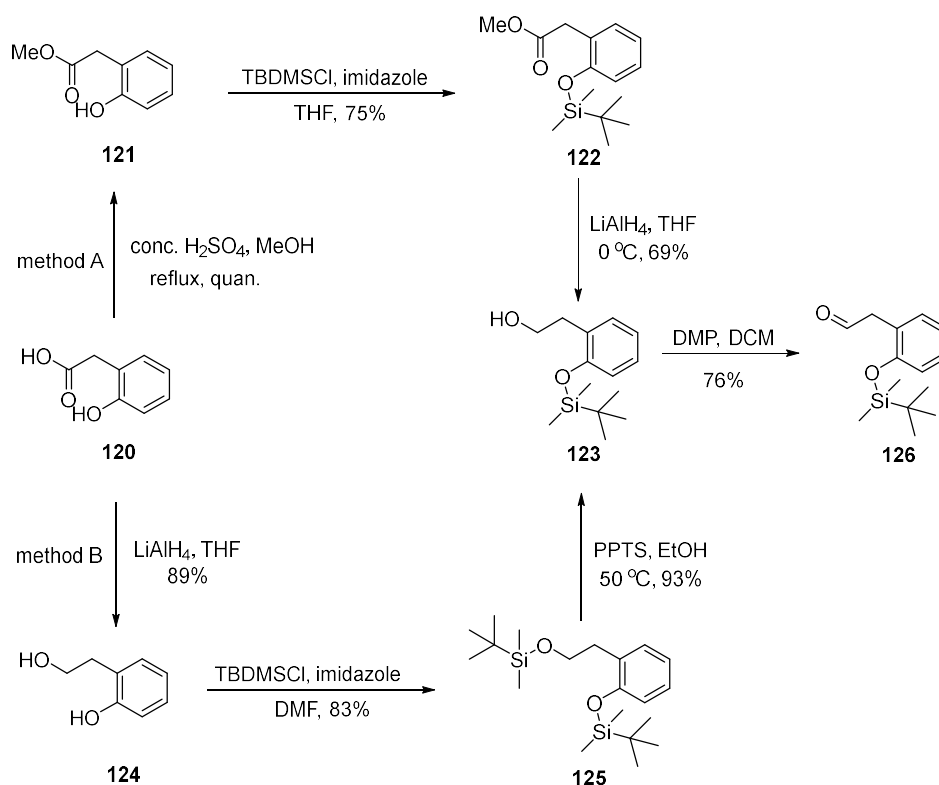
for antibiotic activity. The simplification made the target **115** easier to achieve and less synthetic steps were needed to provide proof of concept for the required Kabachnik-Fields reaction (Scheme 32).



Scheme 32. Retrosynthetic analysis of simplified cyclic phosphonate **115**

#### 4.6 Two Synthetic Routes towards Benzeneacetaldehyde

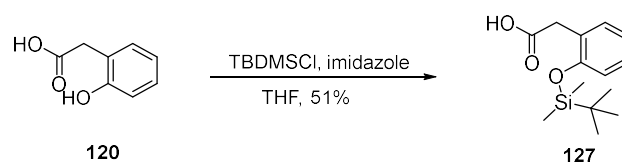
The starting material of Kabachnik-Fields reaction, the aryl acetaldehyde **126**, was prepared in two different ways, which both started from 2-hydroxybenzeneacetic acid **120** (Scheme 33).



Scheme 33. Synthetic routes to aryl acetaldehyde **126**.

In method A, the methylation of 2-hydroxybenzeneacetic acid **120** led to methyl ester **121** in quantitative yield, by heating at reflux in methanol with concentrated sulphuric acid. Secondly, *tert*-butyldimethylsilyl chloride was used as a silylation agent to protect the hydroxy group of phenol **121** in presence of imidazole and THF, and the resulting *tert*-butyldimethylsilyl ether **122** was obtained in 75% yield. After that, the carboxylic ester **122** was reduced to the corresponding alcohol **123** by lithium aluminium hydride at 0 °C (69% yield). The direct silylation of the starting material 2-hydroxybenzeneacetic acid **120**, without the methylation of the carboxyl group, was also attempted using *tert*-butyldimethylsilyl chloride in presence of imidazole and THF. The resulting *tert*-butyldimethylsilyl ether **127** was isolated in 51% yield (Scheme 34). However, *tert*-butyldimethylsilyl ether **127** was not as stable as the one with methyl protection **122**. The

*tert*-butyldimethylsilyl group was found to be very labile and it returned to the starting material **120** quickly, which was proved by <sup>1</sup>H NMR spectroscopy. The low temperature storage avoiding light was necessary to store *tert*-butyldimethylsilyl ether **127**.



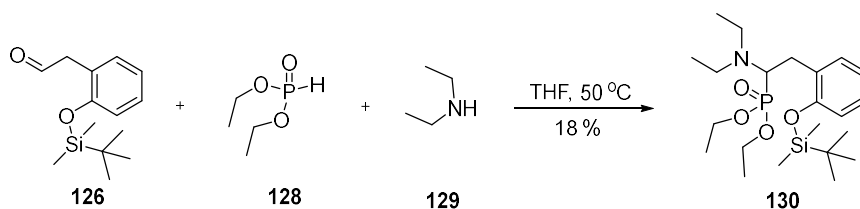
Scheme 34. Synthetic route to *tert*-butyldimethylsilyl ether **127**.

In method B, 2-hydroxybenzoic acid **120** was reduced by lithium aluminium hydride in THF, affording the corresponding diol **124** in 89% yield. Then, *tert*-butyldimethylsilyl chloride was used to protect the two hydroxy groups of diol **124** in presence of imidazole and DMF (83% yield), followed by the selective deprotection of *tert*-butyldimethylsilyl ether **125** using pyridinium *p*-toluenesulfonate in ethanol at 50 °C, affording the compound **123** in 93% yield (Scheme 33).

Finally, the prepared alcohol **123** from methods A and B was oxidised by Dess–Martin periodinane in ethanol to afford the target aryl acetaldehyde **126** in 76% yield (Scheme 33).

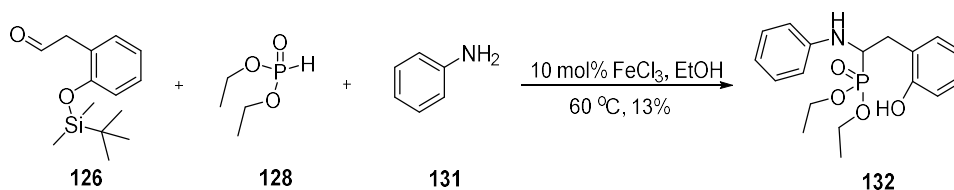
#### 4.7 Kabachnik-Fields Reaction

Diethylamine **129** and aniline **131** as active nucleophiles are able to take part in Kabachnik-Fields reactions to form  $\alpha$ -amino phosphonates by reaction with aryl acetaldehyde **126** and diethyl phosphite **128**. The three-component coupling of diethylamine **129**, benzeneacetaldehyde **126** and diethyl phosphite **128** in THF at 50 °C afforded the corresponding amino phosphonate **130** in 18% yield (Scheme 35).



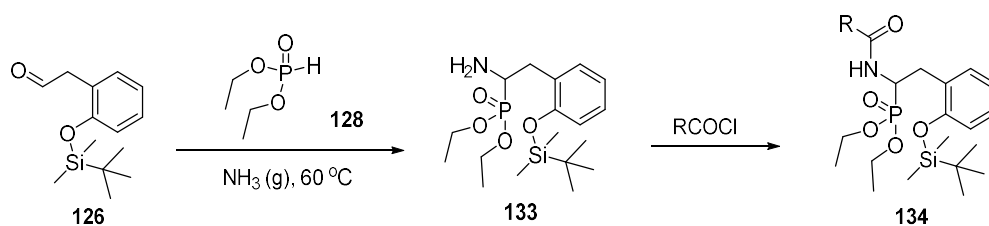
Scheme 35. Kabachnik-Fields reaction to form  $\alpha$ -amino phosphonate **130**.

When aniline **131** was used in the Kabachnik-Fields reaction in reaction with benzeneacetaldehyde **126** and diethyl phosphite **128**, although 10 mol% iron (III) chloride was added to facilitate the synthesis, the amino phosphonate **132** was obtained in a low yield (13%) (Scheme 36). The *tert*-butyldimethylsilyl group was removed from the product possibly during the work-up to remove iron(III) chloride after the reaction.



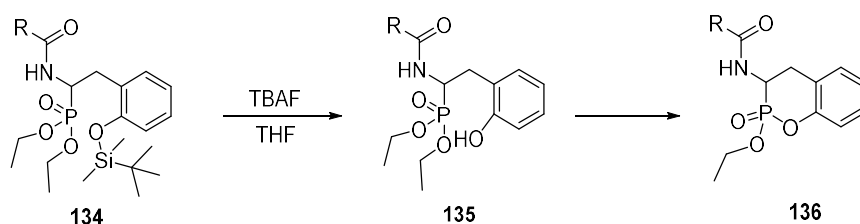
Scheme 36. Kabachnik-Fields reaction to form  $\alpha$ -amino phosphonate **132**.

Whilst the successful preparation of phosphonates **130** and **132**, future research will focus on the optimization of reactions to improve the yields. Other different amines will also be applied in the Kabachnik-Fields reaction, such as ammonia gas (Scheme 37). The product **133** of Kabachnik-Fields reaction using ammonia is able to form different amides **134** by reacting with acyl chlorides.



Scheme 37. Kabachnik-Fields reaction using ammonia gas followed by the formation of amides.

The success of Kabachnik-Fields reactions to prepare phosphonates makes it possible for cyclisation after the deprotection of *tert*-butyldimethylsilyl group, and the cyclised products **136** are expected to be  $\beta$ -lactamase or PBP inhibitors (Scheme 38).



Scheme 38. Possible synthetic route to cyclic phosphonate targets **136**.

## Chapter 5 Conclusion and Future Work

### 5.1 Thiazolidinones

The transglycosylase inhibitor thiazolidinone **4** and thiazolidinone probe I **18** with the PEG linker were successfully synthesised (Figure 34). Based on the MIC test results, thiazolidinone **4** inhibited the growth of *S. aureus* SH1000 at the concentration of 16 µg/mL. However, thiazolidinone probe I **18** did not display antibacterial activity at the concentrations of up to 128 µg/mL for *S. aureus* SH1000, which was not active enough to label bacteria.

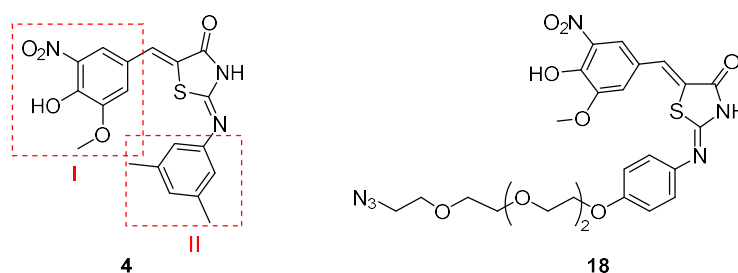


Figure 34. The structures of 2-[(3,5-dimethylphenyl)amino]-5-[(4-hydroxy-3-methoxy-5-nitrophenyl)methylene]-4(5H)-thiazolone **4** and 2-[[4-[2-[2-(2-azidoethoxy)ethoxy]ethoxy]phenyl]imino]-5-(4-hydroxy-3-methoxy-5-nitrobenzylidene)thiazolidin-4-one **18**.

In order to design new thiazolidinone probes with better antibiotic activity, a series of small molecule thiazolidinone derivatives were synthesised to investigate the structure-activity relationship of thiazolidinones (Figure 35). By comparing the activity of thiazolidinone **4** with the derivatives **22** and **28**, it was found that the two methyl groups on the ring II was important, and the PEG linker was not suitable to be added to the ring II. The MIC results of thiazolidinone derivatives **28**, **30** and **33** indicated that the nitro, hydroxy and methyl groups on the aromatic ring I were also necessary. To minimise the

influence of addition of the link, the PEG linker was added to the methyl group instead of replacing it.

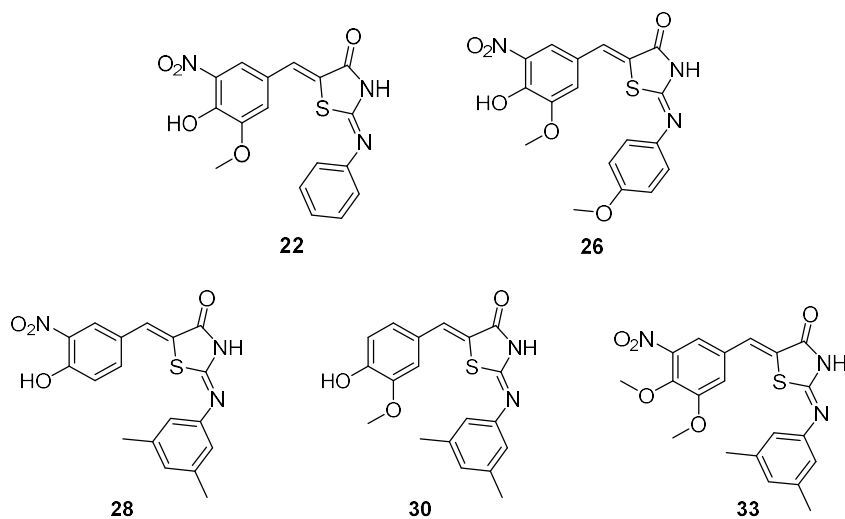


Figure 35. The structures of small molecule thiazolidinone derivatives.

According to the study of the structure-activity relationship, thiazolidinone probe II **42** with PEG linker and BODIPY dye was prepared (Figure 36). Unfortunately, it was still unable to inhibit the growth of *S. aureus* SH1000 at the concentration up to 128  $\mu\text{g/mL}$ .

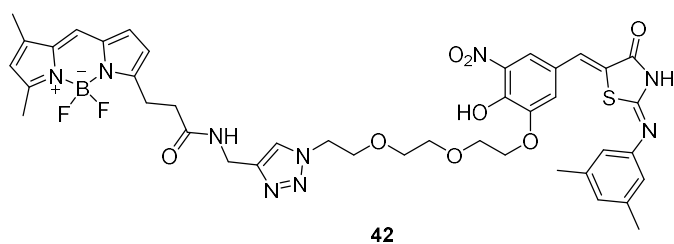


Figure 36. The structures of thiazolidinone probe II **42**.

Although the chemistry was successful to prepare thiazolidinone probes, they did not show good bioactivity qualified for further cell labelling. The structure-activity

relationship study highlights the difficulty for high activity against *S. aureus* when altering the structure of thiazolidinone **4**. In addition, the low solution in aqueous broth is also a problem for biological application. Due to the importance of investigating unknown mechanism of transglycosylation, new transglycosylase inhibitors will be screened and developed for chemical probes.

## 5.2 Quinazolinones

PBP1 and PBP2a inhibitor, quinazolinone **5** was synthesised and tested to show its antibiotic activity against *S. aureus* (Figure 37). Notably, it displayed good inhibitory effect against MSSA (Newman, NewHG) and MRSA (COL, JE2) strains with MIC of 2  $\mu\text{g/mL}$ , but it did not inhibit the growth of *S. aureus* SH1000 at the concentration up to 128  $\mu\text{g/mL}$ .

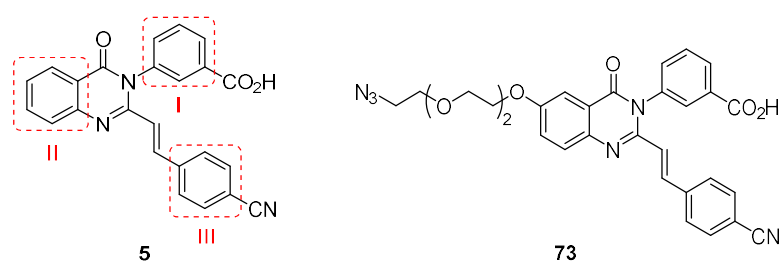


Figure 37. The structures of (*E*)-3-(3-carboxyphenyl)-2-(4-cyanostyryl)quinazolin-4(3*H*)-one **5** and quinazolinone probe **73**.

It was reported that quinazolinone **5** inhibited *S. aureus* PBP2a by binding to the allosteric site of *S. aureus* PBP2a through salt-bridge interactions of the carboxylic acid

group on the aromatic rings I. Therefore, it was not a good idea to attach the linker to the aromatic ring I and the new quinazolinone probes were designed by adding the PEG linker to the aromatic ring II or III.

Quinazolinone probe I **73** was prepared by attaching the PEG linker to the aromatic ring II (Figure 37). It only inhibited the growth of *S. aureus* COL at a concentration of 128  $\mu\text{g/mL}$  and had no effect on other MSSA or MRSA strains (SH1000, Newman, NewHG and JE2).

Quinazolinone (*E* isomer) **84** was synthesised which showed inhibitory effect at the concentration of 32 mg/mL against MSSA (Newman, NewHG) and MRSA (COL, JE2) strains. *E* isomer **84** was sensitive to the light and isomerised to quinazolinone (*Z* isomer) **85** which only had inhibitory effect on *S. aureus* COL at a concentration of 128  $\mu\text{g/mL}$ , but not on other *S. aureus* strains (SH1000, Newman, NewHG and JE2) (Figure 38).

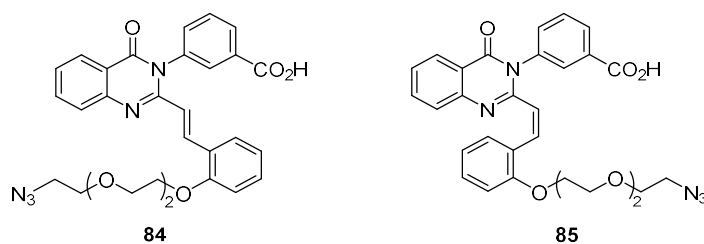


Figure 38. The structures of of quinazolinone *E* isomer **84** and *Z* isomer **85**.

After click reaction with BODIPY dye, quinazolinone probe II was isolated as *E* isomer **86** and *Z* isomer **87** (Figure 39). Both of them had inhibitory effect on *S. aureus* COL at



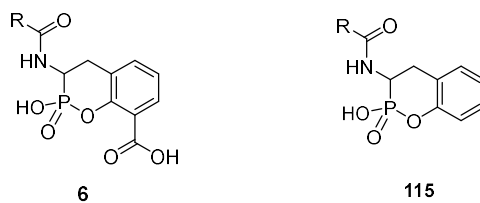


Figure 40. The structures of cyclic phosphonate **6** and the simplified target **115**.

The key intermediates,  $\alpha$ -amino phosphonates **130** and **132**, were successfully synthesised by Kabachnik-Fields reaction (Figure 41). More amines will be attempted in Kabachnik-Fields reaction to prepare novel  $\alpha$ -amino phosphonates.

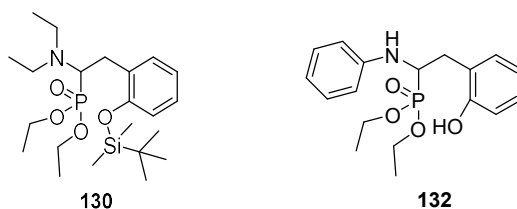


Figure 41. The structures of  $\alpha$ -amino phosphonates **130** and **132**.

The prepared  $\alpha$ -amino phosphonates, including **130** and **132**, will be cyclised to generate the target cyclic phosphonates followed by the biological assays to test the antibiotic activity.

## **Chapter 6 Experimental Procedures**

### **6.1 Biological Experimental**

#### **6.1.1 Growth Media**

All bacterial growth media were prepared in distilled water and sterilised by autoclaving at 121 °C for 20 min, 103 kilopascals.

#### **6.1.2 *Staphylococcus Aureus* Strains**

The strains were taken from glycerol stocks in Microbank storage beads (Pro-lab diagnostics) and streaked for single colonies onto TSB agar plates with or without antibiotics. Plates were incubated at 37 °C overnight and subsequently stored at 4 °C for up to two weeks. Liquid cultures were generally inoculated with a single colony into a culture and grown overnight at 37 °C with shaking at 250 rpm.

#### **6.1.3 Measurement by Optical Density**

To quantify the bacterial yield of a liquid culture, spectrophotometric measurements were conducted at the wavelength of 600 nm (OD<sub>600</sub>). Measurements were taken using a Biochrom WPA Biowave DNA Life Science spectrophotometer. While sterile culture media was used as the blank, necessary culture samples were diluted (1:10) to provide readings within the optimum accuracy range.

#### **6.1.4 Determination of MIC by Microdilution method**

100  $\mu$ L of TSB broth was dispensed into all wells of the 96 well microtitre plate. The test antibiotic solution was diluted in TSB at the double of the top concentration desired. Subsequently, 100  $\mu$ L of diluted antibiotic solution was pipetted into the wells of the first column of the plate. The antibiotics was mixed thoroughly by pipetting up and down without introducing bubbles. 100  $\mu$ L of antibiotic-media mixture was withdrew from the first column and added to the second followed by thorough mixing with pipette. Similarly, the mixture was transferred to the third column and the procedure was repeated to the last desired column (column 10). Finally, 100  $\mu$ L of mixture was discarded from column 10.

An overnight culture was diluted to an OD<sub>600</sub> of  $\sim$ 0.01 using fresh culture media. 100  $\mu$ L of bacteria was inoculated into wells in columns 1 to 11 and column 11 was used as positive control for visible growth. Column 12 was not inoculated and another 100  $\mu$ L of TSB was added as it was sterility control and blank for reading plates. The plates were incubated at 37 °C, 250 rpm overnight. For quinazolinones, aluminium foil was used to avoid light. The readings were measured with a Perkin VICTOR x3 2030 plate reader.

#### **6.1.5 Labelling Peptidoglycan Synthesis**

An SH1000 overnight culture was used to inoculate 50 mL TSB at OD<sub>600</sub> of 0.05 and grown at 37 °C, 250 rpm for 90 min to an OD<sub>600</sub> of  $\sim$ 0.3-0.5. 1 ml Aliquots were taken

and quinazolinone added at a concentration of 100  $\mu\text{g}/\text{mL}$ . Samples were then incubated at 37  $^{\circ}\text{C}$  on a rotary shaker for mixing for 20 min.

Cells were then pelleted by centrifugation and the collected cell pellets were re-suspended in 0.5 mL distilled water and 0.5 ml fixative [0.5mL 16% (w/v) paraformaldehyde in 2 mL PBS] for 20 min at room temperature on a rotator for mixing. Fixed cells were then washed in distilled water and the pellet collected by centrifugation. The click reaction was carried out afterwards. The fixed cells were incubated with 0.5 mL Click-iT reaction buffer mix and 5  $\mu\text{g}$  ATTO 488 dye (1 mg/mL) for 20 mins at room temperature.

#### **6.1.5.1 16% (w/v) Paraformaldehyde**

Paraformaldehyde	8 g
100 mM sodium phosphate buffer (pH 7.0)	50 mL

Paraformaldehyde (8 g) was added to 100 mM sodium phosphate buffer (pH 7.0, 40 mL). The solution was heated to 60  $^{\circ}\text{C}$  with vigorous mixing. While heating and mixing the solution,  $\geq 5$  M NaOH solution was added dropwise until the solution cleared. The solution was stored at 4  $^{\circ}\text{C}$  for up to 3 months.

### 6.1.5.2 Phosphate Buffered Saline (PBS)

NaCl	8 g/L
Na <sub>2</sub> HPO <sub>4</sub>	1.4 g/L
KCl	0.2 g/L
KH <sub>2</sub> PO <sub>4</sub>	0.2 g/L

The pH was adjusted to 7.4 with NaOH.

### 6.1.5.3 Click-iT® Reaction Buffer Mix

All buffer components were made up as per instructions from Molecular Probes.

Click-iT® cell reaction buffer	440 µL
Copper (II) sulphate (100 mM)	10 µL
Click-iT® cell buffer additive	50 µL

### 6.1.6 Fluorescence Microscopy

DeltaVision deconvolution microscope (Applied Precision, GE Healthcare) was used to acquire fluorescence images. All the images obtained were deconvolved using SoftWoRx v.3.5.1 software and processed using Fiji processing package.

## **6.2 Chemical Experimental**

### **6.2.1 Solvents and Reagents**

Anhydrous solvents were obtained from the University of Sheffield Department of Chemistry Grubbs solvent system and stored under a positive pressure of argon with 4Å molecular sieves. All starting materials were purchased from Sigma Aldrich, Alfa Aesar, Fisher Scientific, Fluorochem, Lancaster or Lumiprobe, and used as purchased except where noted. Air sensitive reactions were conducted in flame-dried glassware under an atmosphere of nitrogen or argon unless otherwise stated.

### **6.2.2 Chromatography**

Reactions were monitored using thin layer chromatography (TLC) on precoated aluminium-backed plates (Merck silica gel 60Å F<sub>254</sub>). Materials were visualized by 254 nm ultraviolet light followed by staining with potassium permanganate dip. Purification of products was performed by flash column chromatography using normal phase silica gel 40-63 µm 60Å.

### **6.2.3 Melting point**

All melting points were determined using a Gallenkamp melting point apparatus equipped with a thermometer.

#### **6.2.4 IR spectroscopy**

Infrared spectra were recorded using a Diamond ATR (attenuated total reflection) accessory on a Perkin-Elmer Spectrum 65 or 100 FT-IR spectrometer.

#### **6.2.5 NMR spectroscopy**

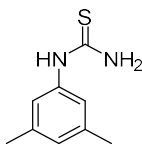
$^1\text{H}$ ,  $^{13}\text{C}$  and  $^{31}\text{P}$  NMR spectra were recorded in  $\text{CDCl}_3$ , MeOD or  $\text{DMSO-d}_6$  on Bruker Avance 400 or Bruker Avance III HD 500 spectrometer at 298 K. Chemical shifts ( $\delta$ ) are reported in parts per million (ppm) relative to the internal reference and coupling constant ( $J$ ) values are given in Hertz (Hz). (s = singlet, d = doublet, t = triplet, q = quartet, m = multiplet, br s = broad singlet, br d = broad doublet, app d = apparent doublet, app t = apparent triplet, dd = doublet of doublets, td = triplet of doublets.)

#### **6.2.6 Mass spectroscopy**

Mass spectra ( $m/z$ ) were recorded using electron ionisation (EI), electrospray ionisation (ESI) or direct infusion using either a Micromass LCT mass spectrometer or a Walter ITC Premier XE instrument.

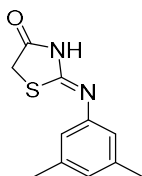
## 6.2.7 Chemical Synthesis

### (3,5-Dimethylphenyl)thiourea **8**



Ammonium thiocyanate (6.13 g, 80.53 mmol) was dissolved in hydrochloric acid (1 M, 75 mL) and 3,5-dimethylaniline **7** (10 mL, 80.53 mmol) added. The reaction mixture was heated at reflux overnight. The reaction mixture was cooled to room temperature and refrigerated for 1.5 h to aid precipitation. The product was filtered under vacuum and washed with water (10 mL) and diethyl ether (20 mL). It was dried under high vacuum to afford the title compound as a light brown solid (5.56 g, 38%); m.p. 179 - 181 °C [lit.<sup>106</sup> m.p. 174 - 176 °C].  $\nu_{\max}(\text{ATR})/\text{cm}^{-1}$  3406, 3170, 3050, 1619, 1609, 1542;  $\delta_{\text{H}}$  (400 MHz, DMSO-*d*<sub>6</sub>) 2.24 (6H, s, 2 × *CH*<sub>3</sub>), 6.77 (1H, s, *ArH*), 6.95 (2H, s, *ArH*), 9.58 (1H, s, *NH*); *m/z* (*ES*<sup>+</sup>) 181 (*M+H*<sup>+</sup>). The data agree with those reported in the literature.<sup>106</sup>

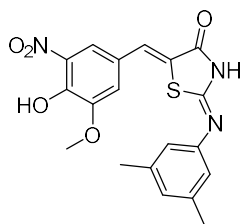
### 2-[(3,5-Dimethylphenyl)amino]-4(5*H*)-thiazolone **9**



(3,5-Dimethylphenyl)thiourea **8** (2.10 g, 11.65 mmol) and sodium acetate (1.33 g, 16.21 mmol) were dissolved in ethanol (20 mL). Ethyl chloroacetate (1.73 mL, 16.21 mmol) was added and the reaction was heated at 90 °C overnight. The reaction mixture was cooled to room temperature and a precipitate formed that was filtered and dried under

vacuum to afford the title compound as a light yellow solid in a quantitative yield (2.98 g). m.p. 222 - 224 °C;  $\nu_{\max}(\text{ATR})/\text{cm}^{-1}$  3165 (NH), 2912, 2730, 1692 (CO), 1618, 1578;  $\delta_{\text{H}}$  (400 MHz,  $\text{CDCl}_3$ ) 2.35 (6H, s,  $2 \times \text{CH}_3$ ), 3.89 (2H, s,  $\text{CH}_2$ ), 6.92 (1H, s,  $\text{ArH}$ ), 6.94 (2H, s,  $\text{ArH}$ );  $\delta_{\text{C}}$  (126 MHz,  $\text{CDCl}_3$ ) 21.3 ( $2 \times \text{CH}_3$ ), 36.7 ( $\text{CH}_2$ ), 120.5 ( $2 \times \text{ArCH}$ ), 128.3 ( $\text{ArCH}$ ), 139.4 ( $2 \times \text{ArCMe}$ ), 140.7 ( $\text{ArCN}$ ), 171.5 (NCNH), 180.3 (CO);  $m/z$  ( $\text{ES}^+$ ) 221.0742 (100%,  $\text{M}+\text{H}^+$ .  $\text{C}_{11}\text{H}_{13}\text{N}_2\text{OS}$  requires 221.0743).

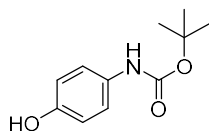
**2-[(3,5-Dimethylphenyl)amino]-5-[(4-hydroxy-3-methoxy-5-nitrophenyl)methylene]-4(5H)-thiazolone 4**



2-[(3,5-Dimethylphenyl)amino]-4(5H)-thiazolone **9** (303 mg, 1.38 mmol) was dissolved in glacial acetic acid (15 mL). 5-Nitrovanillin (272 mg, 1.38 mmol) and sodium acetate (226 mg, 2.75 mmol) were added and the reaction was heated at 130 °C overnight. The reaction mixture was cooled to room temperature and the precipitate formed. The product was filtered and stirred in diethyl ether (30 mL) overnight and then filtered again, dried under vacuum to afford the title compound as an orange solid (305 mg, 55%). m.p. 244 - 246 °C;  $\nu_{\max}(\text{ATR})/\text{cm}^{-1}$  3365 (OH), 2917, 1696 (CO), 1631, 1603, 1586, 1534 (NO);  $\delta_{\text{H}}$  (400 MHz,  $\text{CDCl}_3$ ) 2.38 (6H, s,  $2 \times \text{CH}_3$ ), 3.98 (3H, s,  $\text{OCH}_3$ ), 6.82 (2H, s,  $2 \times \text{ArH}$ ), 6.95 (1H, s,  $\text{ArH}$ ), 7.20 (1H, s,  $\text{Ar-CH}$ ), 7.67 (1H, s,  $\text{ArH}$ ), 7.85 (1H, s,  $\text{ArH}$ );  $\delta_{\text{C}}$  (126

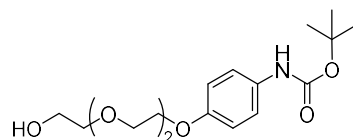
MHz, CDCl<sub>3</sub>) 21.4 (2 × CH<sub>3</sub>), 56.9 (OCH<sub>3</sub>), 117.2 (ArCH), 118.2 (ArCH), 119.7 (2 × ArCH), 124.6 (ArC), 125.3 (ArC), 128.2 (ArCH), 129.2 (Ar-CH), 134.0 (CCO), 139.5 (2 × ArCMe), 143.5 (ArC), 147.3 (ArC), 150.5 (ArC), 156.7 (NCNH), 174.9 (CO); *m/z* (ES<sup>+</sup>) 400.0967 (100%, M+H<sup>+</sup>. C<sub>19</sub>H<sub>18</sub>N<sub>3</sub>O<sub>5</sub>S requires 400.0962).

### ***tert*-Butyl *N*-(4-hydroxyphenyl)carbonate **11****



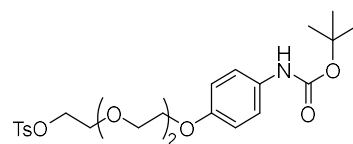
4-Aminophenol **10** (8.3 g, 76.0 mmol) was solubilized in THF (150 mL) at room temperature. A solution of di-*tert*-butyl dicarbonate (16.8 g, 76.0 mmol) in THF (50 mL) was added dropwise to the reaction. The reaction mixture was vigorously stirred at 40 °C for 3 days which was then concentrated in a rotary evaporator under reduced pressure. This was washed with petroleum ether (50 mL), filtered and dried under vacuum to afford the title compound as a white solid (14.9 g, 94%). m.p. 132 - 134 °C [lit.<sup>107</sup> m.p. 142 - 143 °C];  $\nu_{\max}$ (ATR)/cm<sup>-1</sup> 3359 (OH), 1696 (CO), 1512;  $\delta_{\text{H}}$  (400 MHz, DMSO-d<sub>6</sub>) 1.45 (9H, s, 3 × CH<sub>3</sub>), 6.64 [2H, (AX)<sub>2</sub>, ArH], 7.21 (2H, br d, *J* 8.0, ArH), 9.00 (1H, br s, OH), 9.05 (1H, s, NH); *m/z* (ES<sup>-</sup>) 208 [(M-H)<sup>-</sup>]. The data are in broad agreement with those reported in the literature.<sup>107, 108</sup>

***tert*-Butyl *N*-[4-[2-[2-(2-hydroxyethoxy)ethoxy]ethoxy]phenyl]carbamate **12****



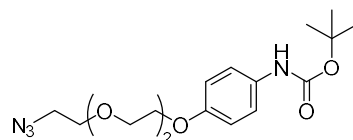
*tert*-Butyl *N*-(4-hydroxyphenyl)carbamate **11** (4.0 g, 19.1 mmol) was dissolved in acetonitrile (20 mL). 2-[2-(2-Chloroethoxy)ethoxy]ethanol (2.3 mL, 15.9 mmol), potassium carbonate (6.6 g, 47.7 mmol) and sodium iodide (238 mg, 1.6 mmol) were added to this solution at room temperature. The reaction mixture was vigorously stirred at 90 °C for 3 days. After cooling to room temperature, the solvent was removed using a rotary evaporator under reduced pressure and water (50 mL) was added to the crude residue. The mixture was extracted with ethyl acetate (3 × 50 mL). The combined organic phases were washed with brine (50 mL), dried over anhydrous MgSO<sub>4</sub>, filtered and the filtrate was evaporated under reduced pressure. The crude residue was purified by dry flash chromatography on silica gel, eluting petroleum ether/EtOAc, EtOAc: 50-100% to afford the title compound as a light yellow oil (5.4 g, 70%).  $\nu_{\text{max}}$ (ATR)/cm<sup>-1</sup> 3316 (OH), 2873, 1700 (CO), 1600, 1512;  $\delta_{\text{H}}$  (400 MHz, CDCl<sub>3</sub>) 1.51 (9H, s, 3 × CH<sub>3</sub>), 3.61 (2H, app t, *J* 4.5, CH<sub>2</sub>), 3.65-3.77 (6H, m, 3 × CH<sub>2</sub>), 3.84 (2H, app t, *J* 4.7, CH<sub>2</sub>), 4.09 (2H, app t, *J* 4.7, CH<sub>2</sub>), 6.57 (1H, br s, NH), 6.85 (2H, d, *J* 8.9, ArH), 7.26 (2H, br d, *J* 7.9, ArH); *m/z* (ES<sup>+</sup>) 380 (15%, M+K<sup>+</sup>), 364 (100, M+Na<sup>+</sup>), 308 (10). The data agree with those reported in the literature.<sup>108</sup>

**2-[2-[2-[4-(*tert*-Butoxycarbonylamino)phenoxy]ethoxy]ethoxy]ethyl-4-methylbenzenesulfonate 13**



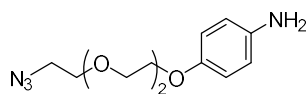
*tert*-Butyl *N*-[4-[2-[2-(2-hydroxyethoxy)ethoxy]ethoxy]phenyl]carbamate **12** (3.18 g, 9.30 mmol) was dissolved in dry DCM (20 mL). *p*-Toluene sulfonyl chloride (3.55 g, 18.6 mmol), 4-dimethylaminopyridine (228 mg, 1.90 mmol) and triethylamine (3.90 mL, 27.9 mmol) were added to the solution and the reaction mixture was stirred at the room temperature under N<sub>2</sub> overnight. The reaction was washed with 1M HCl (15 mL), brine (15 mL), dried over anhydrous MgSO<sub>4</sub>, filtered and the filtrate was evaporated under reduced pressure. The residue was purified by dry flash chromatography (petroleum ether/EtOAc, EtOAc: 30%) to afford the title compound as a viscous yellow oil (3.5 g, 76%).  $\nu_{\max}$ (ATR)/cm<sup>-1</sup> 3338 (NH), 2874, 1717 (CO), 1598, 1513;  $\delta_{\text{H}}$  (400 MHz, MeOD) 1.53 (9H, s, 3 × CH<sub>3</sub>), 2.45 (3H, s, CH<sub>3</sub>), 3.55-3.70 (6H, m, 3 × CH<sub>2</sub>), 3.79 [2H, (AX)<sub>2</sub>, CH<sub>2</sub>], 4.08 [2H, (AX)<sub>2</sub>, CH<sub>2</sub>], 4.16 [2H, (AX)<sub>2</sub>, CH<sub>2</sub>], 6.86 [2H, (AX)<sub>2</sub>, ArH], 7.29 (2H, br d, *J* 8.8, ArH), 7.44 (2H, d, *J* 8.0, ArH), 7.80 [2H, (AX)<sub>2</sub>, ArH]; *m/z* (ES<sup>+</sup>) 518 (55%, M+Na<sup>+</sup>), 496 (25, M+H<sup>+</sup>), 440 (100), 396 (35). The data agree with those reported in the literature.<sup>108</sup>

***tert*-Butyl [4-[2-[2-(2-azidoethoxy)ethoxy]ethoxy]phenyl]carbamate **14****



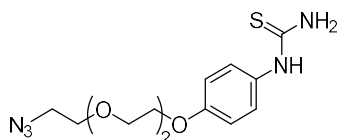
2-[2-[2-[4-(*tert*-Butoxycarbonylamino)phenoxy]ethoxy]ethoxy]ethyl-4-methylbenzenesulfonate **13** (3.36 g, 6.78 mmol) was dissolved in dry DMF (20 mL) under N<sub>2</sub>. Sodium azide (0.53 g, 8.14 mmol) was added to the solution and the reaction mixture was stirred at 50 °C under N<sub>2</sub> overnight. The solvent was evaporated in a rotary evaporator under reduced pressure. Ethyl acetate (50 mL) and water (30 mL) were added, and the organic layer separated, washed with brine (5 × 30 mL), dried over anhydrous MgSO<sub>4</sub>, filtered and concentrated under reduced pressure to afford the title compound that did not require any further purification as a yellow oil (2.43 g, 98%).  $\nu_{\max}(\text{ATR})/\text{cm}^{-1}$  3332 (NH), 2976, 2871, 2097 (N<sub>3</sub>), 1718 (CO), 1599, 1512;  $\delta_{\text{H}}$  (400 MHz, MeOD) 1.52 (9H, s, 3 × CH<sub>3</sub>), 3.37 (2H, br t, *J* 4.9, CH<sub>2</sub>), 3.65-3.75 (6H, m, 3 × CH<sub>2</sub>), 3.84 (2H, app t, *J* 4.7, CH<sub>2</sub>), 4.09 (2H, app t, *J* 4.7, CH<sub>2</sub>), 6.87 [2H, (AX)<sub>2</sub>, ArH], 7.29 (2H, d, *J* 8.6, ArH);  $\delta_{\text{C}}$  (101 MHz, MeOD) 27.4 (3 × CH<sub>3</sub>), 50.4 (CCH<sub>3</sub>), 67.5 (CH<sub>2</sub>), 69.6 (CH<sub>2</sub>), 69.8 (CH<sub>2</sub>), 70.2 (CH<sub>2</sub>), 70.4 (CH<sub>2</sub>), 114.4 (2 × ArCH), 120.3 (2 × ArCH), 132.3 (ArCN), 154.3 (ArCO), 154.7 (C=O); *m/z* (ES<sup>+</sup>) 384.2241 (55%, M+NH<sub>4</sub><sup>+</sup>. C<sub>17</sub>H<sub>30</sub>N<sub>5</sub>O<sub>5</sub> requires 384.2241).

#### 4-[2-[2-(2-Azidoethoxy)ethoxy]ethoxy]aniline **15**



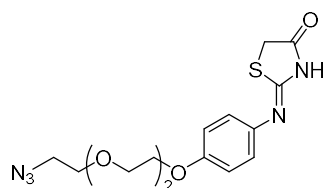
*tert*-Butyl [4-[2-[2-(2-azidoethoxy)ethoxy]ethoxy]phenyl]carbamate **14** (2.25 g, 6.14 mmol) was dissolved in DCM (20 mL). Trifluoroacetic acid (10 mL) was added to the solution and the reaction mixture was stirred at the room temperature overnight. The solvent was removed by co-evaporation with DCM (20 mL) in a rotary evaporator under reduced pressure. The crude product in ethyl acetate (30 mL) was washed with sat. NaHCO<sub>3</sub> (2 × 20 mL). The aqueous phase was back-extracted with ethyl acetate (20 mL). The combined organic phase were washed with brine (30 mL), dried over anhydrous MgSO<sub>4</sub>, filtered and concentrated on a rotary evaporator under reduced pressure to afford the title compound as a brown oil (982 mg, 60%) that did not require any further purification.  $\nu_{\max}(\text{ATR})/\text{cm}^{-1}$  3358 (NH), 2918, 2871, 2096 (N<sub>3</sub>), 1627, 1508;  $\delta_{\text{H}}$  (400 MHz, CDCl<sub>3</sub>) 3.41 (2H, t, *J* 5.1, CH<sub>2</sub>), 3.68-3.78 (6H, m, 3 × CH<sub>2</sub>), 3.85 (2H, app t, *J* 4.9, CH<sub>2</sub>), 4.08 (2H, app t, *J* 4.9, CH<sub>2</sub>), 6.65 [2H, (AX)<sub>2</sub>, ArH], 6.78 [2H, (AX)<sub>2</sub>, ArH]; *m/z* (ES<sup>+</sup>) 305 (30%, M+K<sup>+</sup>), 289 (100%, M+Na<sup>+</sup>), 267 (35%, M+H<sup>+</sup>). The data agree with those reported in the literature.<sup>108</sup>

## 1-[4-[2-[2-(2-Azidoethoxy)ethoxy]ethoxy]phenyl]thiourea **16**



4-[2-[2-(2-Azidoethoxy)ethoxy]ethoxy]aniline **15** (613 mg, 2.30 mmol) was dissolved in 1,4-dioxane (3 mL). Ammonium thiocyanate (176 mg, 2.30 mmol) was added and the reaction mixture was stirred at 110 °C for 2 days. After cooling to room temperature, the solvent was removed using a rotary evaporator under reduced pressure and the residue was purified by flash chromatography on silica gel, eluting with petroleum ether/EtOAc (EtOAc: 50-80%) to afford the title compound as an orange oil (320 mg, 43%).  $\nu_{\text{max}}(\text{ATR})/\text{cm}^{-1}$  2868, 2094 ( $\text{N}_3$ ), 1507;  $\delta_{\text{H}}$  (400 MHz,  $\text{CDCl}_3$ ) 3.41 (2H, app. t,  $J$  5.0,  $\text{CH}_2$ ), 3.67-3.79 (6H, m,  $3 \times \text{CH}_2$ ), 3.90 (2H, app t,  $J$  4.8,  $\text{CH}_2$ ), 4.16 (2H, app t,  $J$  4.8,  $\text{CH}_2$ ), 6.99 [2H, (AX) $_2$ , ArH], 7.18 [2H, (AX) $_2$ , ArH], 7.77 (1H, br s, NH);  $\delta_{\text{C}}$  (101 MHz,  $\text{CDCl}_3$ ) 50.7 ( $\text{CH}_2$ ), 67.8 ( $\text{CH}_2$ ), 69.7 ( $\text{CH}_2$ ), 70.1 ( $\text{CH}_2$ ), 70.8 ( $\text{CH}_2$ ), 70.9 ( $\text{CH}_2$ ), 116.0 ( $2 \times \text{ArCH}$ ), 127.3 ( $2 \times \text{ArCH}$ ), 128.9 (ArC), 158.5 (ArC), 182.2 (CS);  $m/z$  ( $\text{ES}^+$ ) 326.1282 (100%,  $\text{M}+\text{H}^+$ ).  $\text{C}_{13}\text{H}_{20}\text{N}_5\text{O}_3\text{S}$  requires 326.1281).

## 2-[[4-[2-[2-(2-Azidoethoxy)ethoxy]ethoxy]phenyl]imino]thiazolidin-4-one **17**

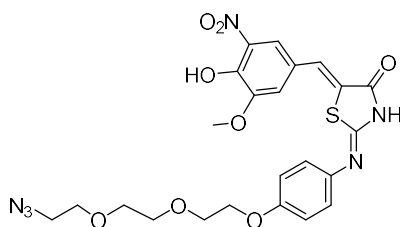


1-[4-[2-[2-(2-Azidoethoxy)ethoxy]ethoxy]phenyl]thiourea **16** (230 mg, 0.71 mmol) and sodium acetate (85 mg, 1.06 mmol) were dissolved in ethanol (2 mL). Ethyl chloroacetate

(0.12 mL, 1.06 mmol) was added and the reaction was heated at 90 °C overnight. The reaction mixture was cooled to room temperature and the solvent was removed using a rotary evaporator under reduced pressure. The crude product in ethyl acetate (20 mL) was washed with water (10 mL), followed by brine (10 mL). The organic phase was dried over anhydrous MgSO<sub>4</sub>, filtered and concentrated on a rotary evaporator under reduced pressure to afford the title compound as a viscous brown oil (252 mg, 97%).

$\nu_{\text{max}}(\text{ATR})/\text{cm}^{-1}$  2869, 2098 (N<sub>3</sub>), 1607, 1505;  $\delta_{\text{H}}$  (400 MHz, CDCl<sub>3</sub>) 3.41 (2H, app. t, *J* 5.1, CH<sub>2</sub>), 3.68-3.80 (6H, m, 3 × CH<sub>2</sub>), 3.87 (2H, s, SCH<sub>2</sub>), 3.90 (2H, app t, *J* 4.8, CH<sub>2</sub>), 4.17 (2H, app t, *J* 4.8, CH<sub>2</sub>), 6.97 [2H, (AX)<sub>2</sub>, ArH], 7.27 [2H, (AX)<sub>2</sub>, ArH];  $\delta_{\text{C}}$  (101 MHz, CDCl<sub>3</sub>) 37.2 (SCH<sub>2</sub>), 50.7 (CH<sub>2</sub>), 67.7 (CH<sub>2</sub>), 69.8 (CH<sub>2</sub>), 70.1 (CH<sub>2</sub>), 70.8 (CH<sub>2</sub>), 70.9 (CH<sub>2</sub>), 115.4 (2 × ArCH), 124.9 (2 × ArCH), 132.6 (ArC), 157.7 (ArC), 175.4 (NCNH), 182.0 (NCO); *m/z* (ES<sup>+</sup>) 366.1 (100%, M+H<sup>+</sup>. C<sub>15</sub>H<sub>20</sub>N<sub>5</sub>O<sub>4</sub>S requires 366.1).

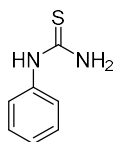
**2-[[4-[2-[2-(2-Azidoethoxy)ethoxy]ethoxy]phenyl]imino]-5-(4-hydroxy-3-methoxy-5-nitrobenzylidene)thiazolidin-4-one 18**



2-[[4-[2-[2-(2-Azidoethoxy)ethoxy]ethoxy]phenyl]imino]thiazolidin-4-one **17** (80 mg, 0.22 mmol) was dissolved in glacial acetic acid (3 mL). 5-Nitrovanillin (43 mg, 0.22 mmol) and sodium acetate (36 mg, 0.44 mmol) were added and the reaction was heated

at 130 °C for 24h. The reaction mixture was cooled to room temperature and the solvent was removed using a rotary evaporator under reduced pressure. The mixture was purified via preparative HPLC using an “Waters Xbridge C 18 4.6 × 250 mm” column [40 to 95% MeCN in aqueous TFA (0.1%) over 20 mins, 240 nm] to afford the title compound as an orange solid (58 mg, 48%). m.p. 136 - 138 °C;  $\nu_{\max}(\text{ATR})/\text{cm}^{-1}$  3206 (OH), 2928, 2870, 2100 (N<sub>3</sub>), 1673 (CO), 1611, 1507 (NO);  $\delta_{\text{H}}$  (400 MHz, CDCl<sub>3</sub>) 3.43 (2H, app t, *J* 4.2, CH<sub>2</sub>), 3.65-3.85 (6H, m, 3 × CH<sub>2</sub>), 3.93 (2H, app t, *J* 4.0, CH<sub>2</sub>), 3.98 (3H, s, CH<sub>3</sub>), 4.20 (2H, app t, *J* 4.0, CH<sub>2</sub>), 7.00-7.10 (2H, m, 2 × ArH), 7.15-7.26 (3H, m, 2 × ArH, Ar-CH), 7.73 (1H, s, ArH), 7.83 (1H, s, ArH);  $\delta_{\text{C}}$  (126 MHz, CDCl<sub>3</sub>) 50.7 (CH<sub>2</sub>), 57.0 (CH<sub>3</sub>), 67.8 (CH<sub>2</sub>), 69.8 (CH<sub>2</sub>), 70.1 (CH<sub>2</sub>), 70.8 (CH<sub>2</sub>), 70.9 (CH<sub>2</sub>), 115.6 (2 × ArCH), 117.2 (ArCH), 118.1 (ArCH), 123.6 (2 × ArCH), 124.7 (ArC), 125.3 (ArC), 129.0 (Ar-CH), 134.0 (CCO), 139.3 (ArC), 147.2 (ArC), 150.5 (ArC), 157.3 (ArC), 157.4 (NCNH), 175.8 (CO); *m/z* (ES<sup>+</sup>) 545.1458 (100%, M+H<sup>+</sup>. C<sub>23</sub>H<sub>25</sub>N<sub>6</sub>O<sub>8</sub>S requires 545.1449).

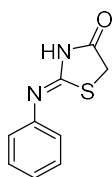
### ***N*-Phenylthiourea 20**



Concentrated hydrochloric acid (4.60 mL, 55.28 mmol) was added dropwise to aniline **19** (5.00 mL, 55.3 mL) with continuous stirring. After 30 min, the solution appeared turbid and a saturated solution of ammonium thiocyanate (5.00 g, 65.68 mmol) in water (10 mL) was added slowly. The reaction mixture was heated at reflux for 1 h until the

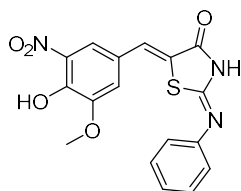
solution appeared turbid again. The turbid solution was poured in ice cold water. The separated precipitate was filtered and recrystallised from water giving the title compound as a white solid (1.70 g, 20%); m.p. 146 - 148 °C [lit.<sup>109</sup> m.p. 148.3 °C];  $\delta_{\text{H}}$  (400 MHz, DMSO- $d_6$ ) 7.03-7.15 (1H, m, *p*-ArH), 7.28-7.35 (2H, m, *o*-ArH), 7.36-7.43 (2H, m, *m*-ArH), 9.70 (1H, s, NH); m/z (ES<sup>-</sup>) 151 [20%, (M-H)<sup>-</sup>], 117 (10), 114 (100). The data agree with those reported in the literature.<sup>109, 110</sup>

### 2-(Phenylamino)-4(5H)-thiazolone **21**



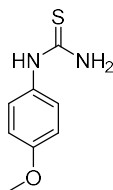
Ethyl chloroacetate (0.50 mL, 4.00 mmol) was added to a magnetically stirred suspension of *N*-phenylthiourea **20** (302 mg, 2.00 mmol) and anhydrous sodium acetate (820 mg, 10.00 mmol) in absolute ethanol (7 mL). The reaction was heated at 90 °C overnight. After cooling to room temperature, a precipitate formed which was cooled in the fridge for 1h for further precipitation. The precipitate was filtered, washed with water (50 mL) and diethyl ether (50 mL), dried under vacuum to afford the title compound as an off-white solid (246 mg, 64%). m.p. 174 - 176 °C [lit.<sup>111</sup> m.p. 172 - 174 °C];  $\delta_{\text{H}}$  (400 MHz, DMSO- $d_6$ ) 3.92 - 4.08 (2H, m, CH<sub>2</sub>), 6.93 - 7.04 (1H, m, ArH), 7.11 - 7.21 (1H, m, ArH), 7.30 - 7.45 (2H, m, 2 × ArH), 7.65 - 7.75 (1H, m, ArH), 10.80 - 12.10 (1H, m, NH); m/z (ES<sup>-</sup>) 191 [100%, (M-H)<sup>-</sup>]. The data agree with those reported in the literature.<sup>111, 112</sup>

**5-[(4-Hydroxy-3-methoxy-5-nitrophenyl)methylene]-2-(phenylamino)-4(5H)-thiazolone 22**



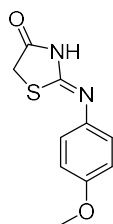
Glacial acetic acid (5 mL) was added to 2-(phenylamino)-4(5H)-thiazolone **21** (100 mg, 0.52 mmol), 5-nitrovanillin (103 mg, 0.52 mmol) and sodium acetate (85 mg, 1.04 mmol). The reaction mixture was stirred and heated at 120 °C overnight. The reaction mixture was cooled to room temperature and the precipitate formed. The crude was filtered and washed with diethyl ether (30 mL), dried under vacuum to afford the title compound as an orange solid (119 mg, 62%). m.p. 280 - 284 °C;  $\nu_{\max}(\text{ATR})/\text{cm}^{-1}$  3238 (OH), 2766, 1707 (CO), 1678, 1647, 1595, 1574, 1543;  $\delta_{\text{H}}$  (400 MHz, DMSO- $d_6$ ) 3.82 – 4.00 (3H, m, OCH<sub>3</sub>), 7.08 (1H, d, *J* 7.1, ArH), 7.22 (1H, t, *J* 7.1, ArH), 7.43 (2H, q, *J* 8.0, 2 × ArH), 7.48 – 7.86 (4H, m, 3 × ArH, Ar-CH), 11.65 (1H, s, OH);  $\delta_{\text{C}}$  (126 MHz, DMSO- $d_6$ ) 57.2 (OCH<sub>3</sub>), 117.4 (2 × ArCH), 120.9 (2 × ArCH), 124.9 (ArC), 125.7 (ArCH), 127.2 (ArC), 128.5 (Ar-CH), 129.7 (ArCH), 130.0 (ArCH), 137.6 (CCO), 138.8 (ArC), 144.5 (ArC), 150.4 (ArC), 170.7 (NCNH), 180.8 (NCO); *m/z* (ES<sup>+</sup>) 372.0656 (100%, M+H<sup>+</sup>. C<sub>17</sub>H<sub>14</sub>N<sub>3</sub>O<sub>5</sub>S requires 372.0649).

### ***N*-(4-Methoxyphenyl)thiourea **24****



Hydrochloric acid (1M, 50 mL) was added to *p*-anisidine **23** (5.00 g, 40.6 mmol) and ammonium thiocyanate (3.09 g, 40.6 mmol). The reaction mixture was stirred and heated at 110 °C overnight. After cooling to room temperature, the reaction mixture was refrigerated for 1.5 h to aid precipitation. The product was filtered under vacuum and washed with water (30 mL) and diethyl ether (30 mL). It was dried under high vacuum to afford the title compound as a purple solid (2.59 g, 35%). m.p. 208 - 210 °C [lit.<sup>113</sup> m.p. 209 - 210 °C];  $\delta_{\text{H}}$  (400 MHz, DMSO- $d_6$ ) 3.73 (3H, s,  $\text{CH}_3$ ), 6.90 [2H, (AX)<sub>2</sub>, 2  $\times$   $\text{ArH}$ ], 7.22 (2H, d,  $J$  8.6, 2  $\times$   $\text{ArH}$ ), 9.49 (1H, s,  $\text{NH}$ );  $m/z$  ( $\text{ES}^+$ ) 183 (100%,  $\text{MH}^+$ ). The data agree with those reported in the literature.<sup>109, 113, 114</sup>

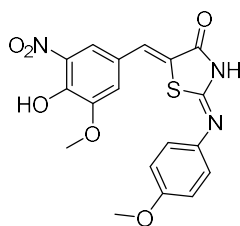
### **2-[(4-Methoxyphenyl)amino]-4(5*H*)-thiazolone **25****



*N*-(4-Methoxyphenyl)thiourea **24** (1.00 g, 5.49 mmol) and sodium acetate (613 g, 7.47 mmol) were dissolved in ethanol (8 mL). Ethyl chloroacetate (0.80 mL, 7.47 mmol) was added and the reaction was heated at 80 °C overnight. The reaction mixture was cooled to room temperature and refrigerated for 1.5 h to aid precipitation. The precipitate formed

was filtered and dried under vacuum to afford the title compound as a brown crystal (1.14 g, 93%). m.p. 178 - 180 °C [lit.<sup>115</sup> m.p. 178.1 – 178.2 °C];  $\nu_{\max}(\text{ATR})/\text{cm}^{-1}$  3006 (NH), 1669 (C=O), 1636, 1612, 1575;  $\delta_{\text{H}}$  (400 MHz, DMSO- $d_6$ ) 3.75 (3H, s,  $\text{CH}_3$ ), 3.94 (1H, s,  $\text{CHH}$ ), 3.99 (1H, s,  $\text{CHH}$ ), 6.90 – 7.05 (3H, m,  $3 \times \text{ArH}$ ), 7.60 (1H, d  $J$  9.0,  $\text{ArH}$ ), 10.70 – 11.95 (1H, m,  $\text{NH}$ );  $m/z$  ( $\text{ES}^+$ ) 223 (100%,  $\text{MH}^+$ ). The data agree with those reported in the literature.<sup>115, 116</sup>

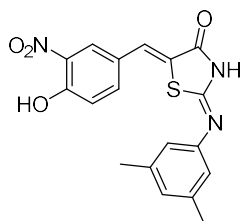
**5-[(4-Hydroxy-3-methoxy-5-nitrophenyl)methylene]-2-[(4-methoxyphenyl)amino]-4(5H)-thiazolone 26**



Glacial acetic acid (20 mL) was added 2-[(4-methoxyphenyl)amino]-4(5H)-thiazolone **25** (500 mg, 2.25 mmol), 5-nitrovanillin (443 mg, 2.25 mmol) and sodium acetate (369 mg, 4.50 mmol). The reaction mixture was stirred and heated at 120 °C overnight. The reaction mixture was cooled to room temperature and the precipitate formed. The crude was filtered and washed with diethyl ether (50 mL), dried under vacuum to afford the title compound as an orange solid (823 mg, 91%). m.p. 240 - 242 °C;  $\nu_{\max}(\text{ATR})/\text{cm}^{-1}$  3395 (OH), 2796, 1695 (CO), 1603, 1532, 1511;  $\delta_{\text{H}}$  (400 MHz, DMSO- $d_6$ ) 3.70 – 3.95 (6H, m,  $2 \times \text{OCH}_3$ ), 6.90 – 7.11 (3H, m,  $3 \times \text{ArH}$ ), 7.32 – 7.80 (4H, m,  $3 \times \text{ArH}$ ,  $\text{Ar-CH}$ ), 11.53 (1H, s,  $\text{OH}$ ), 12.00 (1H, br s,  $\text{NH}$ );  $\delta_{\text{C}}$  (126 MHz, DMSO- $d_6$ ) 55.8 ( $\text{OCH}_3$ ), 56.9

(OCH<sub>3</sub>), 114.7 (2 × ArCH), 116.6 (ArCH), 118.2 (ArCH), 122.2 (ArC), 122.4 (2 × ArCH), 126.0 (ArC), 127.6 (ArC), 129.5 (Ar-CH), 132.1 (ArC), 137.3 (CCO), 139.5 (ArC), 151.3 (ArC), 157.0 (NCNH), 172.7 (NCO); *m/z* (ES<sup>+</sup>) 402.0765 (100%, M+H<sup>+</sup>. C<sub>18</sub>H<sub>16</sub>N<sub>3</sub>O<sub>6</sub>S requires 402.0754).

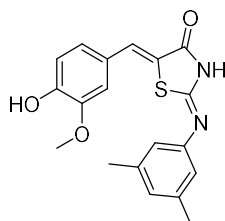
**2-[(3,5-Dimethylphenyl)amino]-5-[(4-hydroxy-3-nitrophenyl)methylene]-4(5*H*)-thiazolone 28**



Glacial acetic acid (10 mL) was added to 2-[(3,5-dimethylphenyl)amino]-4(5*H*)-thiazolone **9** (300 mg, 1.36 mmol), 4-hydroxy-3-nitrobenzaldehyde **27** (228 mg, 1.36 mmol) and sodium acetate (123 mg, 2.72 mmol). The reaction mixture was stirred and heated at 120 °C overnight. The reaction mixture was cooled to room temperature and the precipitate formed. The crude was filtered and washed with diethyl ether (30 mL), dried under vacuum to afford the title compound as a yellow solid (284 mg, 57%). m.p. 294 - 296 °C;  $\nu_{\max}(\text{ATR})/\text{cm}^{-1}$  3314 (OH), 2780, 1718 (CO), 1644, 1622, 1592, 1538;  $\delta_{\text{H}}$  (500 MHz, DMSO-*d*<sub>6</sub>) 2.17 - 2.23 (6H, m, 2 × CH<sub>3</sub>), 6.57 (1H, s, Ar*H*), 6.77 (1H, s, Ar*H*), 7.10 – 7.25 (1H, m, Ar*H*), 7.34 (1H, s, Ar-CH), 7.47 – 7.75 (2H, m, 2 × Ar*H*), 7.93 – 8.10 (1H, m, Ar*H*), 11.56 (1H, s, OH), 12.18 (1H, br s, NH);  $\delta_{\text{C}}$  (126 MHz, DMSO-*d*<sub>6</sub>) 21.4 (CH<sub>3</sub>), 21.5 (CH<sub>3</sub>), 118.6 (ArCH), 120.8 (ArCH), 125.2 (ArC), 127.2 (ArCH), 128.1

(ArCH), 128.9 (Ar-CH), 135.6 (ArCH), 136.6 (ArCH), 137.6 (CCO), 137.8 (ArC), 138.8 (2 × ArCMe), 139.2 (ArC), 148.0 (ArC), 170.5 (NCNH), 180.9 (NCO);  $m/z$  (ES<sup>+</sup>) 370.0867 (100%, M+H<sup>+</sup>. C<sub>18</sub>H<sub>16</sub>N<sub>3</sub>O<sub>4</sub>S requires 370.0856).

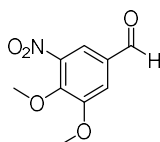
**2-[(3,5-Dimethylphenyl)amino]-5-[(4-hydroxy-3-methoxyphenyl)methylene]-4(5*H*)-thiazolone 30**



Glacial acetic acid (10 mL) was added to 2-[(3,5-dimethylphenyl)amino]-4(5*H*)-thiazolone **9** (150 mg, 0.68 mmol), vanillin **29** (207 mg, 1.36 mmol) and sodium acetate (112 mg, 1.36 mmol). The reaction mixture was stirred and heated at 120 °C overnight. The reaction mixture was cooled to room temperature and the solvent was removed using a rotary evaporator under reduced pressure. The crude mixture in ethyl acetate (30 mL) was washed with water (30 mL), then brine (30 mL), dried over anhydrous MgSO<sub>4</sub>, filtered and concentrated. The crude product was purified via preparative HPLC using an “Waters Xbridge C 18 4.6 × 250 mm” column (40% THF in water over 15 mins, 254 nm) to afford the title compound as a yellow solid (171 mg, 71%). m.p. 166 - 168 °C;  $\nu_{\max}$ (ATR)/cm<sup>-1</sup> 2918, 1694 (CO), 1629, 1589, 1513;  $\delta_{\text{H}}$  (400 MHz, CDCl<sub>3</sub>) 2.36 (6H, s, 2 × CH<sub>3</sub>), 3.92 (3H, s, OCH<sub>3</sub>), 6.80 (2H, s, 2 × ArH), 6.90 (1H, s, ArH), 6.95 - 7.10 (3H, m, 2 × ArH, Ar-CH), 7.69 (1H, s, ArH);  $\delta_{\text{C}}$  (126 MHz, CDCl<sub>3</sub>) 21.4 (2 × CH<sub>3</sub>), 56.0

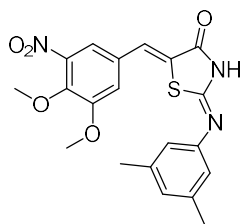
(OCH<sub>3</sub>), 112.7 (ArCH), 115.1 (2 × ArCH), 119.6 (ArCH), 123.9 (ArC), 126.2 (ArC), 127.5 (ArCH), 129.7 (Ar-CH), 132.0 (CCO), 139.3 (2 × ArCMe), 146.8 (ArC), 147.7 (ArC), 150.5 (ArC), 155.1 (NCNH), 169.4 (CO); *m/z* (ES<sup>+</sup>) 355.1129 (100%, M+H<sup>+</sup>). C<sub>19</sub>H<sub>19</sub>N<sub>2</sub>O<sub>3</sub>S requires 355.1111).

### 3,4-Dimethoxy-5-nitrobenzaldehyde 32



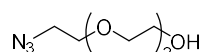
MeI (1.58 mL, 25.4 mmol) was added dropwise to the mixture of 5-nitrovanillin (1.00 g, 5.07 mmol), K<sub>2</sub>CO<sub>3</sub> (1.40 g, 10.1 mmol) and TBAI (188 mg, 0.51 mmol) in DMF (50 mL). The resulting suspension was stirred vigorously under N<sub>2</sub> for 24h. The solvent was removed with a rotary evaporator under reduced pressure. The crude product in diethyl ether (50 mL) was washed with 1M NaOH (2 × 40 mL) to remove unreacted phenol and MeI. The organic layer was further washed with brine (30 mL), dried over anhydrous MgSO<sub>4</sub>, filtered and concentrated with a rotary evaporator. The solid residue was recrystallised from an acetone/water mixture giving the title compound as a light yellow solid (533 mg, 50%); m.p. 78 - 80 °C [lit. m.p. 62 °C,<sup>117</sup> 88 - 89 °C<sup>118</sup>]; δ<sub>H</sub> (400 MHz, CDCl<sub>3</sub>) 4.03 (3H, s, CH<sub>3</sub>), 4.11 (3H, s, CH<sub>3</sub>), 7.65 (1H, d, ArH, *J* 1.8), 7.86 (1H, d, ArH, *J* 1.8), 9.94 (1H, s, CHO); *m/z* (ES<sup>-</sup>) 213 (100%, M+2H<sup>+</sup>), 210 [20%, (M-H)<sup>-</sup>]. The data are in broad agreement with those reported in the literature.<sup>117-119</sup>

**2-[(3,5-Dimethylphenyl)amino]-5-[(3,4-dimethoxy-5-nitrophenyl)methylene]-  
4(5*H*)-thiazolone 33**



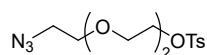
Glacial acetic acid (10 mL) was added to 2-[(3,5-dimethylphenyl)amino]-4(5*H*)-thiazolone **9** (150 mg, 0.68 mmol), 3,4-dimethoxy-5-nitrobenzaldehyde **32** (144 mg, 0.68 mmol) and sodium acetate (112 mg, 1.36 mmol). The reaction mixture was stirred and heated at 120 °C overnight. The reaction mixture was cooled to room temperature and the precipitate formed. The crude was filtered and washed with diethyl ether (30 mL), dried under vacuum to afford the title compound as a light yellow solid (189 mg, 67%).  
m.p. 266 - 268 °C;  $\nu_{\max}(\text{ATR})/\text{cm}^{-1}$  2775, 1722 (CO), 1670, 1630, 1593, 1540;  $\delta_{\text{H}}$  (400 MHz, DMSO- $d_6$ ) 2.22 - 2.31 (6H, m, 2  $\times$  CH<sub>3</sub>), 3.84 - 4.01 (6H, m, 2  $\times$  OCH<sub>3</sub>), 6.62 (1H, s, ArH), 6.74 - 6.84 (1H, m, ArH), 7.34 (1H, s, Ar-CH), 7.42 - 7.72 (3H, m, 3  $\times$  ArH), 12.04 (1H, br s, NH);  $\delta_{\text{C}}$  (101 MHz, DMSO- $d_6$ ) 21.6 (CH<sub>3</sub>), 26.3 (CH<sub>3</sub>), 57.1 (OCH<sub>3</sub>), 62.2(OCH<sub>3</sub>), 115.9 (ArCH), 117.9 (ArCH), 118.4 (ArCH), 119.8 (ArCH), 120.0 (ArCH), 126.1 (ArCH), 131.8 (CCO), 138.2 (ArC), 138.5 (ArC), 142.1 (ArC), 145.0 (ArC), 154.0 (ArC), 154.2 (ArC), 172.5 (NCNH), 180.6 (NCO);  $m/z$  (ES<sup>+</sup>) 414.1126 (100%, M+H<sup>+</sup>. C<sub>20</sub>H<sub>20</sub>N<sub>3</sub>O<sub>5</sub>S requires 414.1118).

### 2-[2-(2-Azidoethoxy)ethoxy]ethanol **35**



Sodium azide (2.68 g, 41.24 mmol) was added to the solution of 2-[2-(2-chloroethoxy)ethoxy]ethanol **34** (5 mL, 34.37 mmol) and potassium iodide (1.14 g, 6.874 mmol) in water (50 mL). The reaction mixture was stirred at 100 °C for 48 h. When cooling to the ambient temperature, the reaction mixture was extracted with DCM (3 × 50 mL), and the organic layer was washed with brine (50 mL) and then dried over anhydrous MgSO<sub>4</sub>. After filtration, the solvent was evaporated and the product was dried under vacuum. Dry flash chromatography on silica gel (petroleum ether/EtOAc, 1:4) was used to purify the title compound as a slight yellow oil (5.45 g, 91 %);  $\delta_{\text{H}}$  (400 MHz, CDCl<sub>3</sub>) 3.41(2H, t, *J* 5.0, CH<sub>2</sub>), 3.59-3.64 (2H, m, CH<sub>2</sub>), 3.65-3.71 (6H, m, 3 × CH<sub>2</sub>), 3.71-3.76 (2H, m, CH<sub>2</sub>); *m/z* (ES<sup>+</sup>) 198 (MNa<sup>+</sup>, 100%), 176 (MH<sup>+</sup>, 85%). The data agree with those reported in the literature.<sup>120</sup>

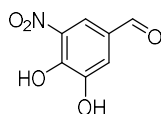
### 2-[2-(2-Azidoethoxy)ethoxy]ethyl-4-methylbenzenesulfonate **36**



4-Toluenesulfonyl chloride (6.84 g, 35.9 mmol) was added to a solution of 2-[2-(2-azidoethoxy)ethoxy]ethanol **35** (5.25 g, 29.9 mmol) in DCM (50 mL) at 0 °C with an ice-water bath. Then KOH (3.36 g, 59.8 mL) was added portion-wise and the reaction was allowed to warm to room temperature and stir overnight. Ice (50 g) and 1M HCl (50 mL) were added to the reaction which was extracted with DCM (3 × 50 mL). The combined

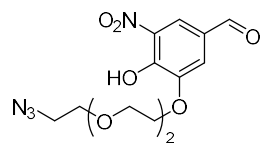
organic layers were washed with brine (50 mL) and then dried over anhydrous MgSO<sub>4</sub>. After filtration, the solvent was evaporated and the product was dried under vacuum. Dry flash chromatography on silica gel (petroleum ether/EtOAc, 3:1) was used to purify the title compound as a mobile colourless oil (8.97 g, 91%);  $\nu_{\max}(\text{ATR})/\text{cm}^{-1}$  2871, 2099 (N=N=N), 1598;  $\delta_{\text{H}}$  (400 MHz, CDCl<sub>3</sub>) 2.47 (3H, s, CH<sub>3</sub>), 3.39 (2H, t, *J* 4.9, CH<sub>2</sub>), 3.59-3.63 (4H, m, 2 × CH<sub>2</sub>), 3.63-3.68 (2H, m, CH<sub>2</sub>), 3.69-3.74 (2H, m, CH<sub>2</sub>), 4.14-4.21 (2H, m, CH<sub>2</sub>), 7.36 (2H, d, *J* 8.0, 2 × ArH), 7.81 (2H, d, *J* 8.0, 2 × ArH); *m/z* (ES<sup>+</sup>) 352 (100%, M+Na<sup>+</sup>), 302 (28). The data agree with those reported in the literature.<sup>121</sup>

### 3,4-Dihydroxy-5-nitrobenzaldehyde **37**



A solution of 5-nitrovanillin **31** (500 mg, 2.54 mmol) in hydrobromic acid (48 wt% in H<sub>2</sub>O, 10 mL) and acetic acid (5 mL) was stirred at 110 °C for 36 h. The reaction mixture was diluted with H<sub>2</sub>O (20 mL) and extracted 5 times with DCM (5 × 30 mL). The combined organic phases were washed with brine (50 mL), dried over anhydrous MgSO<sub>4</sub>, filtered and concentrated under vacuum to afford the title compound as a yellow solid (467 mg, quan.). m.p. 126 - 128 °C [lit.<sup>122</sup> m.p. 134 - 139 °C];  $\delta_{\text{H}}$  (400 MHz, DMSO-*d*<sub>6</sub>) 7.46 (1H, d, *J* 1.8, ArH), 7.99 (1H, d, *J* 1.8, ArH), 9.82 (1H, s, CHO), 10.94 (1H, br s, OH); *m/z* (ES<sup>-</sup>) 182 [100%, (M-H)<sup>-</sup>]; The data are in broad agreement with those reported in the literature.<sup>122, 123</sup>

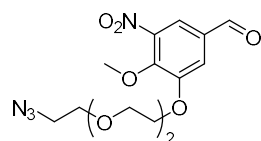
### 3-[2-[2-(2-Azidoethoxy)ethoxy]ethoxy]-4-hydroxy-5-nitrobenzaldehyde **38**



Sodium hydride (87 mg, 2.18 mmol, 60% w/w in mineral oil) was washed three times with petroleum ether (3 × 10 mL) and suspended in dry DMF (2 mL) at 0 °C with an ice-water bath under N<sub>2</sub>. 3,4-Dihydroxy-5-nitrobenzaldehyde **37** (200 mg, 1.09 mmol) in dry DMF (2 mL) was added dropwise to sodium hydride and the reaction mixture was stirred at 0 °C for 30 min. Subsequently, 2-[2-(2-azidoethoxy)ethoxy]ethyl-4-methylbenzenesulfonate **36** (360 mg, 1.09 mmol) in dry DMF (2 mL) was added dropwise to the reaction. The ice-water bath was removed and the reaction was stirred at room temperature overnight. Methanol (10 mL) was added to quench sodium hydride and the solvent was eliminated in a rotary evaporator under reduced pressure. The residue was dissolved in DCM (15 mL) and acidified to pH = 2 with 1M HCl. The aqueous layer was separated and extracted with DCM (3 × 20 mL). The combined organic layers were washed with brine (30 mL), dried over anhydrous MgSO<sub>4</sub>, filtered and the filtrate was eliminated in a rotary evaporator under reduced pressure. The crude residue was purified by flash column chromatography on silica gel, eluting DCM/MeOH, MeOH: 0-10% to afford the title compound as a yellow solid (294 mg, 79%). m.p. 56 - 58 °C;  $\nu_{\max}(\text{ATR})/\text{cm}^{-1}$  3191, 3088, 2910, 2109, 1686 (CO), 1613, 1550;  $\delta_{\text{H}}$  (400 MHz, CDCl<sub>3</sub>) 3.40 (2H, t, *J* 5.0, CH<sub>2</sub>), 3.61 - 3.86 (6H, m, 3 × CH<sub>2</sub>), 4.00 (2H, t, *J* 4.8, CH<sub>2</sub>), 4.32 (2H, t, *J* 4.8, CH<sub>2</sub>), 7.63 (1H, s, ArH), 8.25 (1H, d, *J* 1.8, ArH), 9.85 (1H, s, CHO);  $\delta_{\text{C}}$  (101 MHz, CDCl<sub>3</sub>) 50.7 (CH<sub>2</sub>), 69.4 (CH<sub>2</sub>), 69.7 (CH<sub>2</sub>), 70.1 (CH<sub>2</sub>), 70.7 (CH<sub>2</sub>), 70.0 (CH<sub>2</sub>),

115.4 (ArCH), 116.5 (ArC), 121.8 (ArCH), 125.1 (ArC), 142.9 (ArC), 144.8 (ArC), 188.9 (CHO);  $m/z$  (ES<sup>+</sup>) 363.1 (100%, M+Na<sup>+</sup>. C<sub>13</sub>H<sub>16</sub>N<sub>4</sub>O<sub>7</sub>Na requires 363.1).

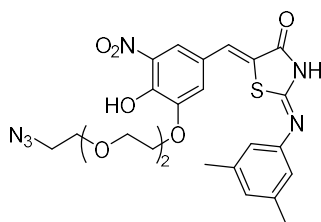
### 3-(2-(2-(2-Azidoethoxy)ethoxy)ethoxy)-4-methoxy-5-nitrobenzaldehyde **39**



Iodomethane (0.05 mL, 0.73 mmol) was added dropwise to the mixture of 3-[2-[2-(2-azidoethoxy)ethoxy]ethoxy]-4-hydroxy-5-nitrobenzaldehyde **38** (50 mg, 0.15 mmol), K<sub>2</sub>CO<sub>3</sub> (40 mg, 0.29 mmol) and TBAI (6 mg, 0.02 mmol) in dry DMF (2 mL). The resulting suspension was stirred under N<sub>2</sub> at room temperature for 24h. The solvent was removed with a rotary evaporator under reduced pressure. The residue was dissolved in EtOAc (10 mL) and 1M NaOH (10 mL) was added to remove unreacted phenol **38** and iodomethane. The organic layer was separated and washed with brine (10 mL), dried over anhydrous MgSO<sub>4</sub>, filtered and concentrated. The aqueous layer was neutralised to pH = 7 with 1M HCl and extracted with EtOAc (2 × 15 mL). The combined organic layers were washed with brine (15 mL), dried over anhydrous MgSO<sub>4</sub>, filtered and the filtrate was eliminated in a rotary evaporator under reduced pressure. The crude residue was purified by flash column chromatography on silica gel, eluting petroleum ether/EtOAc, EtOAc: 50% to afford the title compound as a yellow oil (12 mg, 23%).  $\nu_{\max}$ (ATR)/cm<sup>-1</sup> 2870, 2100, 1698 (CHO), 1604, 1536;  $\delta_{\text{H}}$  (400 MHz, CDCl<sub>3</sub>) 3.40 (2H, t,  $J$  5.0, CH<sub>2</sub>), 3.66 - 3.80 (6H, m, 3 × CH<sub>2</sub>), 3.97 (2H, t,  $J$  4.8, CH<sub>2</sub>), 4.14 (3H, s, OCH<sub>3</sub>),

4.33 (2H, t,  $J$  4.8,  $CH_2$ ), 7.68 (1H, d,  $J$  1.8, ArH), 7.86 (1H, d,  $J$  1.8, ArH), 9.93 (1H, s, CHO);  $\delta_c$  (101 MHz,  $CDCl_3$ ) 50.7 ( $CH_2$ ), 62.3 ( $OCH_3$ ), 69.3 ( $CH_2$ ), 69.5 ( $CH_2$ ), 70.2 ( $CH_2$ ), 70.8 ( $CH_2$ ), 70.9 ( $CH_2$ ), 114.9 (ArCH), 115.6 (ArC), 119.7 (ArCH), 123.3 (ArC), 125.1 (ArC), 140.4 (ArC), 188.9 (CHO);  $m/z$  ( $ES^+$ ) 377.1085 (100%,  $M+Na^+$ .  $C_{14}H_{18}N_4O_7Na$  requires 377.1068).

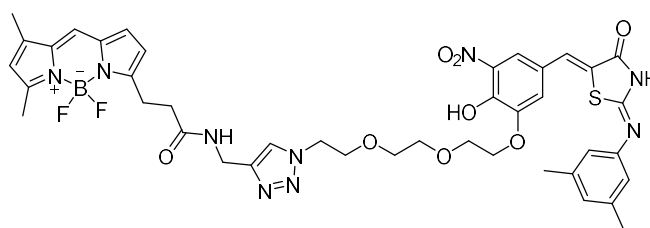
**5-[3-[2-[2-(2-Azidoethoxy)ethoxy]ethoxy]-4-hydroxy-5-nitrobenzylidene]-2-[(3,5-dimethylphenyl)imino]thiazolidin-4-one 40**



2-[(3,5-Dimethylphenyl)amino]-4(5*H*)-thiazolone **9** (65 mg, 0.29 mmol), 3-[2-[2-(2-azidoethoxy)ethoxy]ethoxy]-4-hydroxy-5-nitrobenzaldehyde **38** (100 mg, 0.29 mmol) and sodium acetate (48 mg, 0.59 mmol) were dissolved in glacial acetic acid (4 mL). The reaction was heated at 110 °C for 24h. The reaction mixture was cooled to room temperature and the solvent was removed using a rotary evaporator under reduced pressure. The residue was dissolved in DCM (15 mL) and water (10 mL). The aqueous layer was separated and extracted with DCM (3 × 20 mL). The combined organic layers were washed with brine (30 mL), dried over anhydrous  $MgSO_4$ , filtered and the filtrate was eliminated in a rotary evaporator under reduced pressure. The crude mixture was purified via preparative HPLC using an “Waters Xbridge C 18 4.6 × 250 mm” column

[40% MeCN in aqueous TFA (0.1%) over 25 mins, 354 nm] to afford the title compound as an orange solid (110 mg, 70%). m.p. 210 - 212 °C;  $\nu_{\max}(\text{ATR})/\text{cm}^{-1}$  2922, 2853, 2111 ( $\text{N}_3$ ), 1651, 1632, 1595, 1545;  $\delta_{\text{H}}$  (500 MHz,  $\text{CDCl}_3$ ) 2.37 (6H, s,  $2 \times \text{CH}_3$ ), 3.35 – 3.47 (2H, m,  $\text{CH}_2$ ), 3.64 - 3.82 (6H, m,  $3 \times \text{CH}_2$ ), 3.90 – 4.01 (2H, m,  $\text{CH}_2$ ), 4.24 – 4.35 (2H, m,  $\text{CH}_2$ ), 6.81 (2H, s,  $2 \times \text{ArH}$ ), 6.93 (1H, s,  $\text{ArH}$ ), 7.29 (1H, s,  $\text{Ar-CH}$ ), 7.63 (1H, s,  $\text{ArH}$ ), 7.85 (1H, s,  $\text{ArH}$ );  $\delta_{\text{C}}$  (126 MHz,  $\text{CDCl}_3$ ) 21.4 ( $2 \times \text{CH}_3$ ), 50.7 ( $\text{CH}_2$ ), 69.6 ( $\text{CH}_2$ ), 70.0 ( $\text{CH}_2$ ), 70.1 ( $\text{CH}_2$ ), 70.8 ( $\text{CH}_2$ ), 71.0 ( $\text{CH}_2$ ), 117.9 ( $\text{ArC}$ ), 119.7 ( $2 \times \text{ArC}$ ), 120.8 ( $\text{ArC}$ ), 124.6 ( $\text{ArC}$ ), 125.1 ( $\text{ArC}$ ), 128.1 ( $\text{ArC}$ ), 129.0 ( $\text{ArC}$ ), 134.3 ( $\text{CCO}$ ), 139.5 ( $2 \times \text{ArC}$ ), 144.0 ( $\text{ArC}$ ), 147.6 ( $\text{ArC}$ ), 149.8 ( $\text{ArC}$ ), 155.5 ( $\text{NCNH}$ ), 169.5 ( $\text{CO}$ );  $m/z$  ( $\text{ES}^+$ ) 543.1646 (100%,  $\text{M}+\text{H}^+$ .  $\text{C}_{24}\text{H}_{27}\text{N}_6\text{O}_7\text{S}$  requires 543.1656).

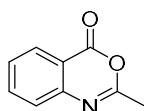
### BODIPY-PEG<sub>3</sub>-thiazolidinone **42**



5-[3-[2-[2-(2-Azidoethoxy)ethoxy]ethoxy]-4-hydroxy-5-nitrobenzylidene]-2-[(3,5-dimethylphenyl)imino]thiazolidin-4-one (1.0 mg,  $1.84 \times 10^{-3}$  mmol) **40** and alkyne-BODIPY-FL **41** (0.6 mg,  $1.84 \times 10^{-3}$  mmol) were dissolved in DMSO (100  $\mu\text{L}$ ). L-Ascorbic acid (6.5 mg) was dissolved in DMSO (2 mL) and portion of this (100  $\mu\text{L}$ ,  $1.84 \times 10^{-3}$  mmol) was added to the reaction.  $\text{CuSO}_4$  (7.37 mg) was dissolved in water (1 mL) and portion of this (20  $\mu\text{L}$ ,  $9.22 \times 10^{-4}$  mmol) was added to the reaction. The reaction

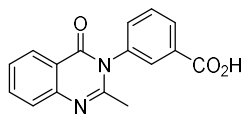
mixture was stirred at room temperature overnight. The crude mixture was directly purified via preparative HPLC using an “Waters Xbridge C 18 4.6 × 250 mm” column [40% MeCN in aqueous TFA (0.1%) over 25 mins, 350 nm, retention time: 17.7 min] to afford the title compound as a brick-red solid (1.0 mg, 63%).  $m/z$  ( $ES^+$ ) 872 (100%,  $M+H^+$ ).

### 2-Methyl-4*H*-3,1-benzoxazin-4-one 47



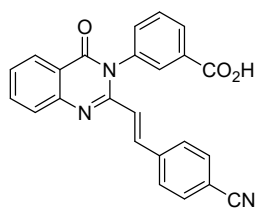
Anthranilic acid **46** (5.08 g, 37.04 mmol) was dissolved in triethyl orthoacetate (11 mL, 60.14 mmol) and heated at reflux for 2.5 h. The reaction mixture was cooled to ambient temperature overnight and the resulting crystals were filtered and washed with hexane to give the title compound as a light brown solid (4.51 g, 76%). m.p. 76 - 80 °C [lit.<sup>124</sup> m.p. 77 - 80 °C];  $\nu_{max}(ATR)/cm^{-1}$  1742 (CO), 1692, 1644, 1606, 1508;  $\delta_H$  (400 MHz,  $CDCl_3$ ) 2.49 (3H, s,  $CH_3$ ), 7.52 (1H, t,  $J$  7.8,  $ArH$ ), 7.56 (1H, d,  $J$  8.1,  $ArH$ ), 7.81 (1H, td,  $J$  7.8, 1.5,  $ArH$ ), 8.20 (1H, dd,  $J$  7.8, 1.5,  $ArH$ );  $m/z$  ( $ES^+$ ) 162 (100%,  $M+H^+$ ). The data agree with those reported in the literature.<sup>87, 124</sup>

### 3-(2-Methyl-4-oxo-3(4*H*)-quinazolinyl)benzoic acid **48**



2-Methyl-4*H*-3,1-benzoxazin-4-one **47** (2.03 g, 12.60 mmol) and 3-aminobenzoic acid (1.74 g, 12.60 mmol) were dissolved in glacial acetic acid (8 mL) and heated to reflux at 130 °C overnight. The reaction mixture was cooled to room temperature and water (5 mL) was added. The resulting precipitate was filtered and washed with water (10 mL), followed by cold ethanol (10 mL) and hexane (10 mL) to give the title compound as a white solid (2.58 g, 73%). m.p. 278 - 282 °C;  $\nu_{\max}(\text{ATR})/\text{cm}^{-1}$  2463 (OH), 1869, 1685 (CO), 1611, 1571;  $\delta_{\text{H}}$  (400 MHz, DMSO- $d_6$ ) 2.13 (3H, s, *CH*<sub>3</sub>), 7.52 (1H, t, *J* 7.5, *ArH*), 7.64 - 7.78 (3H, m, *ArH*), 7.85 (1H, td, *J* 7.6, 1.2, *ArH*), 8.02 (1H, s, *ArH*), 8.10 (2H, t, *J* 7.3, *ArH*); *m/z* ( $\text{ES}^+$ ) 281 ( $\text{M}+\text{H}^+$ ). The data agree with those reported in the literature.<sup>87</sup>

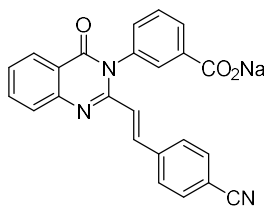
### (*E*)-3-(3-Carboxyphenyl)-2-(4-cyanostyryl)quinazolin-4(3*H*)-one **5**



3-(2-Methyl-4-oxo-3(4*H*)-quinazolinyl)benzoic acid **48** (1.02 g, 3.64 mmol) and 4-formylbenzotrile (0.59 g, 4.50 mmol) were dissolved in glacial acetic acid (5 mL) and heated at 130 °C overnight. The reaction mixture was cooled to room temperature and water (5 mL) was added. The resulting precipitate was filtered and washed with water (10 mL), followed by cold ethanol (10 mL) and hexane (10 mL) to give the title

compound as a yellow solid (1.31 g, 92%). m.p. 276 - 278 °C;  $\nu_{\max}$ (ATR)/ $\text{cm}^{-1}$  2813 (OH), 2224 (CN), 2113, 1681 (CO), 1603, 1573, 1551;  $\delta_{\text{H}}$  (400 MHz, DMSO- $d_6$ ) 6.49 (1H, d,  $J$  15.5, CHCHArCN), 7.53 - 7.64 (3H, m, ArH), 7.71 - 7.77 (2H, m, ArH), 7.80 (3H, d,  $J$  8.4, ArH), 7.87 - 7.96 (2H, m, ArH), 8.05 (1H, s, ArH), 8.11-8.18 (2H, m, ArH, CHArCN), 13.32 (1H, br s,  $\text{CO}_2\text{H}$ );  $m/z$  (ESI $^+$ ) 394 (100%,  $\text{M}+\text{H}^+$ ). The data agree with those reported in the literature.<sup>87</sup>

**Sodium (*E*)-3-(3-Carboxyphenyl)-2-(4-cyanostyryl)quinazolin-4(3*H*)-one 49**

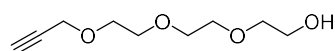


Method A: (*E*)-3-(3-Carboxyphenyl)-2-(4-cyanostyryl)quinazolin-4(3*H*)-one **5** (150 mg, 0.38 mmol) was suspended in hot ethanol (5 mL). Sodium 2-ethylhexanoate (100 mg, 0.60 mmol) was added and the reaction mixture was stirred at 0°C for 2 h. The precipitate was filtered and washed with cold ethanol (15 mL) to give the title compound as a light yellow solid (152 mg, 96%).

Method B: (*E*)-3-(3-Carboxyphenyl)-2-(4-cyanostyryl)quinazolin-4(3*H*)-one **5** (100 mg, 0.25 mmol) was dissolved in THF (5 mL). NaOH (10 mg, 0.25 mmol) was added and the reaction mixture was stirred at room temperature overnight. The solvent was eliminated in a rotary evaporator under reduced pressure to give the title compound as a light yellow solid (114 mg, quantitative). m.p. > 300 °C;  $\nu_{\max}$ (ATR)/ $\text{cm}^{-1}$  3069, 2226 (CN), 1682 (CO),

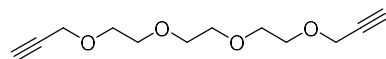
1603, 1572, 1550;  $\delta_{\text{H}}$  (400 MHz, DMSO- $d_6$ ) 6.48 (1H, d,  $J$  15.6, CHCHArCN), 7.40 - 7.47 (1H, m, ArH), 7.50 - 7.61 (4H, m, 4  $\times$  ArH), 7.77 - 7.86 (4H, m, 4  $\times$  ArH), 7.87 - 7.96 (2H, m, ArH, CHArCN), 8.01 - 8.08 (1H, m, ArH), 8.13 - 8.20 (1H, m, ArH);  $m/z$  (ES $^-$ ) 392 [100%, (M-Na) $^-$ ]. The data agree with those reported in the literature.<sup>87</sup>

### 2-[2-[2-(2-Propyn-1-yloxy)ethoxy]ethoxy]ethanol **52**



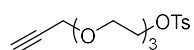
Potassium *tert*-butoxide (2.00 g, 17.8 mmol) was added to triethylene glycol **50** (4.8 mL, 35.6 mmol) in dry THF (40 mL) under N<sub>2</sub>. The mixture was stirred for 30 min at room temperature. A solution of propargyl bromide **51** (2.0 mL, 17.8 mmol, 80% in toluene) diluted in dry THF (10 mL) was added dropwise. The final suspension was continuously stirred for 24 h at room temperature, filtered over Celite Hyflo Supercel (20 g) and washed with DCM (50 mL). The solvent was removed and the resulting residue was purified by flash column chromatography on silica gel, eluting petroleum ether/EtOAc, EtOAc: 50-60% to afford the title compound as a colourless oil (2.54 g, 76%).  $\nu_{\text{max}}$ (ATR)/cm $^{-1}$  3418, 2874, 2115, 1717;  $\delta_{\text{H}}$  (400 MHz, CDCl<sub>3</sub>) 2.44 (1H, t,  $J$  2.4, CH), 2.82 (1H, br s, OH), 3.56 – 3.61 (2H, m, CH<sub>2</sub>OH), 3.63-3.72 (10H, m, 5  $\times$  CH<sub>2</sub>), 4.18 (2H, d,  $J$  2.4, OCH<sub>2</sub>CCH);  $m/z$  (ES $^+$ ) 435 (50), 211 (100%, M+Na $^+$ ). The data agree with those reported in the literature.<sup>125</sup>

### Triethylene glycol dipropargyl ether **53**



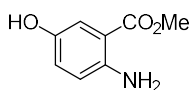
NaH (300 mg, 7.49 mmol, 60% w/w in mineral oil) was washed with petroleum ether (3 × 30 mL). Triethylene glycol **50** (2.00 mL, 14.99 mmol) was added dropwise to the solution of NaH in dry THF (30 mL) at 0 °C with an ice-water bath under N<sub>2</sub>. After stirring for 15 min, propargyl bromide (0.85 mL, 7.49 mmol, 80wt% in toluene) was added slowly and the ice-water bath was removed. The reaction was stirred at the room temperature for 2 h and the solvent was eliminated in a rotary evaporator under reduced pressure. The mixture was extracted between ethyl acetate (30 mL) and water (30 mL) and the aqueous layer was back-extracted with ethyl acetate (30 mL). The combined organic phase was washed with brine (30 mL), dried over anhydrous MgSO<sub>4</sub>, filtered and the filtrate was eliminated in a rotary evaporator under reduced pressure. The crude residue was purified by flash column chromatography (petroleum ether/EtOAc, EtOAc: 60%) to afford 2-[2-[2-(2-propyn-1-yloxy)ethoxy]ethoxy]ethanol **52** (412 mg, 29%) and the title compound **53** as a colourless oil (479 mg, 28%).  $\nu_{\max}(\text{ATR})/\text{cm}^{-1}$  3425, 2920, 2118, 1716;  $\delta_{\text{H}}$  (400 MHz, CDCl<sub>3</sub>) 2.42 (2H, t,  $J$  2.4, 2 × CH), 3.62 - 3.70 (12H, m, 6 × CH<sub>2</sub>), 4.17 (4H, d,  $J$  2.4, 2 × OCH<sub>2</sub>CCH).  $m/z$  (ES<sup>+</sup>) 435 (80), 281 (50), 249 (100%, M+Na<sup>+</sup>). The data agree with those reported in the literature.<sup>126</sup>

## 2-[2-[2-(Prop-2-yn-1-yloxy)ethoxy]ethoxy]ethyl 4-methylbenzenesulfonate **54**



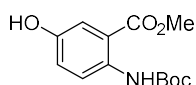
2-[2-[2-(2-Propyn-1-yloxy)ethoxy]ethoxy]ethanol **52** (1.00 g, 5.31 mmol) was dissolved in THF (5 mL). A solution of NaOH (0.64 g, 15.93 mmol) in water (5 mL) was added at 0 °C with an ice-water bath. 4-Toluenesulfonyl chloride (1.32 g, 6.90 mmol) was dissolved in THF (4 mL) and the solution was added to the reaction dropwise. The mixture was stirred at 0 °C and allowed to reach room temperature for 24 h. The solvent was removed and the crude was diluted with water (15 mL) and extracted with diethyl ether (3 × 20 mL). The combined organic phase was dried over anhydrous MgSO<sub>4</sub>, filtered and the filtrate was eliminated in a rotary evaporator under reduced pressure. The crude residue was purified by flash column chromatography eluting with petroleum ether/EtOAc (EtOAc: 30%) to afford the title compound as a colourless oil (1.69 g, 93%).  $\nu_{\text{max}}(\text{ATR})/\text{cm}^{-1}$  3279, 2875, 2117, 1717, 1598;  $\delta_{\text{H}}$  (400 MHz, CDCl<sub>3</sub>) 2.44 (1H, t, *J* 2.4, CH), 2.46 (3H, s, CH<sub>3</sub>), 3.60 (4H, s, 2 × CH<sub>2</sub>), 3.63 - 3.67 (2H, m, CH<sub>2</sub>), 3.68 - 3.72 (4H, m, 2 × CH<sub>2</sub>), 4.15 - 4.19 (2H, m, CH<sub>2</sub>), 4.20 (2H, d, *J* 2.4, OCH<sub>2</sub>CCH), 7.36 (2H, d, *J* 8.2, 2 × ArH), 7.81 (2H, d, *J* 8.2, 2 × ArH). *m/z* (ES<sup>+</sup>) 365 (100%, M+Na<sup>+</sup>), 343 (40, M+H<sup>+</sup>). The data agree with those reported in the literature.<sup>127</sup>

### Methyl 2-amino-5-hydroxybenzoate **56**



A solution of 2-amino-5-hydroxybenzoic acid **55** (1.0 g, 6.53 mmol) in methanol (20 mL) and concentrated sulfuric acid (1 mL) were stirred and heated at 90 °C for 72 h. The solution was cooled and concentrated under reduced pressure, providing a brown solid, that was re-dissolved in deionized water (15 mL). The dark brown solution was neutralized to pH 7-8 with sat. K<sub>2</sub>CO<sub>3</sub> (10 mL). The resultant brown precipitate was filtered, rinsed with ice cold water and dried thoroughly under high vacuum to give the title compound as a brown solid (770 g, 71%). m.p. 148-150 °C [lit.<sup>128</sup> m.p. 154-155 °C];  $\delta_{\text{H}}$  (400 MHz, DMSO-d<sub>6</sub>) 3.77 (3H, s, CH<sub>3</sub>), 6.07 (2H, s, NH<sub>2</sub>), 6.65 (1H, d, *J* 8.8, ArH), 6.81 (1H, dd, *J* 8.8, 2.9, ArH), 7.11 (1H, *J* 2.9, ArH), 8.66 (1H, s, OH); *m/z* (ES<sup>+</sup>) 168 (100%, M+H<sup>+</sup>). The data agree with those reported in the literature.<sup>128, 129</sup>

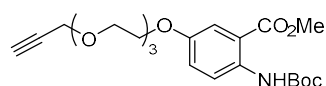
### Methyl 5-hydroxy-2-(*tert*-butoxycarbonylamino)benzoate **57**



A solution of di-*tert*-butyl decarbonate (2.00 g, 9.16 mmol) in ethanol (10 mL) was added to a suspension of methyl 2-amino-5-hydroxybenzoate **56** (1.00 g, 5.98 mmol) in ethanol (10 mL). The reaction was stirred at 30 °C for 24 h, after which a dark brown solution had formed. The solvent was removed in a rotary evaporator under reduced pressure, and the crude material was purified immediately by flash column chromatography on silica gel (petroleum ether/EtOAc 4:1) to give the title compound as a white solid (1.50 g, 94%);

m.p. 162 - 164 °C;  $\nu_{\max}(\text{ATR})/\text{cm}^{-1}$  3408 (OH), 3316 (NH), 2977, 1721 (CO), 1682 (CO), 1527;  $\delta_{\text{H}}$  (400 MHz, DMSO- $d_6$ ) 1.46 (9H, s, 3  $\times$   $\text{CH}_3$ ), 3.82 (3H, s,  $\text{CH}_3$ ), 7.00 (1H, dd,  $J$  9.0, 3.0,  $\text{ArH}$ ), 7.28 (1H, d,  $J$  3.0,  $\text{ArH}$ ), 7.87 (1H,  $J$  9.0,  $\text{ArH}$ ), 9.56 (1H, s, OH), 9.66 (1H, s, NH);  $m/z$  ( $\text{ES}^+$ ) 290 (20%,  $\text{M}+\text{Na}^+$ ), 168 (100), 136 (40). The data agree with those reported in the literature.<sup>129</sup>

**Methyl 2-[(*tert*-butoxycarbonyl)amino]-5-[2-[2-[2-(prop-2-yn-1-yloxy)ethoxy]ethoxy]ethoxy]benzoate **58****

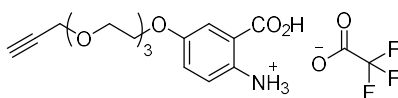


Methyl 5-hydroxy-2-(*tert*-butoxycarbonylamino)benzoate **57** (1.11 g, 4.16 mmol) was dissolved in DMF (20 mL). 2-(2-(2-(Prop-2-yn-1-yloxy)ethoxy)ethoxy)ethyl 4-methylbenzenesulfonate **54** (1.71 g, 4.99 mmol) and potassium carbonate (0.86 g, 6.24 mmol) were added to this solution at room temperature. The reaction mixture was stirred at 80 °C for 24 h. After cooling to room temperature, the solvent was removed using a rotary evaporator under reduced pressure. The crude residue was diluted with ethyl acetate (35 mL) and washed with sat.  $\text{NaHCO}_3$  (25 mL), water (25 mL) and brine (25 mL). The organic phase was dried over anhydrous  $\text{MgSO}_4$ , filtered and the filtrate was evaporated under reduced pressure. The crude was purified by dry flash chromatography on silica gel, eluting petroleum ether/EtOAc, EtOAc: 30% to afford the title compound as a colourless oil (1.67 g, 91%).  $\nu_{\max}(\text{ATR})/\text{cm}^{-1}$  3303, 2872, 1724, 1694 (C=O);  $\delta_{\text{H}}$  (400 MHz,  $\text{CDCl}_3$ ) 1.54 (9H, s, 3  $\times$   $\text{CH}_3$ ), 2.44 (1H, t,  $J$  2.4, CH), 3.69 – 3.78 (8H, m, 4  $\times$



CDCl<sub>3</sub>) 1.55 (9H, s, 3 × CH<sub>3</sub>), 2.45 (1H, t, *J* 2.4, CH), 3.70 – 3.81 (8H, m, 4 × CH<sub>2</sub>), 3.90 (2H, t, *J* 4.8, CH<sub>2</sub>), 4.16 (2H, t, *J* 4.8, CH<sub>2</sub>), 4.23 (2H, d, *J* 2.4, CH<sub>2</sub>), 7.17 (1H, dd, *J* 9.2, 3.1, ArH), 7.62 (1H, d, *J* 3.1, ArH), 8.36 (1H, d, *J* 9.2, ArH), 9.88 (1H, s, NH); δ<sub>c</sub> (101 MHz, CDCl<sub>3</sub>) 28.4 (3 × CH<sub>3</sub>), 58.4 (CH<sub>2</sub>CCH), 67.8 (CH<sub>2</sub>), 69.1 (CH<sub>2</sub>), 69.8 (CH<sub>2</sub>), 70.4 (CH<sub>2</sub>), 70.6 (CH<sub>2</sub>), 70.8 (CH<sub>2</sub>), 74.7 (CCH), 77.2 (CH), 80.5 (CCH<sub>3</sub>), 114.3 (ArC), 116.0 (ArCH), 120.4 (ArCH), 122.8 (ArCH), 136.7 (ArC), 152.7 (ArC), 153.0 (NCO), 171.1 (CO<sub>2</sub>H); *m/z* (ES<sup>+</sup>) 446.1806 (100%, M+Na<sup>+</sup>. C<sub>21</sub>H<sub>29</sub>NO<sub>8</sub>Na requires 446.1785).

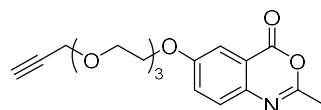
**TFA salt of 2-amino-5-[2-[2-[2-(prop-2-yn-1-yloxy)ethoxy]ethoxy]ethoxy]benzoic acid **60****



2-[(*tert*-Butoxycarbonyl)amino]-5-[2-[2-[2-(prop-2-yn-1-yloxy)ethoxy]ethoxy]ethoxy]benzoic acid **59** (520 mg, 1.23 mmol) was dissolved in DCM (9 mL) and TFA (1 mL). The solution was stirred at room temperature for 2 h. The solvent was removed using compressed air and the residual TFA was co-evaporated with DCM (10 mL) using a rotary evaporator under reduced pressure to afford the title compound as a brown viscous oil in a quantitative yield (553 mg).  $\nu_{\max}$ (ATR)/cm<sup>-1</sup> 2875, 1690 (CO); δ<sub>H</sub> (400 MHz, MeOD) 2.84 (1H, t, *J* 2.4, CH), 3.66 – 3.76 (8H, m, 4 × CH<sub>2</sub>), 3.88 (2H, m, CH<sub>2</sub>), 4.16 – 4.22 (4H, m, 2 × CH<sub>2</sub>), 7.26 (1H, dd, *J* 8.8, 3.0, ArH), 7.36 (1H, d, *J* 8.8, ArH), 7.66 (1H, d, *J* 3.0, ArH); δ<sub>c</sub> (101 MHz, MeOD) 57.6 (CH<sub>2</sub>CCH), 68.0 (CH<sub>2</sub>), 68.7 (CH<sub>2</sub>), 69.4 (CH<sub>2</sub>), 70.0 (CH<sub>2</sub>), 70.1 (CH<sub>2</sub>), 70.3 (CH<sub>2</sub>), 74.5 (CCH),

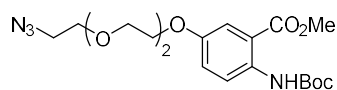
79.1 (CH), 113.7 (ArC), 116.1 (ArCH), 121.6 (ArCH), 121.7 (ArCH), 134.6 (ArC), 147.5 (ArC), 168.3 (CO<sub>2</sub>H); *m/z* (ES<sup>+</sup>) 346.1260 (30, M+Na<sup>+</sup>), 324.1443 (100%, M+H<sup>+</sup>. C<sub>16</sub>H<sub>22</sub>NO<sub>6</sub> requires 324.1442).

**2-Methyl-6-[2-[2-[2-(prop-2-yn-1-yloxy)ethoxy]ethoxy]ethoxy]-4H-benzo[1,3]oxazin-4-one 61**



TFA salt of 2-amino-5-[2-[2-[2-(prop-2-yn-1-yloxy)ethoxy]ethoxy]ethoxy]benzoic acid **60** (292 mg, 0.76 mmol) and triethylamine (0.11 mL, 0.76 mmol) were added to triethyl orthoacetate (2 mL). The reaction mixture was heated and stirred at 80 °C overnight. After cooling to room temperature, the crude mixture was directly purified via flash column chromatography eluting with petroleum ether/EtOAc, EtOAc: 0 - 40%) to afford the title compound as a yellowish-brown viscous oil (77 g, 33%).  $\nu_{\max}(\text{ATR})/\text{cm}^{-1}$  2923, 1683 (CO);  $\delta_{\text{H}}$  (400 MHz, CDCl<sub>3</sub>) 2.24 (3H, s, CH<sub>3</sub>), 2.44 (1H, t, *J* 2.4, CH), 3.71 – 3.82 (8H, m, 4 × CH<sub>2</sub>), 3.91 (2H, t, *J* 4.7, CH<sub>2</sub>), 4.17 (2H, t, *J* 4.7, CH<sub>2</sub>), 4.22 (2H, d, *J* 2.4, CH<sub>2</sub>), 7.16 (1H, dd, *J* 9.2, 3.1, ArH), 7.64 (1H, d, *J* 3.1, ArH), 8.63 (1H, d, *J* 9.2, ArH);  $\delta_{\text{C}}$  (101 MHz, CDCl<sub>3</sub>) 25.3 (CH<sub>3</sub>), 58.4 (CH<sub>2</sub>CCH), 67.8 (CH<sub>2</sub>), 69.1 (CH<sub>2</sub>), 69.8 (CH<sub>2</sub>), 70.4 (CH<sub>2</sub>), 70.7 (CH<sub>2</sub>), 70.8 (CH<sub>2</sub>), 74.7 (CCH), 77.2 (CH), 115.5 (ArC), 116.3 (ArCH), 121.8 (ArCH), 121.9 (ArCH), 136.8 (ArC), 153.6 (ArC), 169.0 (CCH<sub>3</sub>), 170.2 (CO<sub>2</sub>C); *m/z* (ES<sup>+</sup>) 348.1427 (100%, M+H<sup>+</sup>. C<sub>18</sub>H<sub>22</sub>NO<sub>6</sub> requires 348.1442).

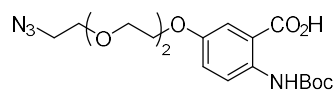
**Methyl 5-[2-[2-(2-azidoethoxy)ethoxy]ethoxy]-2-[(*tert*-  
butoxycarbonyl)amino]benzoate **63****



Methyl 5-hydroxy-2-(*tert*-butoxycarbonylamino)benzoate **57** (240 mg, 0.90 mmol) was dissolved in DMF (5 mL). 2-[2-(2-Azidoethoxy)ethoxy]ethyl-4-methylbenzenesulfonate **36** (377 g, 1.14 mmol) and potassium carbonate (187 g, 1.35 mmol) were added to this solution at room temperature. The reaction mixture was stirred at 90 °C overnight. After cooling to room temperature, the solvent was removed using a rotary evaporator under reduced pressure. The crude residue was diluted with ethyl acetate (35 mL) and washed with sat. NaHCO<sub>3</sub> (25 mL), water (25 mL) and brine (25 mL). The organic phase was dried over anhydrous MgSO<sub>4</sub>, filtered and the filtrate was evaporated under reduced pressure. The crude was purified by flash column chromatography on silica gel, eluting petroleum ether/EtOAc, 4:1 to afford the title compound as a colourless oil (363 g, 95%).  $\nu_{\text{max}}$ (ATR)/cm<sup>-1</sup> 3324, 2872, 2101 (N=N=N), 1725 (C=O), 1694 (C=O), 1591;  $\delta_{\text{H}}$  (400 MHz, CDCl<sub>3</sub>) 1.51 (9H, s, 3 × CH<sub>3</sub>), 3.39 (2H, t, *J* 4.8, CH<sub>2</sub>), 3.64 – 3.76 (6H, m, 3 × CH<sub>2</sub>), 3.85 (2H, t, *J* 4.8, CH<sub>2</sub>), 3.90 (3H, s, CH<sub>3</sub>), 4.12 (2H, t, *J* 4.8, CH<sub>2</sub>), 7.12 (1H, dd, *J* 9.3, 3.0, ArH), 7.51 (1H, d, *J* 3.0, ArH), 8.33 (1H, d, *J* 9.3, ArH), 9.99 (1H, s, NH);  $\delta_{\text{C}}$  (101 MHz, CDCl<sub>3</sub>) 28.4 (3 × CH<sub>3</sub>), 50.7 (CH<sub>2</sub>), 52.3 (CH<sub>3</sub>), 67.9 (CH<sub>2</sub>), 69.8 (CH<sub>2</sub>), 70.1 (CH<sub>2</sub>), 70.8 (CH<sub>2</sub>), 70.9 (CH<sub>2</sub>), 80.3 (CCH<sub>3</sub>), 115.1 (ArC), 115.3 (ArCH), 120.4 (ArCH), 122.1 (ArCH), 136.2 (ArC), 152.7 (ArC), 153.1 (NCO), 168.2 (CO<sub>2</sub>CH<sub>3</sub>); *m/z* (ES<sup>+</sup>) 447.1840 (100%, M+Na<sup>+</sup>, C<sub>19</sub>H<sub>28</sub>N<sub>4</sub>O<sub>7</sub>Na requires 447.1850).

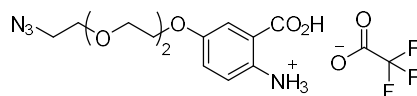
## 5-[2-[2-(2-Azidoethoxy)ethoxy]ethoxy]-2-[(*tert*-butoxycarbonyl)amino]benzoic acid

64



Methyl 5-[2-[2-(2-azidoethoxy)ethoxy]ethoxy]-2-[(*tert*-butoxycarbonyl)amino]benzoate **63** (345 g, 0.81 mmol) was dissolved in methanol (10 mL). 10% NaOH solution (2 mL) was added and the resulting mixture was stirred at room temperature overnight. The solvent was removed using a rotary evaporator under reduced pressure. The residue was re-suspended in water (10 mL) and acidified to pH = 4 with 1M HCl. The mixture was extracted with DCM (2 × 25 mL). The combined organic layer was washed with brine (30 mL), dried over anhydrous MgSO<sub>4</sub> and filtered. The filtrate was removed in a rotary evaporator under reduced pressure to afford the title compound as a light yellow oil in a quantitative yield (337 mg).  $\nu_{\max}(\text{ATR})/\text{cm}^{-1}$  2924, 2103 (N=N=N), 1725 (C=O), 1693 (C=O), 1592;  $\delta_{\text{H}}$  (400 MHz, CDCl<sub>3</sub>) 1.55 (9H, s, 3 × CH<sub>3</sub>), 3.42 (2H, t, *J* 4.9, CH<sub>2</sub>), 3.68 – 3.82 (6H, m, 3 × CH<sub>2</sub>), 3.91 (2H, t, *J* 4.9, CH<sub>2</sub>), 4.17 (2H, t, *J* 4.9, CH<sub>2</sub>), 7.19 (1H, dd, *J* 9.3, 3.1, ArH), 7.62 (1H, d, *J* 3.1, ArH), 8.38 (1H, d, *J* 9.3, ArH), 9.85 (1H, s, NH);  $\delta_{\text{C}}$  (101 MHz, CDCl<sub>3</sub>) 28.4 (3 × CH<sub>3</sub>), 50.7 (CH<sub>2</sub>), 67.9 (CH<sub>2</sub>), 69.9 (CH<sub>2</sub>), 70.1 (CH<sub>2</sub>), 70.7 (CH<sub>2</sub>), 70.9 (CH<sub>2</sub>), 80.6 (CCH<sub>3</sub>), 114.1 (ArC), 116.0 (ArCH), 120.5 (ArCH), 123.0 (ArCH), 136.8 (ArC), 152.7 (ArC), 153.0 (NCO), 171.4 (CO<sub>2</sub>H);  $m/z$  (ES<sup>+</sup>) 433.1710 (100%, M+Na<sup>+</sup>. C<sub>18</sub>H<sub>26</sub>N<sub>4</sub>O<sub>7</sub>Na requires 433.1694).

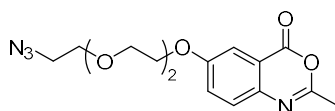
**TFA salt of 2-amino-5-[2-[2-(2-azidoethoxy)ethoxy]ethoxy]benzoic acid 65**



**5-[2-[2-(2-Azidoethoxy)ethoxy]ethoxy]-2-[(*tert*-butoxycarbonyl)amino]benzoic acid 64**

(300 mg, 0.73 mmol) was dissolved in DCM (9 mL) and TFA (1 mL). The solution was stirred at room temperature for 2 h. The solvent was removed using compressed air and the residual TFA was co-evaporated with DCM (10 mL) using a rotary evaporator under reduced pressure to afford the title compound as a brown viscous oil (379 mg, 95%).  $\nu_{\max}(\text{ATR})/\text{cm}^{-1}$  2924, 2108 (N=N=N), 1677 (C=O), 1504;  $\delta_{\text{H}}$  (400 MHz,  $\text{CDCl}_3$ ) 3.43 (2H, t,  $J$  4.8,  $\text{CH}_2$ ), 3.66 – 3.84 (6H, m,  $3 \times \text{CH}_2$ ), 3.89 - 3.98 (2H, m,  $\text{CH}_2$ ), 4.10 – 4.18 (2H, m,  $\text{CH}_2$ ), 7.13 (1H, dd,  $J$  8.8, 2.7,  $\text{ArH}$ ), 7.43 (1H, d,  $J$  8.8,  $\text{ArH}$ ), 7.50 (1H, d,  $J$  2.7,  $\text{ArH}$ );  $\delta_{\text{C}}$  (101 MHz,  $\text{CDCl}_3$ ) 50.6 ( $\text{CH}_2$ ), 67.9 ( $\text{CH}_2$ ), 69.6 ( $\text{CH}_2$ ), 70.0 ( $\text{CH}_2$ ), 70.5 ( $\text{CH}_2$ ), 70.7 ( $\text{CH}_2$ ), 117.1 ( $\text{ArCH}$ ), 121.2 ( $\text{ArCH}$ ), 122.3 ( $\text{ArC}$ ), 125.3 ( $\text{ArCH}$ ), 127.1 ( $\text{ArC}$ ), 157.6 ( $\text{ArC}$ ), 169.5 ( $\text{CO}_2\text{H}$ );  $\delta_{\text{F}}$  (377 MHz,  $\text{CDCl}_3$ ) -75.8;  $m/z$  ( $\text{ES}^+$ ) 333.1174 (20,  $\text{M}+\text{Na}^+$ ). 311.1351 (100%,  $\text{M}+\text{H}^+$ ,  $\text{C}_{13}\text{H}_{19}\text{N}_4\text{O}_5$  requires 311.1350).

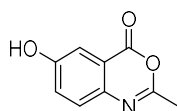
**6-[2-[2-(2-Azidoethoxy)ethoxy]ethoxy]-2-methyl-4*H*-benzo[1,3]oxazin-4-one 66**



TFA salt of 2-amino-5-[2-[2-(2-azidoethoxy)ethoxy]ethoxy]benzoic acid **65** (90 mg, 0.21 mmol) was dissolved in acetonitrile (2 mL). Triethyl orthoacetate (0.06 mL, 0.32 mmol) was added and the reaction mixture was stirred and heated at 90 °C overnight.

After cooling to room temperature, the solvent was removed and the crude mixture was directly purified via flash column chromatography eluting with petroleum ether/EtOAc/AcOH, 33:66:1) to afford the title compound as a light yellow oil (67 mg, 96%).  $\nu_{\max}(\text{ATR})/\text{cm}^{-1}$  2924, 2872, 2101 (N=N=N), 1687 (C=O), 1596, 1518;  $\delta_{\text{H}}$  (400 MHz,  $\text{CDCl}_3$ ) 2.26 (3H, s,  $\text{CH}_3$ ), 3.42 (2H, t,  $J$  4.8,  $\text{CH}_2$ ), 3.66 – 3.84 (6H, m,  $3 \times \text{CH}_2$ ), 3.92 (2H, t,  $J$  4.8,  $\text{CH}_2$ ), 4.17 (2H, t,  $J$  4.8,  $\text{CH}_2$ ), 7.16 (1H, dd,  $J$  9.2, 2.8,  $\text{ArH}$ ), 7.63 (1H, d,  $J$  2.8,  $\text{ArH}$ ), 8.61 (1H, d,  $J$  9.2,  $\text{ArH}$ );  $\delta_{\text{C}}$  (101 MHz,  $\text{CDCl}_3$ ) 25.3 ( $\text{CH}_3$ ), 50.7 ( $\text{CH}_2$ ), 67.7 ( $\text{CH}_2$ ), 69.9 ( $\text{CH}_2$ ), 70.1 ( $\text{CH}_2$ ), 70.7 ( $\text{CH}_2$ ), 70.8 ( $\text{CH}_2$ ), 115.8 ( $\text{ArC}$ ), 116.3 ( $\text{ArCH}$ ), 121.4 ( $\text{ArCH}$ ), 122.0 ( $\text{ArCH}$ ), 135.5 ( $\text{ArC}$ ), 153.7 ( $\text{ArC}$ ), 169.9 ( $\text{CCH}_3$ ), 170.7 ( $\text{CO}_2\text{C}$ );  $m/z$  ( $\text{ES}^+$ ) 335.1365 (100%,  $\text{M}+\text{H}^+$ .  $\text{C}_{15}\text{H}_{19}\text{N}_4\text{O}_5$  requires 335.1350).

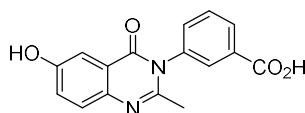
#### 6-Hydroxy-2-methyl-4*H*-3,1-benzoxazin-4-one **68**



5-Hydroxyanthranilic acid **55** (2.00 g, 13.06 mmol) was dissolved in triethyl orthoacetate (3.58 mL, 19.59 mmol) and heated at reflux for 3 h. The reaction mixture was cooled to room temperature and refrigerated for 1 h to aid precipitation. The product was filtered under vacuum and washed with cold hexane (25 mL) to give the title compound as a brown solid (2.16 g, 94%). m.p. 234 - 236 °C;  $\nu_{\max}(\text{ATR})/\text{cm}^{-1}$  2926, 2706, 1764, 1746 (CO), 1637, 1613;  $\delta_{\text{H}}$  (400 MHz,  $\text{DMSO-d}_6$ ) 2.35 (3H, s,  $\text{CH}_3$ ), 7.31 (1H, dd,  $J$  8.7, 2.8,  $\text{ArH}$ ), 7.36 (1H, d,  $J$  2.8,  $\text{ArH}$ ), 7.44 (1H, d,  $J$  8.7,  $\text{ArH}$ ), 10.34 (1H, s,  $\text{OH}$ );  $\delta_{\text{C}}$  (101 MHz,  $\text{DMSO-d}_6$ ) 25.1 ( $\text{CH}_3$ ), 116.8 ( $\text{ArCH}$ ), 119.1 ( $\text{ArC}$ ), 121.2 ( $\text{ArCH}$ ), 122.8 ( $\text{ArCH}$ ), 133.0

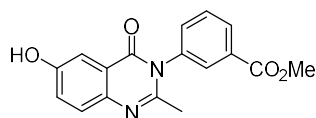
(ArC), 152.9 (ArC), 168.4 (CCH<sub>3</sub>), 169.5 (OCO); *m/z* (ES<sup>+</sup>) 178.0502 (100%, M+H<sup>+</sup>. C<sub>9</sub>H<sub>8</sub>NO<sub>3</sub> requires 178.0499).

### 3-(6-Hydroxy-2-methyl-4-oxoquinazolin-3(4*H*)-yl)benzoic acid **69**



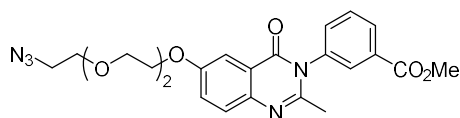
6-Hydroxy-2-methyl-4*H*-3,1-benzoxazin-4-one **68** (1.00 g, 5.64 mmol) and 3-aminobenzoic acid (774 mg, 5.64 mmol) were added to glacial acetic acid (15 mL) and heated at 120 °C for 5 h. The reaction mixture was cooled to room temperature and water (10 mL) was added. The resulting precipitate was filtered and washed with water (20 mL), followed by cold ethanol (20 mL) and hexane (20 mL) to give the title compound as a pale grey solid (1.37 g, 82%). m.p. >300 °C;  $\nu_{\max}$ (ATR)/cm<sup>-1</sup> 3302, 1669 (CO), 1610, 1583, 1503;  $\delta_{\text{H}}$  (400 MHz, DMSO-d<sub>6</sub>) 2.08 (3H, s, CH<sub>3</sub>), 7.30 (1H, dd, *J* 8.8, 2.8, Ar*H*), 7.40 (1H, d, *J* 2.8, Ar*H*), 7.55 (1H, d, *J* 8.8, Ar*H*), 7.66 – 7.74 (2H, m, 2 × Ar*H*), 7.96 (1H, s, Ar*H*), 8.04 – 8.11 (1H, m, Ar*H*), 10.05 (1H, s, OH), 13.22 (1H, s, CO<sub>2</sub>H);  $\delta_{\text{C}}$  (101 MHz, DMSO-d<sub>6</sub>) 24.2 (CH<sub>3</sub>), 109.6 (ArCH), 121.7 (ArC), 124.5 (ArCH), 128.8 (ArCH), 129.9 (ArCH), 130.2 (ArCH), 130.5 (ArCH), 132.8 (ArC), 133.6 (ArCH), 138.8 (ArC), 141.0 (ArC), 151.2 (CCH<sub>3</sub>), 156.4 (ArCOH), 161.7 (NCO), 167.0 (CO<sub>2</sub>H); *m/z* (ES<sup>+</sup>) 297.0884 (100%, M+H<sup>+</sup>. C<sub>16</sub>H<sub>13</sub>N<sub>2</sub>O<sub>4</sub> requires 297.0870).

### Methyl 3-(6-hydroxy-2-methyl-4-oxoquinazolin-3(4*H*)-yl)benzoate **70**



3-[6-Hydroxy-2-methyl-4-oxoquinazolin-3(4*H*)-yl]benzoic acid **69** (300 mg, 1.01 mmol) was suspended in methanol (5 mL). Concentrated sulphuric acid (0.2 mL) was added dropwise and the reaction mixture was stirred and heated at reflux overnight. The mixture was cooled and neutralized to pH = 6 - 7 with sat. NaHCO<sub>3</sub>. The resultant pale brown precipitate was filtered, rinsed with ice cold water (8 mL) and dried thoroughly under high vacuum to give the title compound as a pale grey solid (298 g, 95%). m.p. 120 - 122 °C;  $\nu_{\max}(\text{ATR})/\text{cm}^{-1}$  3570, 3063, 1734 (CO), 1675 (CO);  $\delta_{\text{H}}$  (500 MHz, DMSO-*d*<sub>6</sub>) 2.08 (3H, s, CH<sub>3</sub>), 3.89 (3H, s, CH<sub>3</sub>), 7.30 (1H, dd, *J* 8.8, 2.8, Ar*H*), 7.40 (1H, d, *J* 2.8, Ar*H*), 7.54 (1H, d, *J* 8.8, Ar*H*), 7.69 – 7.78 (2H, m, 2 × Ar*H*), 8.01 (1H, d, *J* 1.7, Ar*H*), 8.09 (1H, dt, *J* 7.1, 1.7, Ar*H*), 10.03 (1H, s, OH);  $\delta_{\text{C}}$  (126 MHz, DMSO-*d*<sub>6</sub>) 24.2 (CH<sub>3</sub>), 52.9 (CH<sub>3</sub>), 109.6 (ArCH), 121.8 (ArC), 124.5 (ArCH), 128.8 (ArCH), 129.9 (ArCH), 130.0 (ArCH), 130.6 (ArCH), 131.6 (ArC), 134.0 (ArCH), 139.0 (ArC), 141.1 (ArC), 151.0 (CCH<sub>3</sub>), 156.4 (ArCOH), 161.7 (NCO), 166.0 (CO<sub>2</sub>Me); *m/z* (ES<sup>+</sup>) 311.1039 (100%, M+H<sup>+</sup>. C<sub>17</sub>H<sub>15</sub>N<sub>2</sub>O<sub>4</sub> requires 311.1026).

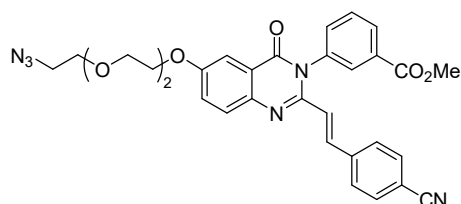
**Methyl 3-[6-[2-[2-(2-azidoethoxy)ethoxy]ethoxy]-2-methyl-4-oxoquinazolin-3(4H)-yl]benzoate 71**



Potassium carbonate (66 mg, 0.48 mmol) was added to methyl 3-(6-hydroxy-2-methyl-4-oxoquinazolin-3(4H)-yl)benzoate **70** (100 mg, 0.32 mmol) and 2-[2-(2-azidoethoxy)ethoxy]ethyl-4-methylbenzenesulfonate **36** (125 mg, 0.38 mmol) in acetonitrile (5 mL). The reaction mixture was stirred and heated at reflux overnight. After cooling to room temperature, the solvent was removed using a rotary evaporator under reduced pressure. The crude residue was diluted with water (10 mL) and ethyl acetate (10 mL). The product was extracted with ethyl acetate (3 × 20 mL), washed with brine (30 mL). The organic phase was dried over anhydrous MgSO<sub>4</sub>, filtered and the filtrate was evaporated under reduced pressure. The crude was purified by flash column chromatography on silica gel, eluting petroleum ether/EtOAc, 1:2 to afford the title compound as a white solid in a quantitative yield (166 mg). m.p. 80 - 82 °C;  $\nu_{\max}$ (ATR)/cm<sup>-1</sup> 2894, 2091 (N<sub>3</sub>), 1718 (CO), 1681 (CO);  $\delta_{\text{H}}$  (400 MHz, CDCl<sub>3</sub>) 2.24 (3H, s, CH<sub>3</sub>), 3.41 (2H, t, *J* 5.1, CH<sub>2</sub>), 3.68 – 3.80 (6H, m, 3 × CH<sub>2</sub>), 3.94 (2H, t, *J* 4.7, CH<sub>2</sub>), 3.96 (3H, s, CH<sub>3</sub>), 4.26 (2H, t, *J* 4.7, CH<sub>2</sub>), 7.44 (1H, dd, *J* 8.9, 2.9, ArH), 7.50 (1H, ddd, *J* 7.9, 2.1, 1.1, ArH), 7.61 – 7.72 (3H, m, 3 × ArH), 7.99 (1H, t, *J* 1.8, ArH), 8.22 (1H, dt, *J* 7.9, 1.3, ArH);  $\delta_{\text{C}}$  (101 MHz, CDCl<sub>3</sub>) 24.3 (CH<sub>3</sub>), 50.7 (CH<sub>2</sub>), 52.5 (CH<sub>3</sub>), 67.9 (CH<sub>2</sub>), 69.7 (CH<sub>2</sub>), 70.1 (CH<sub>2</sub>), 70.7 (CH<sub>2</sub>), 70.9 (CH<sub>2</sub>), 107.3 (ArCH), 121.3 (ArC), 125.3 (ArCH), 128.5 (ArCH), 129.4 (ArCH), 130.2 (ArCH), 130.5 (ArCH), 132.2 (ArC), 132.6 (ArCH), 138.1 (ArC), 142.1 (ArC), 151.4 (CCH<sub>3</sub>), 157.5 (ArC), 162.1 (NCO), 165.8

(CO<sub>2</sub>Me); *m/z* (ES<sup>+</sup>) 490.1712 (50, M+Na<sup>+</sup>), 468.1895 (100%, M+H<sup>+</sup>. C<sub>23</sub>H<sub>26</sub>N<sub>5</sub>O<sub>6</sub> requires 468.1878).

**Methyl (E)-3-[6-[2-[2-(2-azidoethoxy)ethoxy]ethoxy]-2-(4-cyanostyryl)-4-oxoquinazolin-3(4*H*)-yl]benzoate 72**

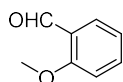


Methyl 3-[6-[2-[2-(2-azidoethoxy)ethoxy]ethoxy]-2-methyl-4-oxoquinazolin-3(4*H*)-yl]benzoate **71** (50 mg, 0.11 mmol) and 4-formylbenzonitrile (17 mg, 0.13 mmol) were dissolved in glacial acetic acid (1 mL) and heated at reflux for 48 h. The reaction mixture was cooled to room temperature and the solvent was removed. The crude was purified by flash column chromatography on silica gel, eluting petroleum ether/EtOAc 1:1 to afford the title compound as a bright yellow solid (13 mg, 20%). m.p. 142 - 146 °C;  $\nu_{\max}$ (ATR)/cm<sup>-1</sup> 2923, 2107 (N<sub>3</sub>), 1731 (CO), 1680 (CO);  $\delta_{\text{H}}$  (400 MHz, CDCl<sub>3</sub>) 3.42 (2H, t, *J* 5.0, CH<sub>2</sub>), 3.67 – 3.83 (6H, m, 3 × CH<sub>2</sub>), 3.91 – 4.00 (5H, m, CH<sub>2</sub>, CH<sub>3</sub>), 4.29 (2H, t, *J* 4.5, CH<sub>2</sub>), 6.41 (1H, d, *J* 15.5, CHCHArCN), 7.39 (2H, d, *J* 8.1, 2 × Ar*H*), 7.49 (1H, dd, *J* 9.0, 2.9, Ar*H*), 7.54 (1H, d, *J* 7.8, Ar*H*), 7.60 (2H, d, *J* 8.1, 2 × Ar*H*), 7.66 – 7.81 (3H, m, 3 × Ar*H*), 7.93 (1H, d, *J* 15.5, CHArCN), 8.05 (1H, s, Ar*H*), 8.29 (1H, d, *J* 7.9, Ar*H*);  $\delta_{\text{C}}$  (101 MHz, CDCl<sub>3</sub>) 50.7 (CH<sub>2</sub>), 52.6 (CH<sub>3</sub>), 68.1 (CH<sub>2</sub>), 69.7 (CH<sub>2</sub>), 70.2 (CH<sub>2</sub>), 70.8 (CH<sub>2</sub>), 71.0 (CH<sub>2</sub>), 107.5 (CHCHArCN), 112.6 (ArC), 118.5 (ArC), 120.9 (ArC), 121.7 (ArC), 122.9 (ArCH), 125.6 (ArCH), 128.0 (2 × ArCH), 129.3 (ArCH), 130.0



t,  $J$  4.6,  $\text{CH}_2$ ), 6.42 (1H, d,  $J$  15.5,  $\text{CHCHArCN}$ ), 7.40 (2H, d,  $J$  8.3,  $2 \times \text{ArH}$ ), 7.50 (1H, dd,  $J$  8.9, 2.9,  $\text{ArH}$ ), 7.58 – 7.63 (3H, m,  $3 \times \text{ArH}$ ), 7.70 (H, d,  $J$  2.9,  $\text{ArH}$ ), 7.73 – 7.80 (2H, m,  $2 \times \text{ArH}$ ), 7.94 (1H, d,  $J$  15.5,  $\text{CHArCN}$ ), 8.08 (1H, s,  $\text{ArH}$ ), 8.32 (1H, d,  $J$  8.0,  $\text{ArH}$ );  $\delta_{\text{C}}$  (101 MHz,  $\text{DMSO-d}_6$ ) 50.5 ( $\text{CH}_2$ ), 68.4 ( $\text{CH}_2$ ), 69.3 ( $\text{CH}_2$ ), 69.8 ( $\text{CH}_2$ ), 70.2 ( $\text{CH}_2$ ), 70.5 ( $\text{CH}_2$ ), 107.9 ( $\text{CHCHArCN}$ ), 111.9 ( $\text{ArC}$ ), 119.1 ( $\text{ArC}$ ), 122.1 ( $\text{ArC}$ ), 124.0 ( $\text{ArCH}$ ), 125.2 ( $\text{ArCH}$ ), 128.6 ( $2 \times \text{ArCH}$ ), 129.7 ( $\text{ArCH}$ ), 130.2 ( $\text{ArCH}$ ), 130.4 ( $\text{ArCH}$ ), 130.5 ( $\text{ArCH}$ ), 132.7 ( $\text{ArC}$ ), 133.3 ( $2 \times \text{ArCH}$ ), 133.8 ( $\text{ArCH}$ ), 136.5 ( $\text{ArCH}$ ), 137.6 ( $\text{ArC}$ ), 139.9 ( $\text{ArC}$ ), 142.2 ( $\text{ArC}$ ), 149.2 ( $\text{ArC}$ ), 157.9 ( $\text{NCN}$ ), 161.4 ( $\text{NCO}$ ), 167.0 ( $\text{CO}_2\text{H}$ );  $m/z$  ( $\text{ES}^+$ ) 567.2000 (100%,  $\text{M}+\text{H}^+$ .  $\text{C}_{30}\text{H}_{27}\text{N}_6\text{O}_6$  requires 567.1987).

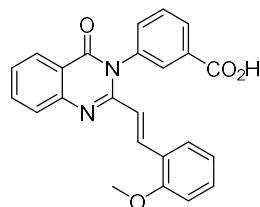
## 2-Methoxybenzaldehyde 78



Salicylaldehyde **77** (0.5 mL, 4.69 mmol), sodium carbonate (600 mg, 5.66 mmol), THF (20 mL) and methanol (5 mL) were mixed in a two-neck round-bottom flask equipped with a reflux condenser. Iodomethane (1.0 mL, 16.06 mmol) was added dropwise and the resulting suspension was stirred and heated at 70 °C for 48 h. Water (60 mL) was added and the crude mixture was extracted with DCM three times ( $3 \times 30$  mL). The combined organic phases were washed with brine (50 mL), dried over anhydrous  $\text{MgSO}_4$ , filtered and the filtrate was eliminated in a rotary evaporator under reduced pressure. The crude residue was purified by flash column chromatography on silica gel, eluting petroleum ether/EtOAc, EtOAc: 2% to afford the title compound as an off-white solid

(115 mg, 18%). m.p. 36 - 38 °C [lit.<sup>130</sup> m.p. 36 - 38 °C];  $\nu_{\max}(\text{ATR})/\text{cm}^{-1}$  2865, 1682 (CO), 1664, 1596;  $\delta_{\text{H}}$  (400 MHz,  $\text{CDCl}_3$ ) 3.93 (3H, s,  $\text{CH}_3$ ), 7.02 (1H, d,  $J$  8.4, ArH), 7.06 (1H, t,  $J$  7.5, ArH), 7.58 (1H, td,  $J$  7.8, 1.8, ArH), 7.85 (1H, dd,  $J$  7.7, 1.8, ArH), 10.50 (1H, s, CHO);  $m/z$  ( $\text{ES}^+$ ) 137 (100%,  $\text{M}+\text{H}^+$ ). The data agree with those reported in the literature.<sup>130</sup>

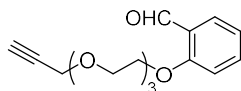
**(E)-3-[2-(2-methoxystyryl)-4-oxoquinazolin-3(4H)-yl]benzoic acid 79**



3-[2-Methyl-4-oxo-3(4H)-quinazolinyl]benzoic acid **48** (178 mg, 0.63 mmol) and 2-methoxybenzaldehyde **78** (72 mg, 0.53 mmol) were dissolved in glacial acetic acid (4 mL) and heated at 130 °C overnight. After cooling to room temperature, the solvent was removed and the residue was co-evaporated with cyclohexane ( $3 \times 10$  mL). The crude was washed with water (10 mL), followed by cold ethanol (10 mL) and hexane (10 mL). The crude residue was purified by flash column chromatography on silica gel, eluting EtOAc/MeOH, MeOH: 0 - 5% to afford the title compound as a yellow solid (72 mg, 34%). m.p. 258 - 260 °C;  $\nu_{\max}(\text{ATR})/\text{cm}^{-1}$  2936, 1678 (CO), 1546;  $\delta_{\text{H}}$  (400 MHz,  $\text{DMSO-d}_6$ ) 3.67 (3H, s,  $\text{CH}_3$ ), 6.56 (1H, d,  $J$  15.6,  $\text{CHCHAr}$ ), 6.93 (1H, t,  $J$  7.4, ArH), 7.02 (1H, d,  $J$  8.2, ArH), 7.25 - 7.38 (2H, m,  $2 \times \text{ArH}$ ), 7.54 (1H, t,  $J$  7.1, ArH), 7.72 - 7.82 (3H, m,  $3 \times \text{ArH}$ ), 7.89 (1H, t,  $J$  7.6, ArH), 7.97 - 8.06 (2H, m,  $2 \times \text{ArH}$ ), 8.11-8.18 (2H, m, ArH,  $\text{CHAr}$ ), 13.27 (1H, br s,  $\text{CO}_2\text{H}$ );  $\delta_{\text{C}}$  (101 MHz,  $\text{DMSO-d}_6$ ) 55.6 ( $\text{CH}_3$ ), 112.2

(CHCHAr), 121.0 (ArC), 121.3 (ArCH), 121.6 (ArCH), 123.7 (ArC), 126.8 (ArCH), 126.9 (ArCH), 127.7 (ArCH), 130.2 (ArCH), 130.3 (ArCH), 130.4 (ArCH), 130.5 (ArCH), 131.6 (ArCH), 132.9 (ArC), 134.0 (ArCH), 135.3 (ArCH), 135.5 (ArCH), 138.1 (ArC), 148.0 (ArC), 152.2 (ArC), 158.4 (NCN), 161.9 (NCO), 167.0 (CO<sub>2</sub>H); *m/z* (ES<sup>+</sup>) 399.1353 (100%, M+H<sup>+</sup>. C<sub>24</sub>H<sub>19</sub>N<sub>2</sub>O<sub>4</sub> requires 399.1339).

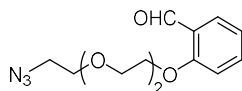
### 2-[2-[2-[2-(Prop-2-yn-1-yloxy)ethoxy]ethoxy]ethoxy]benzaldehyde **80**



Salicylaldehyde **77** (0.03 mL, 0.29 mmol) and 2-[2-[2-(prop-2-yn-1-yloxy)ethoxy]ethoxy]ethyl 4-methylbenzenesulfonate **54** (120 mg, 0.35 mmol) were dissolved in acetonitrile (2 mL) and potassium carbonate (61 mg, 0.44 mmol) was added. The reaction mixture was stirred and heated at 90 °C for 48 h. After cooling to room temperature, the solvent was removed using a rotary evaporator under reduced pressure. Water (15 mL) was added and the crude mixture was extracted with ethyl acetate three times (3 × 20 mL). The combined organic phase was washed with brine (40 mL), dried over anhydrous MgSO<sub>4</sub>, filtered and the filtrate was eliminated in a rotary evaporator under reduced pressure. The crude residue was purified by flash column chromatography on silica gel, eluting petroleum ether/EtOAc, EtOAc: 30 - 50% to afford the title compound as a yellow oil (74 mg, 87%).  $\nu_{\max}$ (ATR)/cm<sup>-1</sup> 3258, 2869, 1684 (C=O), 1598;  $\delta_{\text{H}}$  (400 MHz, CDCl<sub>3</sub>) 2.45 (1H, t, *J* 2.4, CH), 3.68 – 3.78 (8H, m, 4 × CH<sub>2</sub>), 3.93 (2H, t, *J* 4.7, CH<sub>2</sub>), 4.21 (2H, d, *J* 2.4, CH<sub>2</sub>), 4.27 (2H, t, *J* 4.7, CH<sub>2</sub>), 7.01 (1H, d, *J* 8.4, ArH),

7.05 (1H, t, *J* 7.5, ArH), 7.55 (1H, td, *J* 7.7, 1.8, ArH), 7.85 (1H, dd, *J* 7.7, 1.8, ArH), 10.53 (1H, s, CHO);  $\delta_c$  (101 MHz, CDCl<sub>3</sub>) 58.4 (CH<sub>2</sub>CCH), 68.2 (CH<sub>2</sub>), 69.1 (CH<sub>2</sub>), 69.5 (CH<sub>2</sub>), 70.5 (CH<sub>2</sub>), 70.7 (CH<sub>2</sub>), 71.0 (CH<sub>2</sub>), 74.6 (CCH), 79.6 (CH), 112.8 (ArCH), 121.0 (ArCH), 125.1 (ArC), 128.3 (ArCH), 135.9 (ArCH), 161.3 (ArC), 190.0 (CHO); *m/z* (ES<sup>+</sup>) 293.1397 (100%, M+H<sup>+</sup>. C<sub>16</sub>H<sub>21</sub>O<sub>5</sub> requires 293.1384).

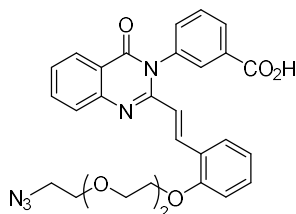
### 2-[2-[2-(2-Azidoethoxy)ethoxy]ethoxy]benzaldehyde **83**



Salicylaldehyde **77** (0.5 mL, 4.69 mmol) and 2-[2-(2-azidoethoxy)ethoxy]ethyl-4-methylbenzenesulfonate **36** (1.85 g, 5.63 mmol) were dissolved in acetonitrile (10 mL) and potassium carbonate (973 mg, 7.04 mmol) was added. The reaction mixture was stirred and heated at 90 °C overnight. After cooling to room temperature, the solvent was removed using a rotary evaporator under reduced pressure. Water (20 mL) was added and the crude mixture was extracted with ethyl acetate three times (3 × 30 mL). The combined organic phases were washed with brine (40 mL), dried over anhydrous MgSO<sub>4</sub>, filtered and the filtrate was eliminated in a rotary evaporator under reduced pressure. The crude residue was purified by flash column chromatography on silica gel, eluting petroleum ether/EtOAc 4:1 to afford the title compound as a colourless oil in a quantitative yield (1.42 g).  $\nu_{\max}$ (ATR)/cm<sup>-1</sup> 2869, 2098 (N<sub>3</sub>), 1685 (C=O), 1598;  $\delta_H$  (400 MHz, CDCl<sub>3</sub>) 3.41 (2H, t, *J* 5.1, CH<sub>2</sub>), 3.68 – 3.80 (6H, m, 3 × CH<sub>2</sub>), 3.95 (2H, t, *J* 4.7, CH<sub>2</sub>), 4.28 (2H, t, *J* 4.7, CH<sub>2</sub>), 7.02 (1H, d, *J* 8.4, ArH), 7.06 (1H, t, *J* 7.5, ArH), 7.55

(1H, td, *J* 7.7, 1.8, ArH), 7.86 (1H, dd, *J* 7.7, 1.8, ArH), 10.55 (1H, s, CHO);  $\delta_c$  (101 MHz, CDCl<sub>3</sub>) 50.7 (CH<sub>2</sub>), 68.3 (CH<sub>2</sub>), 69.6 (CH<sub>2</sub>), 70.2 (CH<sub>2</sub>), 70.8 (CH<sub>2</sub>), 71.0 (CH<sub>2</sub>), 112.7 (ArCH), 121.0 (ArCH), 125.1 (ArC), 128.3 (ArCH), 135.9 (ArCH), 161.3 (ArC), 190.0 (CHO); *m/z* (ES<sup>+</sup>) 280.1280 (100%, M+H<sup>+</sup>. C<sub>13</sub>H<sub>18</sub>N<sub>3</sub>O<sub>4</sub> requires 280.1292).

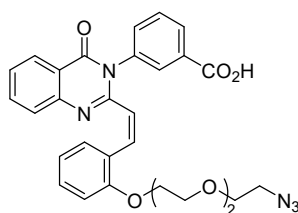
**(*E*)-3-[2-[2-[2-[2-(2-Azidoethoxy)ethoxy]ethoxy]styryl]-4-oxoquinazolin-3(4*H*)-yl]benzoic acid **84****



3-(2-Methyl-4-oxo-3(4*H*)-quinazoliny)benzoic acid **48** (480 mg, 1.71 mmol) and 2-[2-[2-(2-azidoethoxy)ethoxy]ethoxy]benzaldehyde **83** (600 mg, 2.15 mmol) were suspended in glacial acetic acid (15 mL) and heated at 120 °C overnight. The reaction mixture was cooled to room temperature and the solvent was removed using a rotary evaporator under reduced pressure. The crude residue was purified by flash column chromatography on silica gel, eluting DCM/MeOH, MeOH: 0 – 5% to afford the title compound as a yellow solid (422 mg, 46%). m.p. 66 - 68 °C;  $\nu_{\max}$ (ATR)/cm<sup>-1</sup> 2872, 2099 (N<sub>3</sub>), 1680 (CO), 1544;  $\delta_H$  (400 MHz, MeOD) 3.28 (2H, t, *J* 5.0, CH<sub>2</sub>), 3.58 – 3.74 (8H, m, 4 × CH<sub>2</sub>), 4.09 – 4.17 (2H, m, CH<sub>2</sub>), 6.69 (1H, d, *J* 15.6, CHCHAr), 6.92 (1H, t, *J* 7.5, ArH), 7.01 (H, d, *J* 8.2, ArH), 7.25 – 7.34 (2H, m, 2 × ArH), 7.56 (1H, t, *J* 7.5, ArH), 7.67 (1H, d, *J* 7.9, ArH), 7.75 – 7.93 (3H, m, 3 × ArH), 8.05 – 8.10 (1H, m, ArH), 8.15

(1H, d, *J* 15.6, CHAr), 8.26 (2H, dd, *J* 7.9, 1.3, ArH);  $\delta_C$  (101 MHz, MeOD) 50.3 (CH<sub>2</sub>), 67.6 (CH<sub>2</sub>), 69.1 (CH<sub>2</sub>), 69.8 (CH<sub>2</sub>), 70.2 (CH<sub>2</sub>), 70.5 (CH<sub>2</sub>), 112.3 (CHCHAr), 120.2 (ArC), 120.5 (ArCH), 120.7 (ArCH), 123.9 (ArC), 126.4 (ArCH), 126.5 (ArCH), 126.9 (ArCH), 129.7 (ArCH), 129.9 (ArCH), 130.0 (ArCH), 130.3 (ArCH), 130.8 (ArCH), 132.7 (ArC), 133.2 (ArCH), 134.8 (ArCH), 136.6 (ArCH), 137.5 (ArC), 147.8 (ArC), 152.8 (ArC), 157.7 (NCN), 162.7 (NCO), 167.1 (CO<sub>2</sub>H); *m/z* (ES<sup>+</sup>) 542.2044 (100%, M+H<sup>+</sup>. C<sub>29</sub>H<sub>28</sub>N<sub>5</sub>O<sub>6</sub> requires 542.2034).

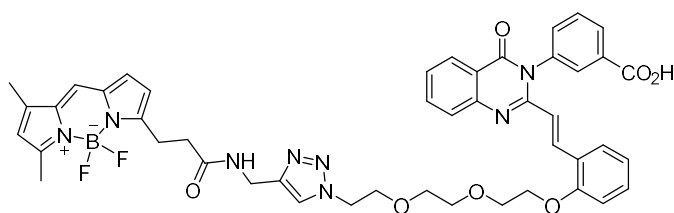
**(*Z*)-3-[2-[2-[2-[2-(2-Azidoethoxy)ethoxy]ethoxy]styryl]-4-oxoquinazolin-3(*4H*)-yl]benzoic acid **85****



A solution of (*E*)-3-[2-[2-[2-[2-(2-azidoethoxy)ethoxy]ethoxy]styryl]-4-oxoquinazolin-3(*4H*)-yl]benzoic acid **84** (50 mg, 0.092 mmol) in MeOD (3 mL) was exposed to a lamp with a regular light (23 W) for 3 h. The solvent was removed using a rotary evaporator under reduced pressure. The crude residue was purified via preparative HPLC using an “Waters Xbridge C 18 4.6 × 250 mm” column [50% MeCN in aqueous TFA (0.1%) over 20 mins, 280 nm, retention time: 8.2 min] to afford the title compound as a yellow solid (41 mg, 82%). *m.p.* 62 - 64 °C;  $\nu_{\max}$ (ATR)/cm<sup>-1</sup> 2925, 2102 (N<sub>3</sub>), 1684 (CO), 1547;  $\delta_H$  (400 MHz, MeOD) 3.25 (2H, t, *J* 5.0, CH<sub>2</sub>), 3.57 – 3.74 (8H, m, 4 × CH<sub>2</sub>), 4.00 (2H, t, *J*

4.7, CH<sub>2</sub>), 6.19 (1H, d, *J* 12.4, CHCHAR), 6.78 – 6.97 (3H, m, 3 × ArH), 7.20 (1H, dd, *J* 7.9, 1.0, ArH), 7.29 (1H, td, *J* 7.7, 1.5, ArH), 7.37 (1H, dd, *J* 7.9, 1.0, ArH), 7.52 – 7.66 (3H, m, 2 × ArH, CHAR), 7.69 – 7.73 (1H, m, ArH), 7.89 (1H, td, *J* 7.7, 1.5, ArH), 8.11 (1H, d, *J* 7.9, ArH), 8.27 (1H, dd, *J* 7.9, 1.0, ArH); δ<sub>c</sub> (101 MHz, MeOD) 50.3 (CH<sub>2</sub>), 67.5 (CH<sub>2</sub>), 69.2 (CH<sub>2</sub>), 69.8 (CH<sub>2</sub>), 70.1 (CH<sub>2</sub>), 70.4 (CH<sub>2</sub>), 111.8 (CHCHAR), 120.1 (ArCH), 120.5 (ArC), 120.7 (ArCH), 124.4 (ArC), 126.2 (ArCH), 126.6 (ArCH), 127.3 (ArCH), 128.9 (ArCH), 129.3 (ArCH), 129.6 (ArCH), 129.8 (ArCH), 130.2 (ArCH), 131.7 (ArC), 132.4 (ArCH), 133.0 (ArCH), 135.0 (ArCH), 136.9 (ArC), 146.7 (ArC), 153.6 (ArC), 156.5 (NCN), 162.1 (NCO), 167.1 (CO<sub>2</sub>H); *m/z* (ES<sup>+</sup>) 542.2031 (100%, M+H<sup>+</sup>. C<sub>29</sub>H<sub>28</sub>N<sub>5</sub>O<sub>6</sub> requires 542.2034).

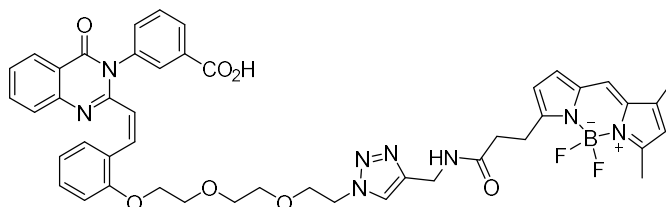
**(E)-BODIPY-PEG<sub>3</sub>-quinazolinone 86**



(*E*)-3-[2-[2-[2-(2-Azidoethoxy)ethoxy]ethoxy]styryl]-4-oxoquinazolin-3(4*H*)-yl]benzoic acid **84** (2.5 mg,  $4.56 \times 10^{-3}$  mmol) and alkyne-BODIPY-FL **41** (1.0 mg,  $3.04 \times 10^{-3}$  mmol) were dissolved in DMSO (100 μL). L-Ascorbic acid (10.7 mg) was dissolved in DMSO (1 mL) and portion of this (100 μL,  $6.08 \times 10^{-3}$  mmol) was added to the reaction. CuSO<sub>4</sub> (24 mg) was dissolved in water (1 mL) and portion of this (20 μL,  $3.04 \times 10^{-3}$  mmol) was added to the reaction. The reaction mixture was covered with

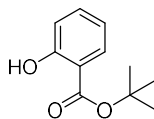
aluminium foil and stirred at room temperature overnight. The crude mixture was directly purified via preparative HPLC using an “Waters Xbridge C 18 4.6 × 250 mm” column [50% MeCN in aqueous TFA (0.1%) over 15 mins, 500 nm, retention time: 11.7 min] to afford the title compound as an orange-red solid (2.6 mg, 100%).  $m/z$  ( $ES^+$ ) 871.3557 (100%,  $M+H^+$ .  $C_{46}H_{46}BF_2N_8O_7$  requires 871.3545).

### (Z)-BODIPY-PEG<sub>3</sub>-quinazolinone **87**



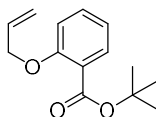
(Z)-3-[2-[2-[2-(2-Azidoethoxy)ethoxy]ethoxy]styryl]-4-oxoquinazolin-3(4H)-yl]benzoic acid **85** (2.5 mg,  $4.56 \times 10^{-3}$  mmol) and alkyne-BODIPY-FL **41** (1.0 mg,  $3.04 \times 10^{-3}$  mmol) were dissolved in DMSO (100  $\mu$ L). L-Ascorbic acid (10.7 mg) was dissolved in DMSO (1 mL) and portion of this (100  $\mu$ L,  $6.08 \times 10^{-3}$  mmol) was added to the reaction.  $CuSO_4$  (24 mg) was dissolved in water (1 mL) and portion of this (20  $\mu$ L,  $3.04 \times 10^{-3}$  mmol) was added to the reaction. The reaction mixture was covered with aluminium foil and stirred at room temperature overnight. The crude mixture was directly purified via preparative HPLC using an “Waters Xbridge C 18 4.6 × 250 mm” column [45% MeCN in aqueous TFA (0.1%) over 15 mins, 500 nm, retention time: 6.9 min] to afford the title compound as vermilion solid (2.5 mg, 96%).  $m/z$  ( $ES^+$ ) 871.3533 (100%,  $M+H^+$ .  $C_{46}H_{46}BF_2N_8O_7$  requires 871.3545).

### ***tert*-Butyl 2-hydroxybenzoate **108****



Salicylic acid **107** (1.00 g, 7.24 mmol), *N*-hydroxysuccinimide (35 mg, 0.30 mmol) and *tert*-butyl alcohol (6 mL) were dissolved in dry DCM (6 mL) under argon. A solution of *N,N'*-dicyclohexylcarbodiimide in dry DCM (5 mL) was added dropwise. The reaction mixture was stirred at room temperature under argon for 24 h, followed by filtration. The filtrate was washed with sat. NaHCO<sub>3</sub> (30 mL) and brine (30 mL). The organic phase was dried over anhydrous MgSO<sub>4</sub>, filtered and the filtrate was evaporated under reduced pressure. The crude was purified by flash column chromatography on silica gel, eluting petroleum ether/EtOAc, EtOAc: 2 – 3% to afford the title compound as a colourless mobile oil (1.05 g, 74%).  $\nu_{\max}(\text{ATR})/\text{cm}^{-1}$  2979, 1668 (C=O), 1614;  $\delta_{\text{H}}$  (400 MHz, CDCl<sub>3</sub>) 1.64 (9H, s, 3 × CH<sub>3</sub>), 6.87 (1H, td, *J* 7.5, 1.0, ArH), 6.98 (1H, dd, *J* 8.4, 0.9, ArH), 7.44 (1H, td, *J* 7.7, 1.7, ArH), 7.80 (1H, dd, *J* 8.0, 1.7, ArH), 11.08 (1H, s, OH); *m/z* (EI<sup>+</sup>) 194 (30%, M<sup>+</sup>), 121 (100), 92 (80). The data agree with those reported in the literature.<sup>131</sup>

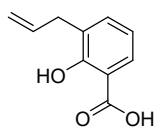
### ***tert*-Butyl 2-(allyloxy)benzoate **109****



*tert*-Butyl 2-hydroxybenzoate **108** (854 mg, 4.37 mmol) and potassium carbonate (907 mg, 6.56 mmol) were suspended in DMF (10 mL). A solution of allyl bromide (0.57 mL, 6.56 mmol) was added dropwise. The reaction mixture was stirred at room temperature

overnight. Ice (30 g) was poured into the reaction mixture with constant stirring. The emulsified content was extracted with diethyl ether (3 × 50 mL). The combined organic phases were dried over anhydrous MgSO<sub>4</sub>, filtered and the filtrate was evaporated under reduced pressure. The crude was purified by flash column chromatography on silica gel, eluting petroleum ether/EtOAc, EtOAc: 5% to afford the title compound as a colourless oil (966 mg, 94%).  $\nu_{\max}(\text{ATR})/\text{cm}^{-1}$  2979, 1701 (C=O), 1601;  $\delta_{\text{H}}$  (400 MHz, CDCl<sub>3</sub>) 1.61 (9H, s, 3 × CH<sub>3</sub>), 4.63 (2H, dt, *J* 5.0, 1.5, CH<sub>2</sub>), 5.31 (1H, dq, *J* 10.6, 1.4, CHH), 5.50 (1H, dq, *J* 17.3, 1.6, CHH), 6.09 (H, ddt, *J* 17.2, 10.6, 5.1 CH), 6.90 – 7.01 (2H, m, 2 × ArH), 7.40 (1H, ddd, *J* 8.3, 7.5, 1.8, ArH), 7.72 (1H, dd, *J* 7.7, 1.8, ArH);  $\delta_{\text{C}}$  (101 MHz, CDCl<sub>3</sub>) 28.3 (3 × CH<sub>3</sub>), 69.5 (CH<sub>2</sub>), 81.0 (CCH<sub>3</sub>), 113.5 (ArCH), 117.5 (C=CH<sub>2</sub>), 120.3 (ArCH), 122.8 (ArC), 131.2 (ArCH), 132.6 (ArCH), 133.0 (CH), 157.7 (ArCO), 165.9 (OCO); *m/z* (ES<sup>+</sup>) 257.1157 (100%, M+Na<sup>+</sup>. C<sub>14</sub>H<sub>18</sub>O<sub>3</sub>Na requires 257.1148).

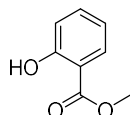
### 3-Allyl-2-hydroxybenzoic acid **110**



*tert*-Butyl 2-(allyloxy)benzoate (384 mg, 1.64 mmol) **109** was dissolved in 1,2-dichlorobenzene (2 mL) and heated at 150 °C for 2 days. The resulting brownish oil was purified via flash column chromatography on silica gel, eluting petroleum ether/EtOAc, EtOAc: 3% to afford the title compound as a brown oil (137 mg, 47%).  $\delta_{\text{H}}$  (400 MHz, CDCl<sub>3</sub>) 3.47 (2H, d, *J* 6.5, CH<sub>2</sub>), 5.06 – 5.16 (2H, m, CH<sub>2</sub>), 5.97 – 6.11 (1H, m, CH), 6.91 (1H, t, *J* 7.7, ArH), 7.42 (1H, d, *J* 7.3, ArH), 7.84 (1H, dd, *J* 7.9, 1.3, ArH), 10.74

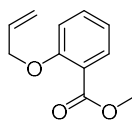
(1H, s, OH);  $m/z$  (EI<sup>+</sup>) 178 (100%, M<sup>+</sup>). The data agree with those reported in the literature.<sup>132</sup>

### Methyl 2-hydroxybenzoate 114



Salicylic acid **107** (5.00 g, 36.2 mmol) was dissolved in methanol (60 mL). Concentrated sulphuric acid (2 mL) was added dropwise to the solution. The reaction mixture was stirred and heated at reflux for 18 h. After cooling to room temperature, the solvent was removed using a rotary evaporator under reduced pressure. The pH of the residue was adjusted to 6 with sat. aq. NaHCO<sub>3</sub>. The aqueous solution was extracted with DCM (3 × 30 mL). The combined organic phases were washed with brine (50 mL), dried over anhydrous Na<sub>2</sub>SO<sub>4</sub>, filtered and the filtrate was evaporated under reduced pressure to afford the title compound as a colourless oil (4.61 g, 84%).  $\delta_{\text{H}}$  (400 MHz, CDCl<sub>3</sub>) 3.97 (3H, s, CH<sub>3</sub>), 6.90 (1H, t,  $J$  7.5, ArH), 7.00 (1H, d,  $J$  8.2, ArH), 7.48 (1H, td,  $J$  7.7, 1.8, ArH), 7.86 (1H, dd,  $J$  8.0, 1.8, ArH), 10.80 (1H, s, OH);  $m/z$  (ES<sup>+</sup>) 191 (100%, M+K<sup>+</sup>). The data agree with those reported in the literature.<sup>104</sup>

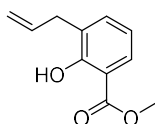
### Methyl 2-(allyloxy)benzoate **112**



Potassium carbonate (4.99 g, 36.12 mmol) and allyl bromide (3.13 mL, 36.12 mmol) were added to a solution of methyl 2-hydroxybenzoate **114** (4.58 g, 30.10 mmol) in DMF (10 mL). The reaction mixture was stirred at room temperature for 18 h. Water (50 mL) was poured into the reaction mixture with constant stirring. The emulsified content was extracted with diethyl ether (3 × 50 mL). The combined organic phases were washed with brine (60 mL), dried over anhydrous MgSO<sub>4</sub>, filtered and the filtrate was evaporated under reduced pressure to afford the title compound as a light-yellow oil (5.71 g, 99%).

$\delta_{\text{H}}$  (400 MHz, CDCl<sub>3</sub>) 3.92 (3H, s, CH<sub>3</sub>), 4.65 (2H, dt, *J* 4.8, 1.7, CH<sub>2</sub>), 5.32 (1H, dq, *J* 10.6, 1.6, CHH), 5.53 (1H, dq, *J* 17.2, 1.7, CHH), 6.09 (1H, ddt, *J* 17.2, 10.6, 4.8, CH), 6.95 – 7.04 (2H, m, 2 × ArH), 7.46 (1H, ddd, *J* 8.4, 7.4, 1.8, ArH), 7.82 (1H, dd, *J* 7.7, 1.8, ArH); *m/z* (ES<sup>+</sup>) 215 (100%, M+Na<sup>+</sup>), 193 (80, M+H<sup>+</sup>). The data agree with those reported in the literature.<sup>104</sup>

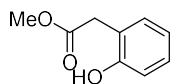
### Methyl 3-allyl-2-hydroxybenzoate **113**



Methyl 2-(allyloxy)benzoate **112** (3.00 g, 15.6 mmol) was neatly heated at 150 °C for 2 days. The resulting brownish oil was purified via flash column chromatography on silica gel, eluting petroleum ether/EtOAc, EtOAc: 0 – 5% to afford the title compound as a

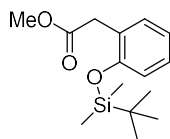
colourless oil (1.47 g, 49%).  $\delta_{\text{H}}$  (400 MHz,  $\text{CDCl}_3$ ) 3.46 (2H, d,  $J$  6.5,  $\text{CH}_2$ ), 3.97 (3H, s,  $\text{CH}_3$ ), 5.07 – 5.15 (2H, m,  $\text{CH}_2$ ), 5.96 – 6.11 (1H, m,  $\text{CH}$ ), 6.85 (1H, t,  $J$  7.7,  $\text{ArH}$ ), 7.36 (1H, d,  $J$  7.4,  $\text{ArH}$ ), 7.75 (1H, dd,  $J$  8.0, 1.6,  $\text{ArH}$ ), 11.09 (1H, s,  $\text{OH}$ );  $m/z$  ( $\text{EI}^+$ ) 192 (50%,  $\text{M}^+$ ), 160 (70), 131 (100). The data agree with those reported in the literature.<sup>104</sup>

### Methyl 2-(2-hydroxyphenyl)acetate **121**



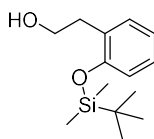
2-Hydroxybenzeneacetic acid **120** (2.00 g, 13.14 mmol) was dissolved in methanol (40 mL). Concentrated sulphuric acid (0.4 mL) was added dropwise to the solution. The reaction yellow solution was stirred and heated at reflux for overnight. After cooling to room temperature, the solvent was removed using a rotary evaporator under reduced pressure. The pH of the residue was adjusted to 6 with sat. aq.  $\text{NaHCO}_3$ . The aqueous solution was extracted with DCM (3  $\times$  20 mL). The combined organic phases were washed with brine (30 mL), dried over anhydrous  $\text{MgSO}_4$ , filtered and the filtrate was removed under reduced pressure to afford the title compound as a pale yellow solid in a quantitative yield (2.23 g). m.p. 70 - 72  $^{\circ}\text{C}$  [lit.<sup>133</sup> m.p. 70 - 71  $^{\circ}\text{C}$ ];  $\delta_{\text{H}}$  (400 MHz,  $\text{CDCl}_3$ ) 3.71 (2H, s,  $\text{CH}_2$ ), 3.78 (3H, s,  $\text{CH}_3$ ), 6.91 (1H, td,  $J$  7.5, 0.9,  $\text{ArH}$ ), 6.97 (1H, d,  $J$  7.5,  $\text{ArH}$ ), 7.12 (1H, d,  $J$  7.5,  $\text{ArH}$ ), 7.23 (1H, td,  $J$  8.0, 1.6,  $\text{ArH}$ ), 7.36 (1H, s,  $\text{OH}$ );  $m/z$  ( $\text{ES}^+$ ) 189 (70,  $\text{M}+\text{Na}^+$ ), 167 (100%,  $\text{M}+\text{H}^+$ ). The data agree with those reported in the literature.<sup>133, 134</sup>

## Methyl 2-[2-[(*tert*-butyldimethylsilyl)oxy]phenyl]acetate **122**



Methyl 2-(2-hydroxyphenyl)acetate **121** (1.00 g, 6.02 mmol) and imidazole (492 mg, 7.22 mmol) were dissolved in dry THF (20 mL) at 0 °C with an ice bath. A solution of *tert*-butyldimethylsilyl chloride (1.09 g, 7.22 mmol) in dry THF (10 mL) was added dropwise. The flask was removed from the ice bath and stirred at room temperature under N<sub>2</sub> for 2 days. Brine (30 mL) was added and the mixture was extracted with diethyl ether (3 × 30 mL). The combined organic phases were dried over anhydrous MgSO<sub>4</sub>, filtered and the filtrate was removed in a rotary evaporator under reduced pressure. The crude residue was purified by flash column chromatography on silica gel, eluting with hexane/EtOAc 9:1 to afford the title compound as a colourless oil (1.42 g, 84%).  $\nu_{\max}(\text{ATR})/\text{cm}^{-1}$  2953, 2931, 2859, 1740 (CO);  $\delta_{\text{H}}$  (400 MHz, CDCl<sub>3</sub>) 0.26 (6H, s, 2 × CH<sub>3</sub>), 1.02 (9H, s, 3 × CH<sub>3</sub>), 3.65 (2H, s, CH<sub>2</sub>), 3.70 (3H, s, CH<sub>3</sub>), 6.85 (1H, d, *J* 8.0, Ar*H*), 6.94 (1H, td, *J* 7.4, 1.0, Ar*H*), 7.15 – 7.24 (2H, m, 2 × Ar*H*); *m/z* (ES<sup>+</sup>) 281.1579 (100%, M+H<sup>+</sup>. C<sub>15</sub>H<sub>25</sub>O<sub>3</sub>Si requires 281.1567). The data agree with those reported in the literature.<sup>135</sup>

## 2-[2-[(*tert*-Butyldimethylsilyl)oxy]phenyl]ethan-1-ol **123**



### Method A:

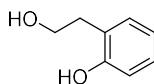
Anhydrous THF (1 mL) was added to lithium aluminium hydride (8.1 mg, 0.21 mmol) with an ice bath under N<sub>2</sub>. A solution of methyl 2-[2-[(*tert*-butyldimethylsilyl)oxy]phenyl]acetate **122** (50 mg, 0.18 mmol) in THF (1 mL) was added dropwise. The mixture was stirred at 0 °C for 3 h. Water (0.1 mL) was added slowly, and sat. NH<sub>4</sub>Cl solution (10 mL) was added in sequence. The aqueous phase was extracted with diethyl ether (3 × 10 mL). The combined organic phases were washed with brine (15 mL), dried over anhydrous MgSO<sub>4</sub>, filtered and the filtrate was evaporated under reduced pressure. The crude residue was purified by flash column chromatography on silica gel, eluting hexane/EtOAc 9:1 to afford the title compound as a colourless oil (31 mg, 69%).

### Method B:

*tert*-Butyl[2-[2-[(*tert*-butyldimethylsilyl)oxy]ethyl]phenoxy]dimethylsilane **125** (1.00 g, 2.73 mmol) was dissolved in EtOH (10 mL). Pyridinium *p*-toluenesulfonate (69 mg, 0.27 mmol) was added and the reaction solution was heated at 50 °C for 1 h. The solvent was removed under reduced pressure and the crude residue was purified by flash column chromatography on silica gel, eluting hexane/EtOAc 9:1 to afford the title compound as a colourless oil (639 mg, 93%).  $\delta_{\text{H}}$  (400 MHz, CDCl<sub>3</sub>) 0.27 (6H, s, 2 × CH<sub>3</sub>), 1.04 (9H,

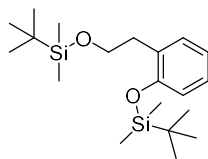
s,  $3 \times \text{CH}_3$ ), 1.58 (1H, t,  $J$  5.8,  $\text{CH}_2\text{OH}$ ), 2.91 (2H, t,  $J$  6.5,  $\text{CH}_2$ ), 3.86 (2H, q,  $J$  6.5,  $\text{CH}_2$ ), 6.84 (1H, d,  $J$  8.0, ArH), 6.93 (1H, td,  $J$  7.4, 3.7, ArH), 7.14 (1H, td,  $J$  7.8, 1.7, ArH), 7.19 (1H, dd,  $J$  7.4, 1.5, ArH);  $m/z$  ( $\text{ES}^+$ ) 275 (20,  $\text{M}+\text{Na}^+$ ), 253 (100%,  $\text{M}+\text{H}^+$ ). The data agree with those reported in the literature.<sup>136</sup>

### 2-(2-Hydroxyethyl)phenol **124**



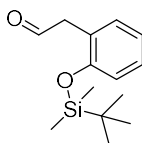
Anhydrous THF (25 mL) was added to lithium aluminium hydride (600 mg, 15.81 mmol) with an ice bath under  $\text{N}_2$ . A solution of 2-hydroxybenzeneacetic acid **120** (2.00 g, 13.14 mmol) in THF (10 mL) was added dropwise. The mixture was stirred at room temperature for 30 min and heated at reflux overnight. After it was cooled to room temperature, water (0.6 mL) was added slowly, and then 15% NaOH solution (0.6 mL) and water (1.8 mL) were added in sequence. After stirring for 30 min, the mixture was filtered, dried over anhydrous  $\text{MgSO}_4$ , filtered and the filtrate was removed under reduced pressure. The crude residue was purified by flash column chromatography on silica gel, eluting hexane/EtOAc, EtOAc: 0 - 10% to afford the title compound as a colourless oil (1.62 g, 89%).  $\delta_{\text{H}}$  (400 MHz,  $\text{CDCl}_3$ ) 2.59 (1H, s,  $\text{CH}_2\text{OH}$ ), 2.92 (2H, t,  $J$  5.3,  $\text{CH}_2$ ), 4.00 (2H, t,  $J$  5.3,  $\text{CH}_2$ ), 6.88 (1H, td,  $J$  7.4, 1.1, ArH), 6.93 (1H, dd,  $J$  8.0, 0.8, ArH), 7.09 (1H, dd,  $J$  7.4, 1.5, ArH), 7.18 (1H, td,  $J$  8.0, 1.7, ArH), 7.92 (1H, s, ArOH);  $m/z$  ( $\text{EI}^+$ ) 138 (50%,  $\text{M}^+$ ), 107 (100). The data agree with those reported in the literature.<sup>137</sup>

***tert*-Butyl[2-[2-[(*tert*-butyldimethylsilyl)oxy]ethyl]phenoxy]dimethylsilane 125**



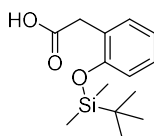
Imidazole (1.48 g, 21.72 mmol) was added to a solution of 2-(2-hydroxyethyl)phenol **124** (1.00 g, 7.24 mmol) in dry DMF (20 mL) at 0 °C with an ice bath under N<sub>2</sub>. A solution of *tert*-butyldimethylsilyl chloride (3.27 g, 21.72 mmol) in dry DMF (10 mL) was added dropwise. The flask was removed from the ice bath and the colourless solution was stirred at room temperature under N<sub>2</sub> for 2 days. Water (20 mL) was added and the mixture was extracted with diethyl ether (3 × 30 mL). The combined organic phases were washed with brine (30 mL), dried over anhydrous MgSO<sub>4</sub>, filtered and the filtrate was removed in a rotary evaporator under reduced pressure. The crude residue was purified by flash column chromatography on silica gel, eluting with hexane/EtOAc, EtOAc: 2% to afford the title compound as a colourless oil (2.21 g, 83%).  $\nu_{\max}(\text{ATR})/\text{cm}^{-1}$  2956, 2929, 2858;  $\delta_{\text{H}}$  (400 MHz, CDCl<sub>3</sub>) 0.01 (6H, s, 2 × CH<sub>3</sub>), 0.26 (6H, s, 2 × CH<sub>3</sub>), 0.89 (9H, s, 3 × CH<sub>3</sub>), 1.04 (9H, s, 3 × CH<sub>3</sub>), 2.86 (2H, t, *J* 7.2, CH<sub>2</sub>), 3.80 (2H, t, *J* 7.2, CH<sub>2</sub>), 6.80 (1H, d, *J* 8.0, ArH), 6.89 (1H, td, *J* 7.4, 1.0, ArH), 7.10 (1H, td, *J* 7.8, 1.7, ArH), 7.19 (1H, dd, *J* 7.4, 1.7, ArH); *m/z* (ES<sup>+</sup>) 389 (30%, M+Na<sup>+</sup>), 235 (100). The data agree with those reported in the literature.<sup>136</sup>

## 2-[2-[(*tert*-Butyldimethylsilyl)oxy]phenyl]acetaldehyde **126**



2-[2-[(*tert*-Butyldimethylsilyl)oxy]phenyl]ethan-1-ol **123** (28 mg, 0.11 mmol) was dissolved in DCM (1 mL) at 0 °C. Dess–Martin periodinane (94 mg, 0.22 mmol) was added and the reaction mixture was stirred at 0 °C for 1 h. The mixture was warmed to room temperature and stirred for additional 1 h. After that, the mixture was diluted with DCM (10 mL) and washed with sat. aq. NaHCO<sub>3</sub> (8 mL), dried over anhydrous MgSO<sub>4</sub>, filtered and the filtrate was evaporated under reduced pressure. The crude residue was purified by flash column chromatography on silica gel, eluting hexane/EtOAc 19:1 to afford the title compound as a colourless oil (21 mg, 76%).  $\nu_{\text{max}}(\text{ATR})/\text{cm}^{-1}$  2956, 2931, 2859, 1726 (CO);  $\delta_{\text{H}}$  (400 MHz, CDCl<sub>3</sub>) 0.27 (6H, s, 2 × CH<sub>3</sub>), 1.01 (9H, s, 3 × CH<sub>3</sub>), 3.66 (2H, d, *J* 1.9, CH<sub>2</sub>), 6.89 (1H, d, *J* 8.0, ArH), 6.97 (1H, t, *J* 7.4, ArH), 7.17 (1H, d, *J* 7.5, ArH), 7.22 (1H, td, *J* 7.5, 1.5, ArH), 9.72 (1H, t, *J* 2.1, CHO); *m/z* (ES<sup>+</sup>) 273 (100%, M+Na<sup>+</sup>), 251 (80, M+H<sup>+</sup>). The data agree with those reported in the literature.<sup>136</sup>

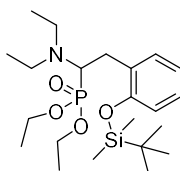
## 2-[2-[(*tert*-Butyldimethylsilyl)oxy]phenyl]acetic acid **127**



2-Hydroxybenzeneacetic acid **120** (1.00 g, 6.57 mmol) and imidazole (536 mg, 7.88 mmol) were dissolved in dry THF (20 mL) at 0 °C with an ice bath. A solution of *tert*-

butyldimethylsilyl chloride (1.19 g, 7.88 mmol) in dry THF (10 mL) was added dropwise. The flask was removed from the ice bath and stirred at room temperature under N<sub>2</sub> for 2 days. Brine (30 mL) was added and the mixture was extracted with diethyl ether (3 × 30 mL). The combined organic phases were dried over anhydrous MgSO<sub>4</sub>, filtered and the filtrate was removed in a rotary evaporator under reduced pressure. The crude residue was purified by flash column chromatography on silica gel, eluting with hexane/EtOAc 4:1 to afford the title compound as a yellow solid (887 mg, 51%). m.p. 62 - 64 °C;  $\nu_{\text{max}}(\text{ATR})/\text{cm}^{-1}$  2953, 2930, 2860, 1703 (CO);  $\delta_{\text{H}}$  (400 MHz, CDCl<sub>3</sub>) 0.26 (6H, s, 2 × CH<sub>3</sub>), 1.01 (9H, s, 3 × CH<sub>3</sub>), 3.67 (2H, s, CH<sub>2</sub>), 6.86 (1H, d, *J* 8.0, ArH), 6.95 (1H, td, *J* 7.5, 0.9, ArH), 7.16 – 7.24 (2H, m, 2 × ArH), 10.81 (1H, br s, CO<sub>2</sub>H);  $\delta_{\text{C}}$  (101 MHz, CDCl<sub>3</sub>) -4.2 (2 × CH<sub>3</sub>), 18.2 (CCH<sub>3</sub>), 25.7 (3 × CH<sub>3</sub>), 36.0 (CH<sub>2</sub>), 118.2 (ArCH), 121.1 (ArCH), 124.5 (ArC), 128.6 (ArCH), 131.3 (ArCH), 153.9 (ArC), 177.6 (CO<sub>2</sub>H); *m/z* (ES<sup>+</sup>) 289.1243 (100%, M+Na<sup>+</sup>. C<sub>14</sub>H<sub>22</sub>O<sub>3</sub>SiNa requires 289.1230).

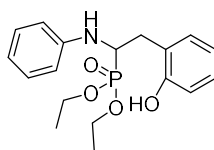
**Diethyl [2-[2-[(*tert*-butyldimethylsilyl)oxy]phenyl]-1-(diethylamino)ethyl]phosphonate 130**



A mixture of 2-[2-[(*tert*-Butyldimethylsilyl)oxy]phenyl]acetaldehyde **126** (100 mg, 0.40 mmol), diethylamine **129** (41  $\mu$ L, 0.40 mmol), diethyl phosphite **128** (52  $\mu$ L, 0.40 mmol) in THF (1 mL) was stirred and heated at 50 °C overnight. After cooling down, the solvent

was removed and the crude residue was purified by flash column chromatography on silica gel, eluting hexane/EtOAc 3:2 to afford the title compound as a colourless oil (32 mg, 18%).  $\nu_{\max}(\text{ATR})/\text{cm}^{-1}$  2930, 2859, 1600;  $\delta_{\text{H}}$  (400 MHz,  $\text{CDCl}_3$ ) 0.27 (6H, s,  $2 \times \text{CH}_3$ ), 0.89 (6H, t,  $J$  7.1,  $2 \times \text{CH}_3$ ), 1.04 (9H, s,  $3 \times \text{CH}_3$ ), 1.31 (6H, dt,  $J$  12.8, 7.1,  $2 \times \text{CH}_3$ ), 2.52 – 2.64 (2H, m,  $\text{CH}_2$ ), 2.70 – 2.82 (2H, m,  $\text{CH}_2$ ), 2.93 – 3.11 (2H, m,  $\text{CH}_2$ ), 3.59 – 3.70 (1H, m, CH), 4.02 – 4.23 (4H, m,  $2 \times \text{CH}_2$ ), 6.77 (1H, dd,  $J$  8.1, 0.9, ArH), 6.86 (1H, td,  $J$  7.4, 1.0, ArH), 7.08 (1H, td,  $J$  7.8, 1.7, ArH), 7.22 (1H, dd,  $J$  7.5, 1.6, ArH);  $\delta_{\text{C}}$  (101 MHz,  $\text{CDCl}_3$ ) -4.0 ( $2 \times \text{CH}_3$ ), 14.6 ( $2 \times \text{CH}_3$ ), 16.6 (CH), 18.4 ( $\text{CCH}_3$ ), 25.9 ( $3 \times \text{CH}_3$ ), 28.8 ( $\text{CH}_2$ ), 44.9 ( $2 \times \text{CH}_2$ ), 56.2 ( $\text{CH}_3$ ), 57.6 ( $\text{CH}_3$ ), 60.6 ( $\text{CH}_2$ ), 62.1 ( $\text{CH}_2$ ), 118.3 (ArCH), 120.6 (ArCH), 127.1 (ArCH), 129.8 (ArC), 132.0 (ArCH), 154.0 (COH);  $\delta_{\text{P}}$  (162 MHz,  $\text{CDCl}_3$ ) 27.9;  $m/z$  ( $\text{ES}^+$ ) 444.2707 (100%,  $\text{M}+\text{H}^+$ ).  $\text{C}_{22}\text{H}_{43}\text{NO}_4\text{PSi}$  requires 444.2693).

### Diethyl [2-(2-hydroxyphenyl)-1-(phenylamino)ethyl]phosphonate **132**



A mixture of 2-[2-[(*tert*-butyldimethylsilyl)oxy]phenyl]acetaldehyde **126** (50 mg, 0.20 mmol), aniline **131** (18  $\mu\text{L}$ , 0.20 mmol), diethyl phosphite **128** (26  $\mu\text{L}$ , 0.20 mmol) and  $\text{FeCl}_3$  (3 mg, 0.02 mmol) in EtOH (1 mL) was stirred at 60 °C overnight. The solvent was removed and the residue was diluted with ethyl acetate (10 mL). The mixture was washed with water (10 mL), brine (10 mL), dried over anhydrous  $\text{MgSO}_4$ , filtered and the

filtrate was evaporated under reduced pressure. The crude residue was purified by flash column chromatography on silica gel, eluting hexane/EtOAc 3:2 to afford the title compound as a light yellow oil (9 mg, 13%).  $\nu_{\max}(\text{ATR})/\text{cm}^{-1}$  2925, 1602, 1503;  $\delta_{\text{H}}$  (400 MHz,  $\text{CDCl}_3$ ) 1.26 (6H, q,  $J$  7.1,  $2 \times \text{CH}_3$ ), 3.92 – 4.20 (4H, m,  $2 \times \text{CH}_2$ ), 4.68 (1H, t,  $J$  7.4,  $\text{CHH}$ ), 4.92 (1H, dd,  $J$  22.6, 6.2,  $\text{CHH}$ ), 6.70 (2H, dd,  $J$  8.6, 0.9,  $2 \times \text{ArH}$ ), 6.80 (1H, t,  $J$  7.4,  $\text{ArH}$ ), 6.91 (1H, t,  $J$  7.5,  $\text{ArH}$ ), 6.99 (1H, d,  $J$  7.6,  $\text{ArH}$ ), 7.13 – 7.27 (4H, m,  $4 \times \text{ArH}$ ), 7.28 (1H, s,  $\text{NH}$ ), 8.79 (1H, s,  $\text{OH}$ );  $\delta_{\text{C}}$  (101 MHz,  $\text{CDCl}_3$ ) 16.3 ( $2 \times \text{CH}_3$ ), 26.0 ( $\text{CH}$ ), 55.1 ( $\text{CH}_2$ ), 63.7 ( $\text{CH}_2$ ), 64.4 ( $\text{CH}_2$ ), 114.6 ( $2 \times \text{ArCH}$ ), 119.4 ( $\text{ArCH}$ ), 119.7 ( $\text{ArCH}$ ), 121.1 ( $\text{ArCH}$ ), 121.7 ( $\text{ArC}$ ), 129.1 ( $\text{ArCH}$ ), 129.3 ( $2 \times \text{ArCH}$ ), 129.6 ( $\text{ArCH}$ ), 146.3 ( $\text{ArC}$ ), 155.7 ( $\text{COH}$ );  $\delta_{\text{P}}$  (162 MHz,  $\text{CDCl}_3$ ) 24.3.

## References

1. R. Gaynes, *Emerging Infect. Dis.*, 2017, **23**, 849-853.
2. S. L. Derderian, *River Academic Journal*, 2007, **3**, 1-5.
3. R. Sanjuan and P. Domingo-Calap, *Cell Mol Life Sci*, 2016, **73**, 4433-4448.
4. G. Subramaniam and M. Girish, *Indian J Pediatr*, 2020, **87**, 937-944.
5. S. Duffy, *PLoS Biol*, 2018, **16**, 1-6.
6. D. A. Wirtz, K. C. Ludwig, M. Arts, C. E. Marx, S. Krannich, P. Barac, S. Kehraus, M. Josten, B. Henrichfreise, A. Muller, G. M. Konig, A. J. Peoples, A. Nitti, A. L. Spoering, L. L. Ling, K. Lewis, M. Crusemann and T. Schneider, *Angew Chem Int Ed Engl*, 2021, **60**, 13579-13586.
7. C. L. Ventola, *Pharm. Ther.*, 2015, **40**, 277-283.
8. D. M. Chenoweth, *Chemical Tools for Imaging, Manipulating, and Tracking Biological Systems: Diverse Methods for Prokaryotic and Eukaryotic Systems*, Academic Press, 1st edn., 2020.
9. S. Bernatova, O. Samek, Z. Pilat, M. Sery, J. Jezek, P. Jakl, M. Siler, V. Krzyzanek, P. Zemanek, V. Hola, M. Dvorackova and F. Ruzicka, *Mol.*, 2013, **18**, 13188-13199.
10. F. Li, J. G. Collins and F. R. Keene, *Chem Soc Rev*, 2015, **44**, 2529-2542.
11. G. Kapoor, S. Saigal and A. Elongavan, *J Anaesthesiol Clin Pharmacol.*, 2017, **33**, 300-305.
12. S. P. Singh, A. Qureshi and W. Hassan, *Mcgill J Med*, 2021, **19**, 1-10.
13. K.-F. Kong, L. Schneper and K. Mathee, *APMIS*, 2010, **118**, 1-36.

14. L. Poirel, A. Jayol and P. Nordmann, *Clin Microbiol Rev*, 2017, **30**, 557-596.
15. G. Wang and K. Vasquez, *Genes*, 2017, **8**, 1-18.
16. E. A. Campbell, N. Korzheva, A. Mustaev, K. Murakami, S. Nair, A. Goldfarb and S. A. Darst, *Cell*, 2001, **104**, 901-912.
17. B. S. Laursen, H. P. Sorensen, K. K. Mortensen and H. U. Sperling-Petersen, *Microbiol Mol Biol Rev*, 2005, **69**, 101-123.
18. D. N. Wilson, *Nat Rev Microbiol*, 2014, **12**, 35-48.
19. W. Hong, J. Zeng and J. Xie, *Acta Pharm Sin B*, 2014, **4**, 258-265.
20. P. A. de Boer, *EMBO J*, 2009, **28**, 1193-1194.
21. T. J. Silhavy, D. Kahne and S. Walker, *Cold Spring Harb Perspect Biol*, 2010, **2**, a000414.
22. D. J. Scheffers and M. G. Pinho, *Microbiol Mol Biol Rev*, 2005, **69**, 585-607.
23. C. Schaffer and P. Messner, *Microbiology*, 2005, **151**, 643-651.
24. W. Vollmer, D. Blanot and M. A. de Pedro, *FEMS Microbiol Rev*, 2008, **32**, 149-167.
25. V. Prajapati, H. D. Karen, P. H. Prajapati, D. J. Sen and C. N. Patel, *World J. Pharm. Res.*, 2018, **7**, 490-535.
26. L. Brown, J. M. Wolf, R. Prados-Rosales and A. Casadevall, *Nat Rev Microbiol*, 2015, **13**, 620-630.
27. V. van Dam, N. Orlachs and E. Breukink, *Chembiochem*, 2009, **10**, 617-624.
28. A. El Zoeiby, F. Sanschagrín and R. C. Levesque, *Mol Microbiol*, 2003, **47**, 1-12.
29. H. Mohammad, W. Younis, L. Chen, C. E. Peters, J. Pogliano, K. Pogliano, B.

- Cooper, J. Zhang, A. Mayhoub, E. Oldfield, M. Cushman and M. N. Seleem, *J Med Chem*, 2017, **60**, 2425-2438.
30. R. T. Guo, T. P. Ko, A. P. Chen, C. J. Kuo, A. H. Wang and P. H. Liang, *J Biol Chem*, 2005, **280**, 20762-20774.
31. H. Y. Chang, C. C. Chou, M. F. Hsu and A. H. Wang, *J Biol Chem*, 2014, **289**, 18719-18735.
32. H. Mohammad, W. Younis, H. G. Ezzat, C. E. Peters, A. AbdelKhalek, B. Cooper, K. Pogliano, J. Pogliano, A. S. Mayhoub and M. N. Seleem, *PLoS One*, 2017, **12**, e0182821.
33. G. Manat, S. Roure, R. Auger, A. Bouhss, H. Barreteau, D. Mengin-Lecreulx and T. Touzé, *Microb. Drug Resist.*, 2014, **20**, 199-214.
34. B. C. Chung, J. Zhao, R. A. Gillespie, D. Y. Kwon, Z. Guan, J. Hong, P. Zhou and S. Y. Lee, *Science*, 2013, **341**, 1012-1016.
35. J. v. Heijenoort, *Glycobiology*, 2001, **11**, 25R-36R.
36. J.-V. Höltje, *Microbiol Mol Biol Rev*, 1998, **62**, 181-203.
37. A. L. Lovering, S. S. Safadi and N. C. Strynadka, *Annu Rev Biochem*, 2012, **81**, 451-478.
38. A. Typas, M. Banzhaf, C. A. Gross and W. Vollmer, *Nat. Rev. Microbiol.*, 2011, **10**, 123-136.
39. R. Kosmol, L. Hennig, P. Welzel, M. Findesien, D. Müller, A. Markus and J. van Heijenoort, *J. Prakt. Chem.*, 1997, **339**, 340-358.
40. J. van Heijenoort, *Glycobiology*, 2001, **11**, 25r-36r.

41. M. Yamada, T. Watanabe, T. Miyara, N. Baba, J. Saito, Y. Takeuchi and F. Ohsawa, *Antimicrob. Agents Chemother.*, 2007, **51**, 3902-3907.
42. B. M. Meberg, A. L. Paulson, R. Priyadarshini and K. D. Young, *J. Bacteriol.*, 2004, **186**, 8326-8336.
43. M. A. McDonough, J. W. Anderson, N. R. Silvaggi, R. F. Pratt, J. R. Knox and J. A. Kelly, *J. Mol. Biol.*, 2002, **322**, 111-122.
44. E. Sauvage, F. Kerff, M. Terrak, J. A. Ayala and P. Charlier, *FEMS Microbiol Rev*, 2008, **32**, 234-258.
45. A. M. D. Guilmi, A. Dessen, O. Dideberg and T. Vernet, *J. Bacteriol.*, 2003, **185**, 1650-1658.
46. M. Haenni, P. A. Majcherczyk, J.-L. Barblan and P. Moreillon, *Antimicrob. Agents Chemother.*, 2006, **50**, 4062-4069.
47. D. E. Nelson and K. D. Young, *J. Bacteriol.*, 2001, **183**, 3055-3064.
48. V. V. Loi, N. T. T. Huyen, T. Busche, Q. N. Tung, M. C. H. Gruhlke, J. Kalinowski, J. Bernhardt, A. J. Slusarenko and H. Antelmann, *Free Radic. Biol. Med.*, 2019, **139**, 55-69.
49. H. W. Boucher and G. R. Corey, *Clin Infect Dis*, 2008, **46 Suppl 5**, S344-349.
50. F. D. Lowy, *J Clin Invest*, 2003, **111**, 1265-1273.
51. H. F. Chambers and F. R. Deleo, *Nat. Rev. Microbiol.*, 2009, **7**, 629-641.
52. G. G. Zhanel, G. Sniezek, F. Schweizer, S. Zelenitsky, P. R. Lagacé-Wiens, E. Rubinstein, A. S. Gin, D. J. Hoban and J. A. Karlowsky, *Drugs*, 2009, **69**, 809-831.

53. D. M. Sievert, J. T. Rudrik, J. B. Patel, L. C. McDonald, M. J. Wilkins and J. C. Hageman, *Clin Infect Dis*, 2008, **46**, 668-674.
54. C. Duplessis and N. F. Crum-Cianflone, *Clin Med Rev Ther*, 2011, **3**, a2466.
55. P. V. Ingle, S. Z. Samsudin, P. Q. Chan, M. K. Ng, L. X. Heng, S. C. Yap, A. S. Chai and A. S. Wong, *Ther Clin Risk Manag*, 2016, **12**, 445-455.
56. P. Reed, H. Veiga, A. M. Jorge, M. Terrak and M. G. Pinho, *J. Bacteriol.*, 2011, **193**, 2549-2556.
57. T. M. da Costa, C. R. de Oliveira, H. F. Chambers and S. S. Chatterjee, *Microorganisms*, 2018, **6**, 57.
58. M. Roch, E. Lelong, O. O. Panasenko, R. Sierra, A. Renzoni and W. L. Kelley, *Commun. Biol.*, 2019, **2**, 417.
59. S. L. Schreiber, J. D. Kotz, M. Li, J. Aube, C. P. Austin, J. C. Reed, H. Rosen, E. L. White, L. A. Sklar, C. W. Lindsley, B. R. Alexander, J. A. Bittker, P. A. Clemons, A. de Souza, M. A. Foley, M. Palmer, A. F. Shamji, M. J. Wawer, O. McManus, M. Wu, B. Zou, H. Yu, J. E. Golden, F. J. Schoenen, A. Simeonov, A. Jadhav, M. R. Jackson, A. B. Pinkerton, T. D. Chung, P. R. Griffin, B. F. Cravatt, P. S. Hodder, W. R. Roush, E. Roberts, D. H. Chung, C. B. Jonsson, J. W. Noah, W. E. Severson, S. Ananthan, B. Edwards, T. I. Oprea, P. J. Conn, C. R. Hopkins, M. R. Wood, S. R. Stauffer, K. A. Emmitte and N. I. H. M. L. P. Team, *Cell*, 2015, **161**, 1252-1265.
60. R. Weissleder and U. Mahmood, *Radiology*, 2001, **219**, 316-333.
61. T. F. Massoud and S. S. Gambhir, *Genes Dev*, 2003, **17**, 545-580.

62. K. Chen and X. Chen, *Curr. Top. Med. Chem.*, 2010, **10**, 1227-1236.
63. Y. Zhang, Y. Yang and W. Cai, *Theranostics*, 2011, **1**, 135-148.
64. R. Haubner, H. J. Wester, W. A. Weber, C. Mang, S. I. Ziegler, S. L. Goodman, R. Senekowitsch-Schmidtke, H. Kessler and M. Schwaiger, *Cancer Res.*, 2001, **61**, 1781-1785.
65. H. Liu, G. Ren, Z. Miao, X. Zhang, X. Tang, P. Han, S. S. Gambhir and Z. Cheng, *PLoS One*, 2010, **5**, e9470.
66. T. Terai and T. Nagano, *Pflugers Arch - Eur J Physiol* 2013, **465**, 347-359.
67. S. Liu and D. S. Edwards, *Bioconjugate Chem.*, 2001, **12**, 7-34.
68. R. Slusarz, M. Szulc and J. Madaj, *Carbohydr Res*, 2014, **389**, 154-164.
69. E. Sauvage and M. Terrak, *Antibiotics (Basel)*, 2016, **5**, 12.
70. Y. Yuan, S. Fuse, B. Ostash, P. Sliz, D. Kahne and S. Walker, *ACS Chem Biol*, 2008, **3**, 429-436.
71. T.-J. R. Cheng, M.-T. Sung, H.-Y. Liao, Y.-F. Chang, C.-W. Chen, C.-Y. Huang, L.-Y. Chou, Y.-D. Wu, Y.-H. Chen, Y.-S. E. Cheng, C.-H. Wong, C. Ma and W.-C. Cheng, *Proc. Natl. Acad. Sci.*, 2008, **105**, 431-436.
72. B. Ostash and S. Walker, *Nat Prod Rep*, 2010, **27**, 1594-1617.
73. K. Bush and P. A. Bradford, *Cold Spring Harb Perspect Med*, 2016, **6**, a025247.
74. S. Sharifzadeh, N. W. Brown, J. D. Shirley, K. E. Bruce, M. E. Winkler and E. E. Carlson, *Methods Enzymol*, 2020, **638**, 27-55.
75. S. Sharifzadeh, M. J. Boersma, O. Kocaoglu, A. Shokri, C. L. Brown, J. D. Shirley, M. E. Winkler and E. E. Carlson, *ACS Chem Biol*, 2017, **12**, 2849-2857.

76. W. L. Parker, M. L. Rathnum and W. C. Liu, *J. Antibiot.*, 1982, **35**, 900-902.
77. A. Buchynskyy, U. Kempin, S. Vogel, L. Hennig, M. Findeisen, D. Müller, S. Giesa, H. Knoll and P. Welzel, *Eur. J. Org. Chem.*, 2002, **2002**, 1149-1162.
78. J. G. Taylor, X. Li, M. Oberthür, W. Zhu and D. E. Kahne, *J. Am. Chem. Soc.*, 2006, **128**, 15084-15085.
79. R. C. Goldman and D. Gange, *Curr. Med. Chem.*, 2000, **7**, 801-820.
80. P. Butaye, L. A. Devriese and F. Haesebrouck, *Clin Microbiol Rev*, 2003, **16**, 175-188.
81. C. L. Ventola, *P & T*, 2015, **40**, 277-283.
82. P. Gallo, S. Fabbrocino, L. Serpe, M. Fiori, C. Civitareale and P. Stacchini, *Rapid Commun. Mass Spectrom*, 2010, **24**, 1017-1024.
83. M. A. Pfaller, *Diagn. Microbiol. Infect. Dis*, 2006, **56**, 115-121.
84. C. M. Gampe, H. Tsukamoto, E. H. Doud, S. Walker and D. Kahne, *J. Am. Chem. Soc.*, 2013, **135**, 3776-3779.
85. J. C. Thenmozhiyal, P. T. Wong and W. K. Chui, *J Med Chem*, 2004, **47**, 1527-1535.
86. S.-F. Tan, K.-P. Ang and Y.-F. Fong, *J. Chem. Soc., Perkin Trans. 2*, 1986, 1941-1944.
87. R. Bouley, M. Kumarasiri, Z. Peng, L. H. Otero, W. Song, M. A. Suckow, V. A. Schroeder, W. R. Wolter, E. Lastochkin, N. T. Antunes, H. Pi, S. Vakulenko, J. A. Hermoso, M. Chang and S. Mobashery, *J Am Chem Soc*, 2015, **137**, 1738-1741.
88. R. Bouley, D. Ding, Z. Peng, M. Bastian, E. Lastochkin, W. Song, M. A. Suckow,

- V. A. Schroeder, W. R. Wolter, S. Mobashery and M. Chang, *J Med Chem*, 2016, **59**, 5011-5021.
89. J. N. Pendleton, S. P. Gorman and B. F. Gilmore, *Expert Rev. Anti-Infect. Ther*, 2013, **11**, 297-308.
90. L. B. Rice, *J Infect Dis*, 2008, **197**, 1079-1081.
91. K. V. Mahasenan, R. Molina, R. Bouley, M. T. Batuecas, J. F. Fisher, J. A. Hermoso, M. Chang and S. Mobashery, *J Am Chem Soc*, 2017, **139**, 2102-2110.
92. A. J. O'Neill, *Lett Appl Microbiol*, 2010, **51**, 358-361.
93. G. McVicker, T. K. Prajsnar, A. Williams, N. L. Wagner, M. Boots, S. A. Renshaw and S. J. Foster, *PLoS Pathog*, 2014, **10**, e1003959.
94. M. Mainiero, C. Goerke, T. Geiger, C. Gonser, S. Herbert and C. Wolz, *J Bacteriol*, 2010, **192**, 613-623.
95. J. Janardhanan, R. Bouley, S. Martinez-Caballero, Z. Peng, M. Batuecas-Mordillo, J. E. Meisel, D. Ding, V. A. Schroeder, W. R. Wolter, K. V. Mahasenan, J. A. Hermoso, S. Mobashery and M. Chang, *Antimicrob Agents Chemother*, 2019, **63**, e02637-18.
96. M. A. Foxley, A. W. Friedline, J. M. Jensen, S. L. Nimmo, E. M. Scull, J. B. King, S. Strange, M. T. Xiao, B. E. Smith, K. J. Thomas Iii, D. T. Glatzhofer, R. H. Cichewicz and C. V. Rice, *J. Antibiot.*, 2016, **69**, 871-878.
97. D. E. Lorke, A. Stegmeier-Petroianu and G. A. Petroianu, *J Appl Toxicol*, 2017, **37**, 13-22.
98. A. M. Faisca Phillips, M. T. Barros, M. Pacheco and R. Dias, *Bioorg Med Chem*

- Lett*, 2014, **24**, 49-53.
99. K. Kaur, S. A. Adediran, M. J. Lan and R. F. Pratt, *Biochemistry*, 2003, **42**, 1529-1536.
100. K. Bush, *Int J Antimicrob Agents*, 2015, **46**, 483-493.
101. D. M. Livermore and S. Mushtaq, *J Antimicrob Chemother*, 2013, **68**, 1825-1831.
102. J. Brem, R. Cain, S. Cahill, M. A. McDonough, I. J. Clifton, J. C. Jimenez-Castellanos, M. B. Avison, J. Spencer, C. W. Fishwick and C. J. Schofield, *Nat Commun*, 2016, **7**, 12406.
103. J. M. Frere and M. G. Page, *Curr Opin Pharmacol*, 2014, **18**, 112-119.
104. M. R. Patel, A. Bhatt, J. D. Steffen, A. Chergui, J. Murai, Y. Pommier, J. M. Pascal, L. D. Trombetta, F. R. Fronczek and T. T. Talele, *J Med Chem*, 2014, **57**, 5579-5601.
105. T. Shimizu, Y. Hayashi, Y. Nagano and K. Teramura, *Bull. Chem. Soc. Jpn.*, 1980, **53**, 429-434.
106. M. P. Hay, S. Turcotte, J. U. Flanagan, M. Bonnet, D. A. Chan, P. D. Sutphin, P. Nguyen, A. J. Giaccia and W. A. Denny, *J Med Chem*, 2010, **53**, 787-797.
107. Y. Saito, H. Ouchi and H. Takahata, *Tetrahedron*, 2006, **62**, 11599-11607.
108. G. Burgy, T. Tahtouh, E. Durieu, B. Foll-Josselin, E. Limanton, L. Meijer, F. Carreaux and J. P. Bazureau, *Eur J Med Chem*, 2013, **62**, 728-737.
109. S. P. Gangadhar, D. K. Ramesh and S. K. Mahajan, *IJRPC*, 2013, **3**, 793-796.
110. H. Brand, P. Mayer, A. Schulz, T. Soller and A. Villinger, *Chem Asian J*, 2008, **3**, 1050-1058.

111. S. V. Bhandari, K. G. Bothara, A. A. Patil, T. S. Chitre, A. P. Sarkate, S. T. Gore, S. C. Dangre and C. V. Khachane, *Bioorg Med Chem*, 2009, **17**, 390-400.
112. M. Arfeen, S. Bhagat, R. Patel, S. Prasad, I. Roy, A. K. Chakraborti and P. V. Bharatam, *Eur J Med Chem*, 2016, **121**, 727-736.
113. A. Katritzky, N. Kirichenko, B. Rogovoy, J. Kister and H. Tao, *Synthesis*, 2004, **2004**, 1799-1805.
114. C. Goodyer, *Bioorg. Med. Chem.*, 2003, **11**, 4189-4206.
115. S. Mahboobi, A. Sellmer, H. Hoher, E. Eichhorn, T. Bar, M. Schmidt, T. Maier, J. F. Stadlwieser and T. L. Beckers, *J Med Chem*, 2006, **49**, 5769-5776.
116. S. Guiheneuf, L. Paquin, F. Carreaux, E. Durieu, H. Benedettid, R. Guevel, A. Corlu, L. Meijer and J.-P. Bazureau, *Curr. Microw. Chem.*, 2014, **1**, 33-40.
117. A. Kamal, R. Reddy Ch, M. V. Vishnuvardhan, R. Mahesh, V. Lakshma Nayak, S. Prabhakar and C. S. Reddy, *Bioorg Med Chem Lett*, 2014, **24**, 2309-2314.
118. R. G. Andrew and R. A. Raphael, *Tetrahedron*, 1987, **43**, 4803-4816.
119. R. Schobert, B. Biersack, A. Dietrich, K. Effenberger, S. Knauer and T. Mueller, *J Med Chem*, 2010, **53**, 6595-6602.
120. W. Shi, S. Dolai, S. Averick, S. S. Fernando, J. A. Saltos, W. L'Amoreaux, P. Banerjee and K. Raja, *Bioconjugate Chem.*, 2009, **20**, 1595-1601.
121. S. Eising, F. Lelivelt and K. M. Bongers, *Angew Chem Int Ed Engl*, 2016, **55**, 12243-12247.
122. W. Zhou, H. B. Li, C. N. Xia, X. M. Zheng and W. X. Hu, *Bioorg Med Chem Lett*, 2009, **19**, 1861-1865.

123. B. M. Trost and B. M. O'Boyle, *Org Lett*, 2008, **10**, 1369-1372.
124. K. Suzuki, E. K. Weisburger and J. H. Weisburger, *J. Org. Chem.*, 1961, **26**, 2239-2242.
125. O. Michel and B. J. Ravoo, *Langmuir*, 2008, **24**, 12116-12118.
126. Y. Feng, J. Li, L. Jiang, Z. Gao, W. Huang, F. Jiang, N. Luo, S. Han, R. Zeng and D. Yang, *Eur. J. Org. Chem.*, 2011, **2011**, 562-568.
127. G. Lu, S. Lam and K. Burgess, *Chem Commun*, 2006, **15**, 1652-1654.
128. C. v. d. Stelt, B. G. Suurmond and W. T. Nauta, *Recl. Trav. Chim. Pays-Bas*, 1953, **72**, 195-201.
129. C. S. McKay and M. G. Finn, *Angew Chem Int Ed Engl*, 2016, **55**, 12643-12649.
130. C.-X. Miao, L.-N. He, J.-L. Wang and F. Wu, *J. Org. Chem.*, 2010, **75**, 257-260.
131. S. W. Wright, D. L. Hageman, A. S. Wright and L. D. McClure, *Tetrahedron Lett.*, 1997, **38**, 7345-7348.
132. P. Stanetty, H. Koller and G. Pürstinger, *Monatsh. Chem.*, 1990, **121**, 883-891.
133. J. Lin, B. S. Gerstenberger, N. Y. Stessman and J. P. Konopelski, *Org Lett*, 2008, **10**, 3969-3972.
134. M. V. W. Rekowski, V. Kumar, Z. Zhou, J. Moschner, A. Marazioti, M. Bantzi, G. A. Spyroulias, F. van den Akker, A. Giannis and A. Papapetropoulos, *J Med Chem*, 2013, **56**, 8948-8952.
135. Y. Wang, B. Tian, M. Ding and Z. Shi, *Chemistry*, 2020, **26**, 4297-4303.
136. *U.S. Pat.*, WO 2014/159959 A1, 2014.
137. B. S. Bodnar and P. F. Vogt, *J. Org. Chem.*, 2009, **74**, 2598-2600.